Roraima Mount, Venezuela

ΕΛΛΗΝΙΚΗ
ΕΠΙΣΤΗΜΟΝΙΚΗ
ΕΤΑΙΡΕΙΑ
ΕΔΑΦΟΜΗΧΑΝΙΚΗΣ
& ΓΕΩΤΕΧΝΙΚΗΣ
ΜΗΧΑΝΙΚΗΣ

Τα Νέα της Ε Ε Ε Ε Γ Μ

72Β

Αρ. 72Β – ΝΟΕΜΒΡΙΟΣ 2014

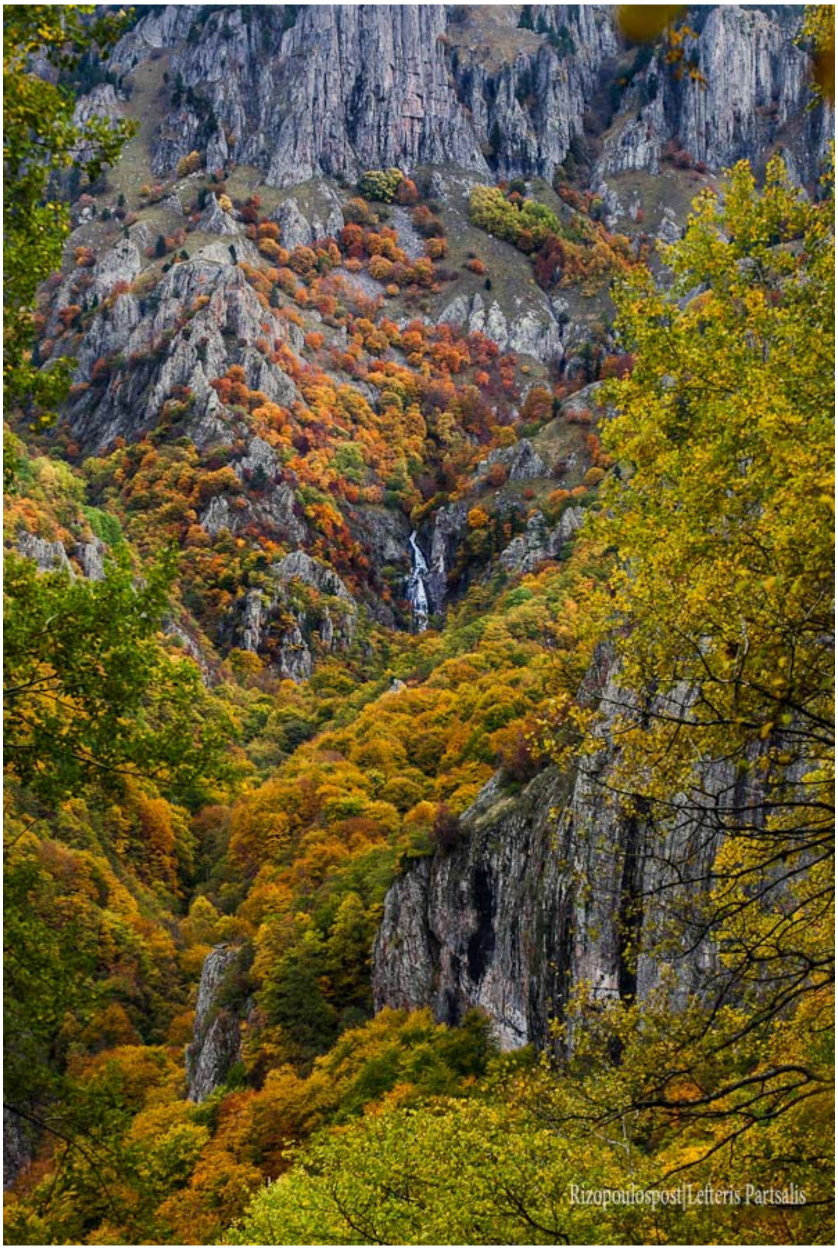

SIMSG ISSMGE

ISRM

Π Ε Ρ Ι Ε Χ Ο Μ Ε Ν Α

ΑΡΘΡΑ

Ishihara Lecture: Soil–Foundation–Structure Systems Beyond Conventional Seismic Failure Thresholds

G. Gazetas
Professor, National Technical University of Athens, Greece

ABSTRACT: A new paradigm has now emerged in performance–based seismic design of soil–foundation–structure systems. Instead of imposing strict safety limits on forces and moments transmitted from the foundation onto the soil (aiming at avoiding pseudo-static failure), the new dynamic approach "invites" the creation of two simultaneous "failure" mechanisms: substantial foundation uplifting and ultimate-bearing-capacity slippage, while ensuring that peak and residual deformations are acceptable. The paper shows that allowing the foundation to work at such extreme conditions not only may not lead to system collapse, but it would help protect (save) the structure from seismic damage. A potential price to pay: residual settlement and rotation, which could be abated with a number of foundation and soil improvements. Numerical studies and experiments demonstrate that the consequences of such daring foundation design would likely be quite beneficial to bridge piers and building frames. It is shown that system collapse could be avoided even under seismic shaking far beyond the design ground motion.

KEYWORDS: seismic analysis, performance-based design, foundation rocking, bearing capacity failure, nonlinear vibrations

1 CURRENT STATE OF PRACTICE : THE CONVENTIONAL "WISDOM"

Seismic design of structures recognises that highly inelastic material response is unavoidable under the strongest possible shaking of the particular location and for the specific soil where the structure is founded. "Ductility" levels of the order of 3 or more are usually allowed to develop under seismic loading, implying that the strength of a number of critical bearing elements is fully mobilized. In the prevailing structural terminology "plastic hinging" is allowed to develop as long as the overall stability is maintained.

By contrast, a crucial goal of current practice in seismic "foundation" design, particularly as entrenched in the respective codes is to *avoid* the mobilisation of "strength" in the foundation. In the words of EC8 (Part 2, § 5.8) :

"…foundations shall not be used as sources of hysteretic energy dissipation, and therefore shall be designed to remain elastic under the design seismic action."

In *structural* terminology : *no* "plastic hinging" is allowed in the foundation. In simple *geotechnical* terms, the designer must ensure that the below-ground (and hence uninspectable) support system will not even reach a number of "thresholds" that would conventionally imply failure. Specifically, the following states are prohibited :

- plastic structural "hinging" in piles, pile-caps, foundation beams, rafts, and so on
- mobilisation of the so-called *bearing-capacity failure* mechanisms under cyclically–uplifting shallow foundations
- sliding at the soil–footing interface or excessive uplifting of a shallow foundation
- passive failure along the normal compressing sides of an embedded foundation
- a combination of two or more of the above "failure" modes.

In this conventional approach to foundation design, "overstrength" factors plus (explicit and implicit) factors of safety larger than 1 (e.g. in the form of "material" factors) are introduced against each of the above "failure" modes, in a way qualitatively similar to the factors of safety of the traditional static design. Thus, the engineer is certain that foundation performance will be satisfactory and there will be no need to inspect and repair after strong earthquake shaking — a task practically considered next to impossible.

Some of the above thresholds stem not just from an understandable engineering conservatism, but also from a purely (pseudo) static thinking. It will be shown that such an approach may lead not only to unnecessarily expensive foundation solutions but also, in many situations, to less safe structures.

2 SOME COMPELLING REASONS TO GO BEYOND CONVENTIONAL THRESHOLDS

A growing body of evidence suggests that soil–foundation plastic yielding under seismic excitation is unavoidable, and at times even desirable; hence, it must be considered in analysis and perhaps allowed in design. *[See for an early recognition : Pecker 1998, Faccioli & Paolucci 1999, Martin & Lam 2000, FEMA-356 2000, Kutter et al 2001, Gazetas & Apostolou 2003.]* The urgent need to explicitly consider the possibility of the foundation system to go beyond "failure" thresholds, and the potential usefulness of doing so, have emerged from :

(a) The large (often huge) effective ground acceleration, A, and velocity, V, levels recorded in several earthquakes in the last 25 years. A f*ew examples :*

- *1994 $M_s \approx 6.8$ Northridge : A = 0.98 g, V = 140 cm/s*
- *1995 $M_J \approx$ 7.2 Kobe : A = 0.85 g, V = 120 cm/s*
- *1986 $M_s \approx 5.6$ San Salvador : A = 0.75 g, V = 84 cm/s*
- *2003 $M_s = 6.4$ Lefkada : A $\approx$ 0.55 g, V = 50 cm/s*
- *2007 $M_J \approx 6.9$ Niigata : A =1.20 g, V = 100cm/s.*

With the correspondingly large accelerations in the (above–ground) structure from such ground motions (spectral S_a values well in excess of 1 g), preventing "plastic hinging" in the foundation system is a formidable task. And in fact, it may not even be desirable**:** enormous ductility demands might be imposed to the structure if soil–foundation "yielding" would not take place to effectively limit the transmitted accelerations. Several present-day critically–important structures on relatively loose soil could not have survived severe ground shaking if "plastic hinging" of some sort had not taken place in the "foundation" — usually unintentionally.

(b) In seismically retrofitting a building or a bridge, allowing for soil and foundation yielding is often the most rational alternative. Because increasing the structural capacity of some elements, or introducing some new stiff elements, would then imply that the forces transmitted onto their foundation will be increased, to the point that it might not be technically or economically feasible to undertake them "elastically". The new American retrofit design guidelines (FEMA 356) explicitly permit some forms of inelastic deformations in the foundation.

A simple hypothetical *example* referring to an existing three–bay multi–story building frame which is to be retrofitted with a single–bay concrete "shear" wall had been introduced by Martin & Lam 2000. Such a wall, being much stiffer than the columns of the frame, would carry most of the inertia-driven shear force and would thus transmit a disproportionately large horizontal force and overturning moment onto the foundation compared with its respective small vertical force. If uplifting, sliding, and mobilisation of bearing capacity failure mechanisms in the foundation had been all spuriously ignored, or had been conversely correctly taken into account, would have led to dramatically different results. With "beyond–threshold" action in the foundation the shear wall would "shed" off some of the load onto the columns of the frame, which must then be properly reinforced ; the opposite would be true when such action (beyond the thresholds) is disallowed.

The Engineer therefore should be able to compute the consequences of "plastic hinging" in the foundation before deciding whether such "hinging" must be accepted, modified, or avoided (through foundation changes).

(c) Many slender historical monuments (e.g. ancient columns, towers, sculptures) may have survived strong seismic shaking during their life (often of thousands of years). While under static conditions such "structures" would have easily toppled, it appears that sliding at, and especially uplifting from, their base during oscillatory seismic motion was a key to their survival (Makris & Roussos 2000, Papantonopoulos 2000). These nonlinear interface phenomena cannot therefore be ignored, even if their geometrically–nonlinear nature presents computational difficulties.

In fact, it is worthy of note that the lack of recognition of the fundamental difference between pseudo-static and seismic overturning threshold accelerations has led humanity to a gross under-estimation of the largest ground accelerations that must have taken place in historic destructive earthquakes. Because, by observing in numerous earthquakes that very slender blocks (of width b and height h, *with* $h >> b$) or monuments in precarious equilibrium that had not overturned, engineers had invariably attributed the fact to very small peak accelerations, less than $(b/h)g$, as would be necessary if accelerations were applied pseudostatically in one direction. Today we know that sometimes even five times as large peak ground acceleration of a high-frequency motion may not be enough to overturn a slender block (Koh et al 1986, Makris & Roussos 2000, Gazetas 2001). Simply stated: even severe uplifting (conventional "failure") may not lead to overturning (true "collapse") under dynamic seismic base excitation.

(d) Compatibility with structural design is another reason for the soil–structure interaction analyst to compute the lateral load needed for collapse of the foundation system, as well as (in more detail) the complete load–displacement or moment–rotation response to progressively increasing loading up to collapse. Indeed, in State of the Art (SOA) structural engineering use is made of the so-called "push-over" analysis, which in order to be complete requires the development of such information from the foundation analyst.

In addition to the above "theoretical" arguments, there is a growing need for estimating the "collapse motion" : insurance coverage of major construction facilities is sometimes based on estimated losses under the worst possible (as opposed to probable) earthquake scenario.

(e) Several persuasive arguments could be advanced on the need *not to* disallow structural plastic "hinging" of piles:

- Yielding and cracking of piles (at various critical depths) is unavoidable with strong seismic shaking in soft soils, as the Kobe 1995 earthquake has amply revealed.

- Refuting the contrary universal belief, post-earthquake inspection of piles is often feasible (with internally placed inclinometers, borehole cameras, integrity shock testing, under-excavation with visual inspection), although certainly not a trivial operation. Again, Kobe offered numerous examples to this effect.

- The lateral confinement provided by the soil plays a very significant role in pile response, by retarding the development of high levels of localised plastic rotation, thereby providing an increase in ductility capacity. Sufficient displacement ductility may be achieved in a pile shaft with transverse reinforcement ratio as low as 0.003 (Butek et al 2004).

- The presence of soil confinement leads to increased plastic hinge lengths, thus preventing high localised curvatures (Tassios 1998). Therefore, the piles retain much of their axial load carrying capacity after yielding.

Thus, a broadly distributed plastic deformation on the pile may reduce the concentrated plastification on the structural column — so detrimental to safety.

Furthermore, when subjected to strong cyclic overturning moment, end-bearing piles in tension will easily reach their full frictional uplifting capacity. It has been shown analytically and experimentally that this does not imply failure. The same argument applies to deeply embedded (caisson) foundations.

(f) The current trend in *structural* earthquake engineering calls for a philosophical change **:** from strength-based design (involving force considerations) to performance-based design (involving displacement considerations) [Pauley 2002, Priestley et al 2000, 2003, Calvi 2007]. *Geotechnical* earthquake engineering has also been slowly moving towards performance–based seismic design**:** gravity retaining structures are indeed allowed to slide during the design earthquake. The time is therefore ripe for soil–foundation–structure interaction (SFSI) to also move from imposing "safe" limits on forces and moments acting on the foundation (aiming at avoiding pseudo-static "failure") to performance–based design in which all possible conventional "failure" mechanisms are allowed to develop, to the extent that maximum and permanent displacements and rotations are kept within acceptable limits.

3 THE CONCEPT OF "ROCKING ISOLATION" IN FOUNDATION DESIGN

The paper addresses the case of structure-foundation systems oscillating mainly in a rotational mode (rocking).

Subjected to strong seismic shaking, structures tend to experience large inertial forces. For tall-slender structures these forces will lead to overturning moments onto the foundation that may be disproportionally large compared to the vertical load. As a result, a shallow foundation may experience detachment (uplifting) of one edge from the supporting soil. This in turn will lead to increased normal stresses under the opposite edge of the foundation. Development of a bearing capacity failure mechanism is quite possible if such a concentration leads to sufficiently large stresses. But, in contrast to a static situation, even *then* failure may not occur. Thanks to the *cyclic* and *kinematic* nature of earthquake induced vibrations : (i) the inertial forces do not act *"forever"* in the same direction to cause failure (as would be the case with static load), but being cyclic, very soon reverse and thereby relieve the distressed soil; and (ii) the developing inertial forces are not externally applied predetermined loads, but are themselves reduced once the soil-foundation system reaches its (limited) ultimate resistance — the foundation system acts like a fuse.

As a result, the system experiences nonlinear-inelastic rocking oscillations, which may or may not result in excessive settlement and rotation. But failure is almost unlikely.

In the last 10 years a number of research efforts have explored the consequences of substantial foundation rocking on the response of the supported structure, theoretically and experimentally : Kutter et al 2003, Gajan et al 2005, Harden et al 2006, Kawashima et al 2007, Apostolou et al 2007, Paolucci et al 2008, Chatzigogos & Pecker 2010, Deng et al 2012. The results of these studies confirmed the idea that strongly-nonlinear rocking oscillations under seismic excitation can be of benefit to the structure.

Taking the whole idea one small step farther, it is proposed that the design of a shallow foundation should actively "invite" the creation of two simultaneous "failure" mechanisms: substantial foundation uplifting and ultimate bearing-capacity sliding. This would be accomplished by substantially under-designing the foundation — e.g., by reducing its width and length to, say, one-half of the values required with current design criteria. This can be thought of as a reversal of the "capacity" design: "plastic hinging" will take place in the foundation-soil system and not at the column(s) of the structure. Fig. 1 elucidates the main idea of Rocking Isolation. The benefits of designing the foundation to work at and beyond its conventional limits will become evident in the sequel. To this end, three examples will elucidate the dynamics of "Rocking Isolation" in comparison with the dynamics of the conventional design :

(a) a bridge pier, free to rotate at its top

(b) a two-storey two-bay asymmetric frame (MRF)

(c) a three-storey retrofitted frame–shearwall structure.

In each case, the two alternatives (the conventional and the rocking-isolated system) are subjected to numerous acceleration time histories the overall intensity of which is either within or well beyond the design earthquake levels.

4 ROTATIONAL MONOTONIC RESPONSE OF SHALLOW FOUNDATIONS

Much of the research in earlier years on dynamic rocking of foundations and dynamic soil–structure interaction had focused on linear response. Elastic stiffness and damping as functions of frequency have been developed and utilised to describe the dynamic action of the foundation system. The various US seismic codes in the last 30$^+$ years have promulgated linear approximations to deal with seismic soil–structure interaction.

The behavior of "Rocking Foundations" significantly deviates from linear visco-elasticity: uplifting introduces strong geometric nonlinearity and even damping due to impact ; soil yielding and plastic deformation generate hysteresis, implying significant frequency-independent damping, while when bearing-capacity slippage mechanisms develop a limiting plateau restricts the passage of high accelerations from the ground into the superstructure.

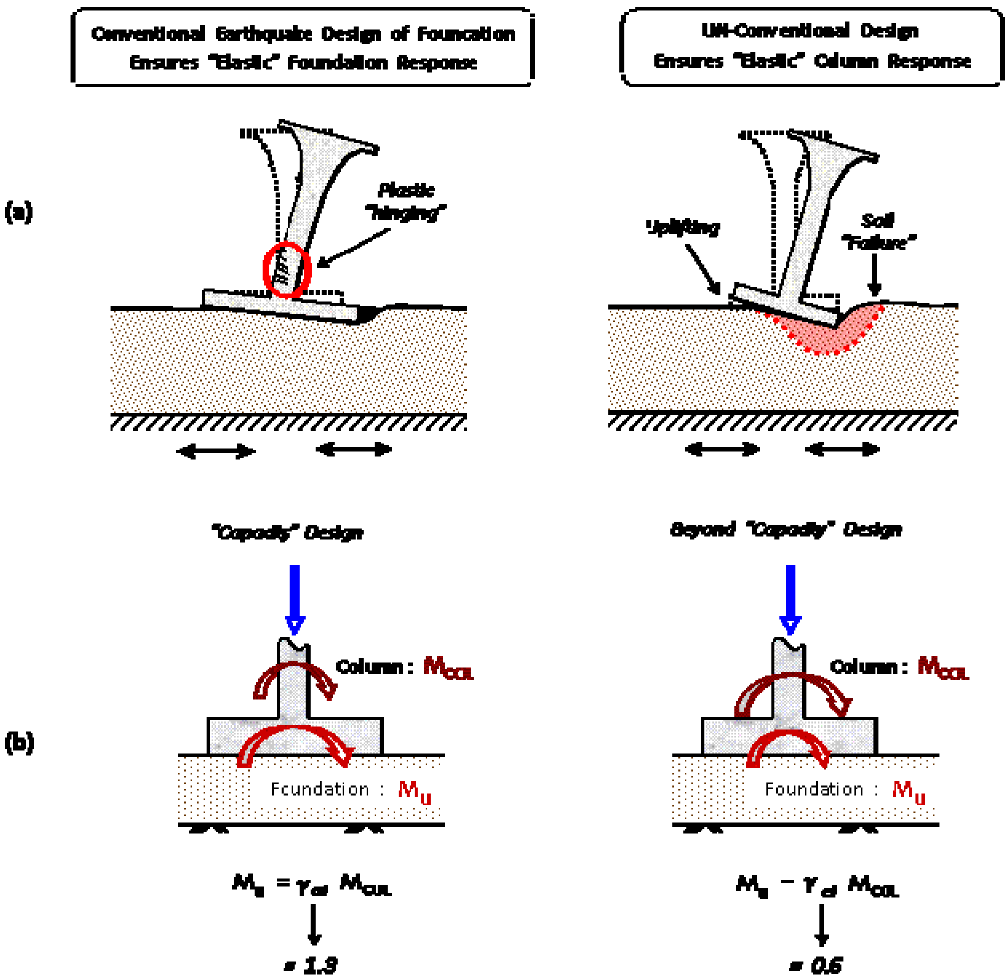

Figure 1. Conceptual illustration of *(a)* the response of a conventional and a "rocking-isolation" design of a bridge-pier foundation; and *(b)* the "capacity" design principle as conventionally applied to foundations, and its reversal in "rocking isolation".

In monotonic loading, a most crucial parameter controlling the moment–rotation, M–θ, relation of a specific foundation is the factor of safety against vertical static bearing capacity failure :

$$F_s = N_{uo}/N \qquad (1)$$

where N_{uo} is the ultimate load under purely vertical loading and N the acting vertical load. Fig. 2 offers typical results for a homogeneous (G and s_u) soil for three F_s values : a very high one (20), a low one (2), and an extremely low one (1.25). M is normalized by N_{uo} B, where B is the width of the footing in the direction of loading. This leads to curves which, for the homogeneous profile considered, depend solely on the so-called "rigidity index", $G/\ u_s$, and the shape of the footing.

Also shown in Fig. 2 are the snapshots of the deformed soil and the contours of plastic strain as they develop when the maximum moment is reached — apparently at different angles of rotation. The following are worthy of note in the figure:

- The foundation with $F_s = 20$ (which can be interpreted either as a very-lightly loaded foundation or as a "normally"-loaded foundation on very stiff soil) despite its largest initial elastic rocking stiffness fails at the smallest value of applied moment:

$$M_u \approx 0.025\ N_{uo}\ B \qquad (2a)$$

Indeed if $F_s \to \infty$, i.e. there is no vertical load onto the foundation, M_u would vanish, due to the tensionless nature of the soil–footing interface.

- As expected from the literature (Meyerhof 1963, Georgiadis and Butterfield 1988, Salençon and Pecker 1995, Allotey and Naggar 2003, Apostolou and Gazetas 2005, Gajan and Kutter 2008, Chatzigogos et al. 2009, Gouvernec 2009, Gajan and Kutter 2008) the largest maximum moment is attained by the $F_s = 2$ footing :

$$M_u \approx 0.13\ N_{uo}\, B \qquad (2b)$$

but its elastic initial rocking stiffness is smaller than for the $F_s = 20$ foundation. Evidently, the extensive plastic deformations upon the application of the vertical (heavy) load soften the soil so that a small applied moment meets less resistance — hence lower stiffness. However, $F_s = 2$ achieves the largest ultimate M_u as it leads to an optimum combination of uplifting and bearing-capacity mobilization.

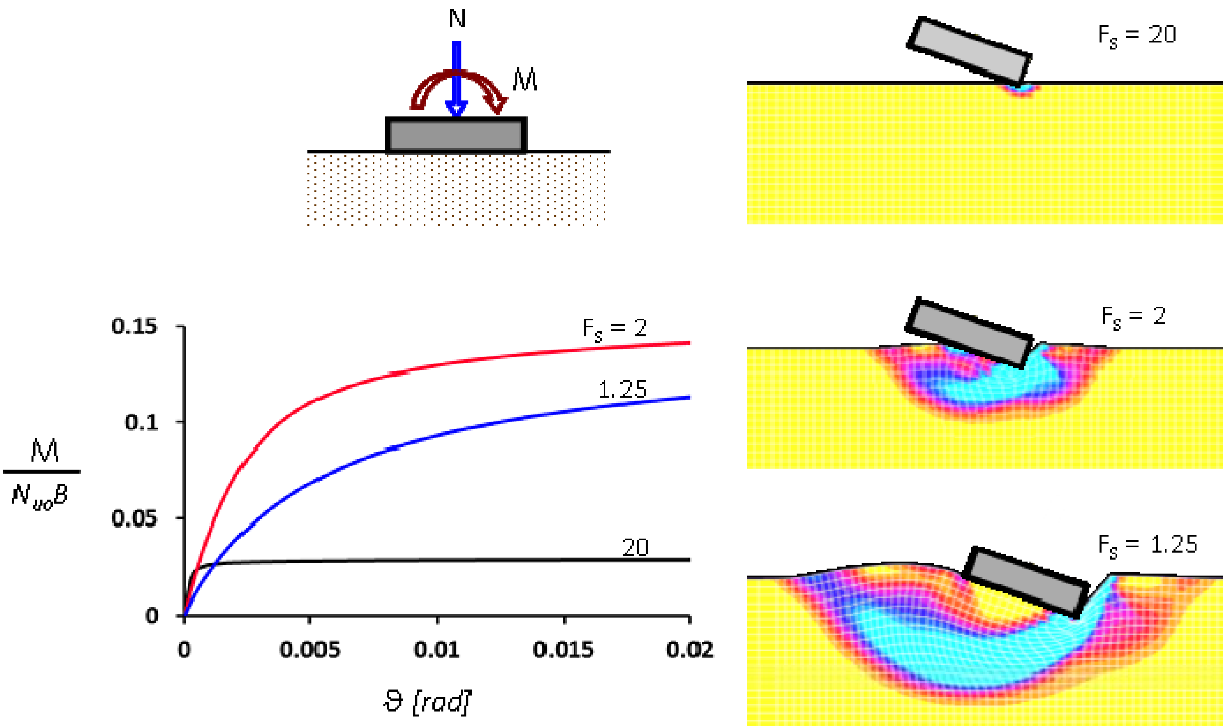

Figure 2. Typical moment–rotation relations of three foundations and corresponding snapshots of their ultimate response with the contours of plastic deformation. The only difference between foundations : their static factor of safety.

- A more severely loaded foundation, however, with the (rather unrealistic) $F_s = 1.25$ will only enjoy an even smaller initial stiffness and a smaller ultimate moment than the $F_s = 2$ foundation. Notice that in this case no uplifting accompanies the plasticification of the soil.

The failure envelope (also called interaction diagram) in N-M space is given in Fig. 3 for the specific example. It was obtained with the same numerical (FE) analysis as the curves and snapshots of Fig. 2, and can be expressed analytically as a function of the static factor of safety (F_S) as

$$M_u = \frac{1}{2F_S}\left(1-\frac{1}{F_S}\right)N_{uo}B \qquad (3)$$

The specific plot is in terms of N/N_{uo} which is $1/F_s$ which ranges between 0 and 1. Notice that heavily and lightly loaded foundations with $1/F_s$ symmetrically located about the $1/F_s = 0.5$ value where the M_u is the largest, have the same moment capacity : yet their behavior especially in cyclic loading is quite different as will be shown subsequently.

5 MONOTONIC RESPONSE ACCOUNTING FOR P–δ EFFECTS

An increasingly popular concept in structural earthquake engineering is the so-called *"pushover"* analysis. It refers to the nonlinear lateral force-displacement relationship of a particular structure subjected to monotonically increasing loading up to failure. The development (theoretical or experimental) of such pushover relationships has served as a key in simplified dynamic response analyses that estimate

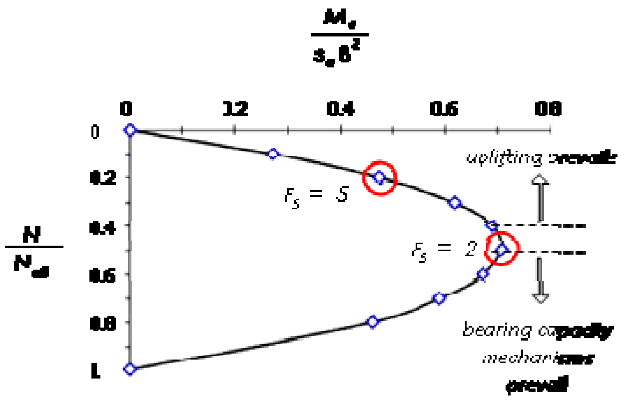

Figure 3. Dimensionless N_u – M_u failure envelope for strip foundation

seismic deformation demands and their ultimate capacity. We apply the pushover idea to a shallow foundation supporting an elevated mass, which represents a tall slender structure with $h/B = 2$ (or "slenderness" ratio $h/b = 4$, *where* $b = B/2$). This mass is subjected to a progressively increasing horizontal displacement until failure by overturning. Since our interest at this stage is only in the behavior of the foundation, the structural column is considered absolutely rigid. The results are shown in Fig: 4(a) and (b) for two F_s values : 5 and 2.

The difference in the *M-θ* response curves from those of Fig. 2 stems from the so-called P-δ effect. As the induced lateral displacement of the mass becomes substantial its weight induces an additional aggravating moment, $mgu = mg\theta h$, where θ is the angle of foundation rotation. Whereas before the ultimate moment M_u is reached the angles of rotation are small and this aggravation is negligible, its role becomes increasingly significant at larger rotation and eventually becomes crucial in driving the system to collapse. Thus, the (rotation controlled) *M-θ* curve decreases with θ until the system topples at an angle θ_c. This critical angle for a rigid structure on a rigid base $(F_S = \infty)$ is simply :

$$\theta_{c,\infty} = \arctan(b/h) \tag{4}$$

where b = the foundation halfwidth. For very slender systems the approximation

$$\theta_{c,\infty} = \approx (b/h) \tag{4a}$$

is worth remembering.

As the static vertical safety factor (F_S) diminishes, the rotation angle (θ_c) at the state of imminent collapse ("critical" overturning rotation) also slowly decreases. Indeed, for rocking on compliant soil, θ_c is always lower than it is on a rigid base (given with **Eq. 4**). For stiff elastic soil (or with a very large static vertical safety factor) θ_c is imperceptibly smaller than that given by Eq. 4, because the soil deforms slightly, only below the (right) edge of the footing, and hence only insignificantly alters the geometry of the system at the point of overturning. As the soil becomes softer, soil inelasticity starts playing a role in further reducing θ_c. However, such a reduction is small as long as the factor of safety (F_S) remains high (say, in excess of 3). Such behaviour changes drastically with a very small F_S: then the soil responds in strongly inelastic fashion, a symmetric bearing-capacity failure mechanism under the vertical load N is almost fully developed, replacing uplifting as the prevailing mechanism leading to collapse θ_c tends to zero.

The following relationship has been developed from FE reults by Kourkoulis et al, 2012, for the overturning angle $\theta_c = \theta_c(F_s)$:

$$\frac{\theta_c}{\theta_{c,\infty}} \approx \left(1 - \frac{1}{F_S}\right) + \frac{1}{3}\left[1 - \frac{\log h}{B}\right]\frac{1}{\sqrt{F_s}} \tag{5}$$

6 CYCLIC RESPONSE ACCOUNTING FOR P–δ EFFECTS

Slow cyclic analytical results are shown for the two aforementioned systems having static factors of safety (F_S = 5 and 2). The displacement imposed on the mass center increased gradually; the last cycle persisted until about 4 or 5 times the angle θ_u of the maximum resisting moment. As can be seen in the moment–rotation diagrams, the loops of the cyclic analyses for the safety factor $F_S = 5$ are well enveloped by the monotonic pushover curves in Figure 7(a). In fact, the monotonic and maximum cyclic curves are indistinguishable. This can be explained by the fact that the plastic deformations that take place under the edges of the foundation during the deformation-controlled cyclic loading are too small to affect to any appreciable degree of response of the system when the deformation alters direction. As a consequence, the residual rotation almost vanishes after a complete set of cycles — an important (and desirable) characteristic. The system largely rebounds, helped by the restoring role of the weight. A key factor of such behaviour is the rather small extent of soil plastification, thanks to the light vertical load on the foundation.

The cyclic response for the F_S = 2 system is also essentially enveloped by the monotonic pushover curves. However, there appears to be a slight overstrength of the cyclic "envelope" above the monotonic curve. For an explanation see Panagiotidou et al, 2012.

But the largest difference between monotonic and cyclic, on one hand, and $F_S = 2$ and 5, on the other, is in the developing settlement. Indeed, monotonic loading leads to monotonically-upward movement ("heave") of the center of the $F_S = 5$ foundation, and slight monotonically-downward movement ("settlement") of the $F_S = 2$ foundation. Cyclic loading with F_S = 5 produces vertical movement of the footing which follows closely its monotonic upheaval.

But the $F_S = 5$ foundation experiences a progressively accumulating settlement — much larger that its monotonic settlement would have hinted at. The hysteresis loops are now wider. Residual rotation may appear upon a full cycle of loading, as inelastic deformations in the soil are now substantial.

The above behavior is qualitatively similar to the results of centrifuge experiments conducted at the University of California at Davis on sand and clay (e.g., Kutter et al. 2003, Gajan et al. 2005) large-scale tests conducted at the European Joint Research Centre, (Negro et al. 2000, Faccioli et al. 1998), and 1-g Shaking Table tests in our laboratory at the National Technical University of Athens on sand (Anastasopoulos et al 2011, 2013, Drosos et al 2012).

In conclusion, the cyclic moment–rotation behavior of foundations on clay and sand exhibits to varying degrees three important characteristics with increasing number of cycles :

- no "strength" degradation (experimentally verified).
- sufficient energy dissipation — large for small F_S values, smaller but still appreciable for large ones. (Loss of energy due to impact will further enhance damping in the latter category, when dynamic response comes into play.)
- relatively low residual drift especially for large FS values — implying a *re-centering* capability of the rocking foundation.

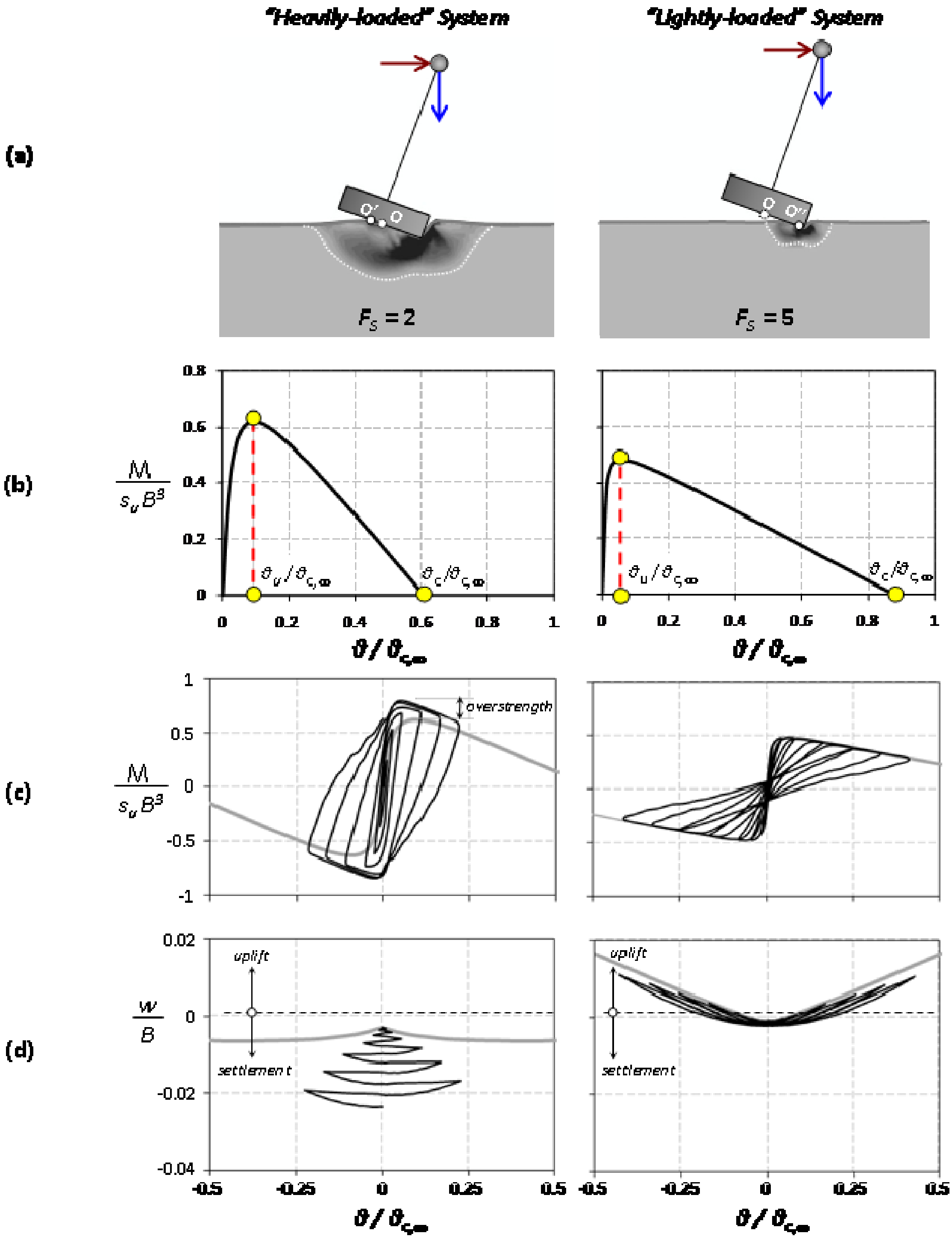

Figure 4. Comparison of two slender systems (differing only in F_S) subjected to monotonic and cyclic loading: *(a)* deformed mesh with plastic strain contours at ultimate state; *(b)* dimensionless monotonic moment–rotation response; *(c)* cyclic moment–rotation response; and *(d)* cyclic settlement–rotation response (the grey line corresponds to the monotonic backbone curves).

These positive attributes not only help in explaining the favorable behavior of "Rocking Foundation", but also enhance the reliability of the geotechnical design.

7 SEISMIC RESPONSE OF BRIDGE PIER ON SHALLOW FOUNDATION

The concept of "Rocking Isolation" is illustrated in Fig. 5 by comparing the response of a 12 m tall bridge pier carrying a deck of four lanes of traffic for a span of about 35 m — typical of elevated highways around the world.

The bridge chosen for analysis is similar to the Hanshin Expressway Fukae bridge, which collapsed spectacularly in the Kobe 1995 earthquake. The example bridge is designed in accordance to (EC8 2000) for a design acceleration A = 0.30 g, considering a (ductility-based) behavior factor q = 2. With an elastic (fixed-base) vibration period T = 0.48 sec the resulting design bending moment $M_{COL} \approx$ 45 MNm.

The pier is founded through a square foundation of width B on an idealized homogeneous 25 m deep stiff clay layer, of undrained shear strength s_u = 150 kPa (representative soil conditions for which a surface foundation would be a realistic solution). Two different foundation widths are considered

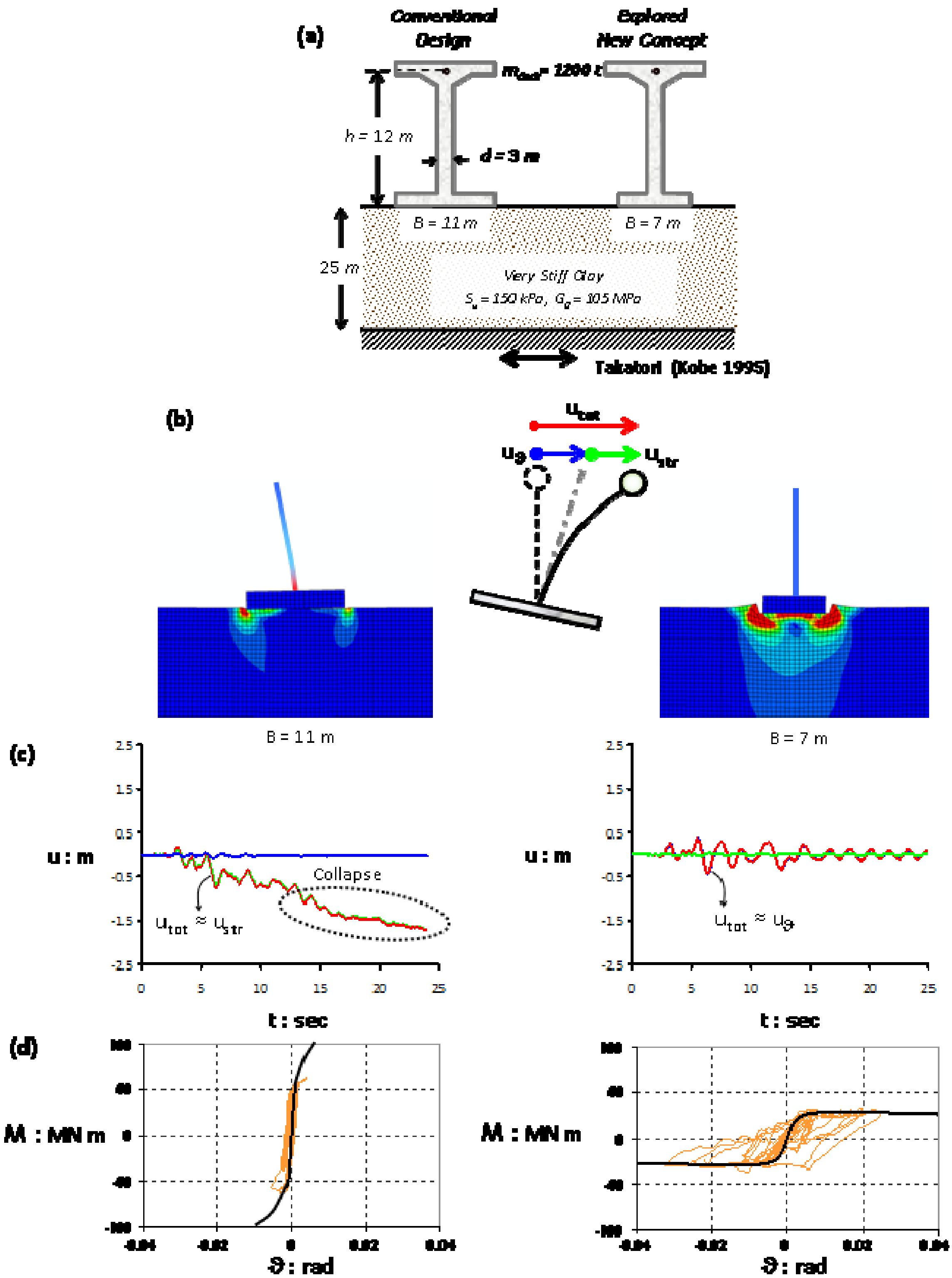

Figure 5. *(a)* Two bridge piers on two alternative foundations subjected to a large intensity shaking, exceeding the design limits; *(b)* deformed mesh with superimposed plastic strain, showing the location of "plastic hinging" at ultimate state; *(c)* time histories of deck drift; *(d)* overturning moment–rotation (M–θ) response of the two foundations.

to represent the two alternatives design approaches. A large square foundation, B = 11 m, is designed in compliance with conventional capacity design, applying an over-strength factor γ_{Rd} = 1.4 to ensure that the plastic "hinge" will develop in the superstructure (base of pier). Taking account of maximum allowable uplift (eccentricity $e = M / N < B/3$, where N is the vertical load), the resulting safety factors for static and seismic loading are F_S = 5.6 and F_E = 2.0, respectively. A smaller, under-designed, B = 7 m foundation is considered in the spirit of the new design philosophy. Its static safety factor F_S= 2.8, but it is designed applying an "*understrength*" factor $1/1.4 \approx 0.7$ for seismic loading. Thus, the resulting safety factor for seismic loading is lower than 1.0 ($F_E \approx 0.7$).

The seismic performance of the two alternatives is investigated through nonlinear FE dynamic time history analysis. An ensemble of 29 real accelerograms is used as seismic excitation of the soil–foundation–structure system. In all cases, the seismic excitation is applied at the bedrock level. Details about the numerical models and the requisite constitutive relations can be seen in Anastasopoulos et al, 2010, 2011.

Results are shown here only for a severe seismic shaking, exceeding the design limits: the Takatori accelerogram of the 1995 M_{JMA} 7.2 Kobe earthquake. With a direct economic loss of more than $100 billion, the Kobe earthquake needs no introduction. Constituting the greatest earthquake disaster in Japan since the 1923 M_s = 8 Kanto earthquake, it is simply considered as one of the most devastating earthquakes of modern times. Of special interest is the damage inflicted to the bridges of Hanshin Expressway, which ranged from collapse to severe damage. The aforementioned bridge chosen for our analysis is very similar to the Fukae section of Hanshin Expressway, 630 m of which collapsed during the earthquake of 1995. It is therefore logical to consider this as a reasonably realistic example of an "*above the limits*" earthquake. In particular, the Takatori record constitutes one of the worst seismic motions ever recorded : PGA = 0.70 g, PGV = 169 cm/s, bearing the "mark" of forward rupture directivity and of soil amplification.

Fig. 5 compares the response of the two alternatives, in terms of deformed mesh at the end of shaking with superimposed the plastic strains. In the conventionally designed system there is very little inelastic action in the soil; the red regions of large plastic deformation are seen only under the severely "battered" edges of the rocking foundation — but without extending below the foundation. "Plastic hinging" forms at the base of the pier, leading to a rather intense accumulation of curvature (deformation scale factor = 2).The P–δ effect of the mass will further aggravate the plastic deformation of the column, leading to collapse.

In stark contrast, with the new design scheme the "plastic hinge" takes the form of mobilization of the bearing capacity failure mechanisms in the underlying soil, leaving the superstructure totally intact. Notice that the red regions of large plastic shearing are of great extent, covering both half-widths of the foundation and indicating alternating mobilization of the bearing capacity failure mechanisms, left and right.

The above observations are further confirmed by the time history of deck drift shown in Fig. 5(c). The two components of drift, are shown, one due to footing rotation in blue and one due to structural distortion in green. Their sum is shown in red. Evidently, the conventional design experiences essentially only structural distortion which leads to uncontrollable drifting — collapse. In marked contrast, the system designed according to the new philosophy easily survives. It experiences substantial *maximum* deck drift (about 40 cm), almost exclusively due to foundation rotation. Nevertheless, the *residual* foundation rotation leads to a tolerable 7 cm deck horizontal displacement at the end of shaking.

Fig. 5(d) further elucidates the action of the foundation-soil system. The M-θ relationship shows for the 11m^2 foundation a nearly linear viscoelastic response, well below its ultimate capacity and apparently with no uplifting. On the contrary, the 7m^2 (under-designed) foundation responds well past its ultimate moment capacity, reaching a maximum *θ ≈ 30 mrad*, generating hysteretic energy dissipation, but returning almost to its original position, i.e. with a negligible residual rotation.

However, energy dissipation is attained at a cost : increased foundation settlement. While the practically elastic response of the conventional (*over-designed*) foundation leads to a minor 4 cm settlement, the *under-designed* foundation experiences an increased accumulated 15 cm settlement. Although such settlement is certainly not negligible, it can be considered as a small price to pay to avoid collapse under such a severe ground shaking.

Perhaps not entirely fortuitously, the residual rotation in this particular case turned out to be insignificant. The re-centering capability of the design certainly played some role in it.

8 SEISMIC RESPONSE OF TWO–STOREY TWO BAY ASYMMETRIC FRAME

The frame of Fig. 6 was structural designed according to EC8 for an effective ground acceleration A = 0.36 g and ductility-dependent "behavior" factor q = 3.9. The soil remains the stiff clay of the previous example. Two alternative foundation schemes are shown in the figure.

The conventionally *over-designed* footings can mobilize a maximum moment resistance M_u from the underlying soil, larger than the bending moment capacity of the corresponding column M_{COL} . For static vertical loads, a factor of safety $F_S \geq 3$ is required against bearing capacity failure. For seismic load combinations, a factor of safety $F_E = 1$ is acceptable. In the latter case, a maximum allowable eccentricity criterion is also enforced: $e = M/N \leq B/3$. For the investigated soil–structure system this eccentricity criterion was found to be the controlling one, leading to minimum required footing widths B = 2.7 m, 2.5 m and 2.4 m for the left, middle, and right footing, respectively. Bearing capacities and safety factors are computed according to the provisions of EC8, which are basically similar to those typically used in foundation design practice around the world.

The *under-sized* footings of the rocking isolation scheme, are "weaker" than the superstructure, guiding the plastic hinge to or below the soil–footing interface, instead of at the base of the columns. The small width of the footings promotes full mobilization of foundation moment capacity with substantial uplifting. The eccentricity criterion is completely relaxed, while $F_E < 1$ is allowed. The static $F_S \geq 3$ remains a requirement as a measure against uncertainties regarding soil strength. Moreover, it turns out that $F_S \geq 4$ might be desirable in order to promote uplifting–dominated response, and thereby limit seismic settlements [Kutter et al. 2003, Faccioli et al. 2001,Pecker & Pender 2000, Kawashima et al. 2007, Chatzigogos et al. 2009; Panagiotidou et al. 2012]. Applying the methodology which has been outlined in Gelagoti et al. 2012, the footings were designed to be adequately small to promote uplifting, but large enough to limit the settlements. Aiming to minimize differential settlements stemming from asymmetry, the three footings were dimensioned in such a manner so as to have the same F_S. Based on the above criteria, the resulting footing widths for the rocking–isolated design alternative are B = 1.1 m, 1.8 m, and 1.3 m, for the left, middle, and right footing, respectively: indeed, substantially smaller than those of the code-based design. Footing dimensions and static factors of safety against vertical loading of the two designs are summarized in Table 1.

Table 1. Footing dimensions and corresponding factors of safety (computed following the provisions of EC8) against vertical loading for the seismic load combination (G + 0.3Q) for the two design alternatives of Fig. 6.

Conventional Design			*Rocking Isolation*		
Footing	B (m)	F_S	Footing	B (m)	F_S
Left	2.7	32.6	Left	1.1	5.4
Middle	2.5	10.6	Middle	1.8	5.4
Right	2.4	18.1	Right	1.3	5.4

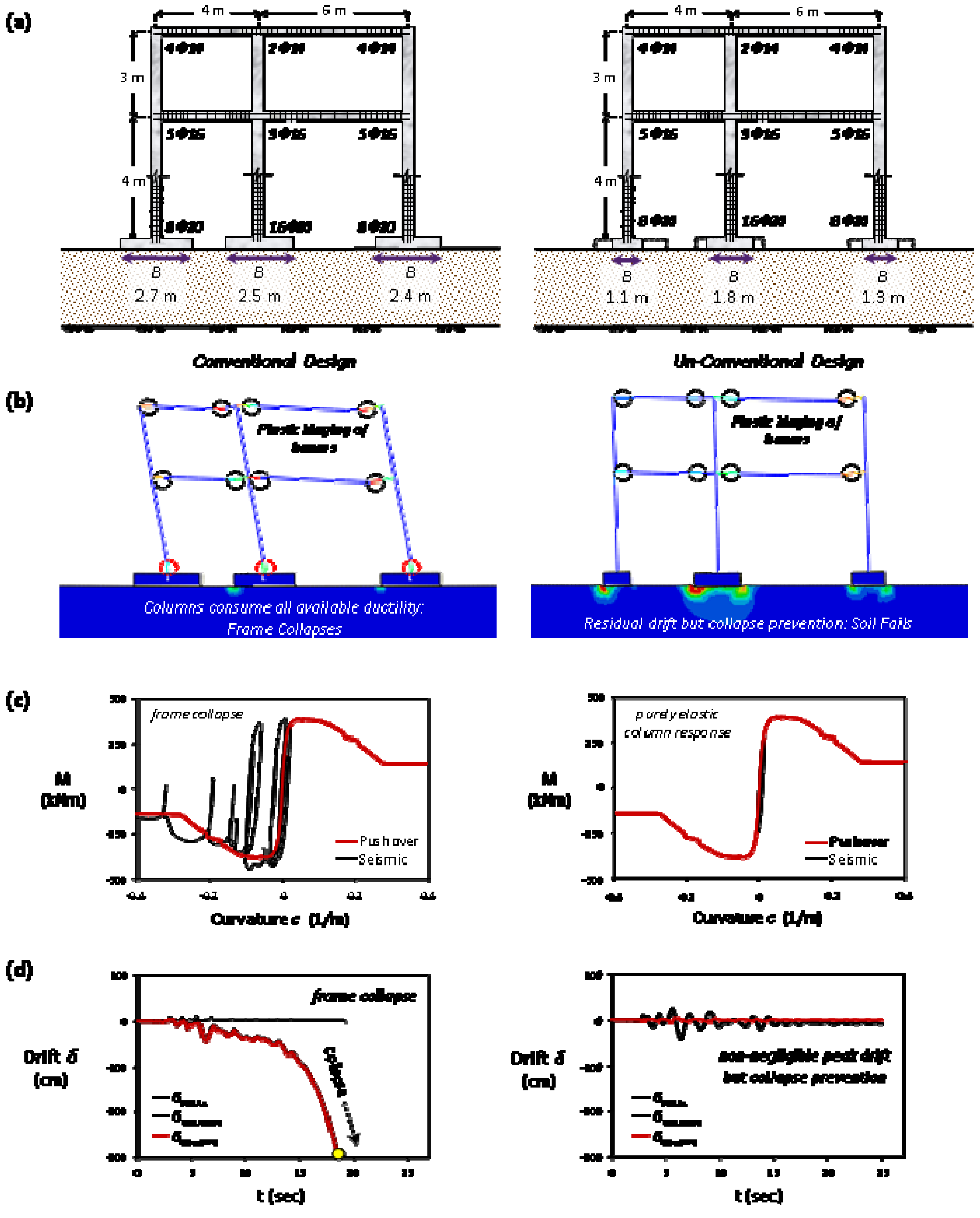

Figure 6. *(a)* Two building frames on two alternative foundation subjected to a large intensity earthquake, exceeding the design limits; *(b)* deformed mesh with superimposed plastic strain, showing the location of "plastic hinging" at ultimate state; *(c)* bending moment–curvature response of the central columns; *(d)* overturning moment–rotation (M–θ) response of the two central foundations.

The performance of the two design alternatives is compared in Fig. 6. The deformed mesh with superimposed plastic strain contours of the two alternatives is portrayed on top (Fig. 6a). With the relentless seismic shaking of the Takatori motion, the conventionally designed frame collapses under its gravity load (due to excessive drift of the structure, the moments produced by *P–δ* effects cannot be sustained by the columns, leading to loss of stability and total collapse). As expected, plastic hinges firstly develop in the beams and subsequently at the base of the three columns, while soil under the footings remains practically elastic. The collapse is also evidenced by the substantial exceedance of the available curvature ductility of the columns (Fig. 6b). Conversely, the rocking–isolated frame withstands the shaking, with plastic hinging taking place only in the beams, leaving the columns almost unscathed (moment-curvature response: elastic). Instead, plastic hinging now develops within the underlying soil in the form of extended soil plastification (indicated by the red regions under the foundation. The time histories of inter-storey drift further elucidate the aforementioned behavior of the two design alternatives (Fig. 6d).

Thanks to the larger bending moment capacity of the column than of the footing, damage is guided "below ground" and at the soil–foundation interface in the form of detachment and uplifting — evidenced in Fig. 6d by the zero residual rotation, unveiling the re-centering capability of the under-designed foundation scheme.

The price to pay: large accumulated settlements. Moreover, despite the fact that the three footings have been dimensioned to have the same static factor of safety F_S (in an attempt to minimize differential settlements exacerbated from asymmetry), the central footing settles more than the two side footings, leading to a differential settlement of the order of 3 cm. The difference in the settlement stems of course from their differences in width. As previously discussed, the central footing was made larger (B = 1.8 m, compared to 1.1 m and 1.3 m of the two side footings) in order to maintain the same F_S. Since the latter is common for the three footings, if the loading is more-or-less the same, their response should be similar. However, such equivalence refers to dimensionless quantities, not absolute values [see Kourkoulis et al., 2012b]. In other words, while the three footings sustain almost the same dimensionless settlement w/B, which is roughly equal to 0.025 (≈ 3 cm/1.2 m) for the two side footings and 0.033 (≈ 6 cm/1.8 m) for the central one, the latter is substantially larger in width and hence its settlement is larger in absolute terms. Naturally, the three footings are not subjected to exactly the same loading, something which further complicates the response. Such differential settlements may inflict additional distress in the superstructure, and are therefore worthy of further investigation.

9 THREE–STOREY FRAME RETROFITTED WITH SHEAR–WALL

The results presented now are not from numerical analysis as the previous one, but from Shaking Table experiments. They refer to a 3-storey two-bay frame which was designed according to the pre-1970 seismic regulations, for a base shear coefficient of 0.06. Because of the small value of this coefficient and the otherwise inadequate design, the frame has columns of cross-section 25 x 25 cm^2 and beams 25 x 50 cm^2 resulting in a strong beam–weak column system. Naturally, it fails by first "soft-story" type of collapse when excited by motions corresponding to today's codes with effective ground accelerations of the order of 0.30g and more. To upgrade the frame, a strong and stiff Shear Wall 1.5 m x 0.3 m in cross-section is constructed replacing the middle column, as shown in Fig. 7.

The 1:10–scale model is supported on dense fine–grained $D_r \approx 80\%$ sand. The original footings of all three columns were 1.5 m square. For the retrofitted frame the two columns retained their original 1.5 x 1.5m^2 footings. The foundation of the Shear Wall (SW) is of special geotechnical interest : due to its disproportionately large lateral stiffness the SW tends to attract most of the seismically induced shear force and hence to transmit onto the foundation a large overturning moment. By contrast, its vertical load is relatively small. To meet the eccentricity limit e = M/N < B/3, a large foundation 6.0m x 0.80 m is thus necessary. Hence, the conventional solution of Fig. 8. Of course the resulting vertical bearing-capacity factor of safety is unavoidably large, $F_S \cong 10$, and the seismic apparent factor of safety against moment bearing-capacity is also far more than adequate : $F_E = 2$.

The decision to reduce the footing width to merely B = 3.5 m is not only economically favorable, but in the harsh reality of old buildings it may often be the only feasible decision in view of the usual space limitations due to pipes, small basements, walls, etc, present in the base. We will see if it is also favorable technically in resisting a strong seismic shaking.

To be practical, in the above sense, no change is made to the column footings. (1.5 m square).

We subject all three structures [i.e., "a" the original frame, "b" the retrofitted with a SW founded on conventionally-conservative footing, and "c" the retrofitted with the underdesigned SW footing] to a number of strong ground excitations. Frame "a" easily fails as sketched in Fig. 8, where the physical collapse was artificially prevented by an external protective barrier in the Shaking Table experiment. The conventionally retrofitted SW-frame "b" could withstand most excitations. But with some of the strongest motions it developed substantial plastification at its base and led to residual top drift of an unacceptable 8%.

The unconventionally–founded system "c" behaved much better with residual top drift of merely 2%.

Figure 8 sketches the deformation pattern of the three systems while Fig. 7 plots the time histories of structural –distortion and foundation–rotation induced top drift ratio. It is seen that not only is the total drift of the Rocking-Isolated system only 2% but at least half of it is solely due to foundation rotation, rather than damage to the SW.

The penalty to pay is the increased settlement (1.5 cm rather 0.8 cm) which nevertheless in this particular case would be acceptable for most applications.

10 CONCLUSIONS

(a) Current seismic design practice leads most often to very conservative foundation solutions. Not only are such foundations un-economical but are sometimes difficult to implement. Most significantly : they are agents of transmitting large accelerations up to the superstructure. The ensuing large inertial forces send back in "return" large overturning moments (and shear forces) onto the foundation — a vicious circle.

(b) On the contrary, seriously under-designed foundations limit the transmitted accelerations to levels proportional to their (small) ultimate moment capacity. This leads to much safer superstructures. In earthquake engineering terminalogy the plastic "hinging" moves from the columns to the foundation-soil system, preventing dangerous structural damage.

(c) For tall-slender systems that respond seismically mainly in rocking, underdesigning the footings "invites" strong uplifting and mobilization of bearing capacity failure mechanisms. It turns out that the statically determined ultimate moment resistance is retained without degradation during cyclic loading, at least for the few numbers of cycles of most events — hence the geotechnical reliability in such a design. Moreover, the cyclic response of such foundations reveals that the amount of damping (due to soil inelasticity and uplifting–retouching impacts) is appreciable, if not large, while the system has a fair re-centering capability. These are some of the secrets of their excellent performance.

(d) The key variable in controlling the magnitude of uplifting versus the extent of bearing–capacity yielding is the static factor of safety F_S against vertical bearing–capacity failure. The designer may for example, choose to intervene in the subsoil to increase F_S and hence enhance uplifting over soil inelasticity. Such intervention need only be of small vertical extent, thanks to the shallow dynamic "pressure bulb" of a rocking foundation.

(e) In classical geotechnical engineering, avoiding bearing capacity failure at any cost is an unquestionably prudent goal. Seismic "loading" is different — it is not even loading, but an imposed displacement. Sliding mechanisms develop under the footing momentarily and hence alternatingly, and may only lead to (increased) settlement. It would be the

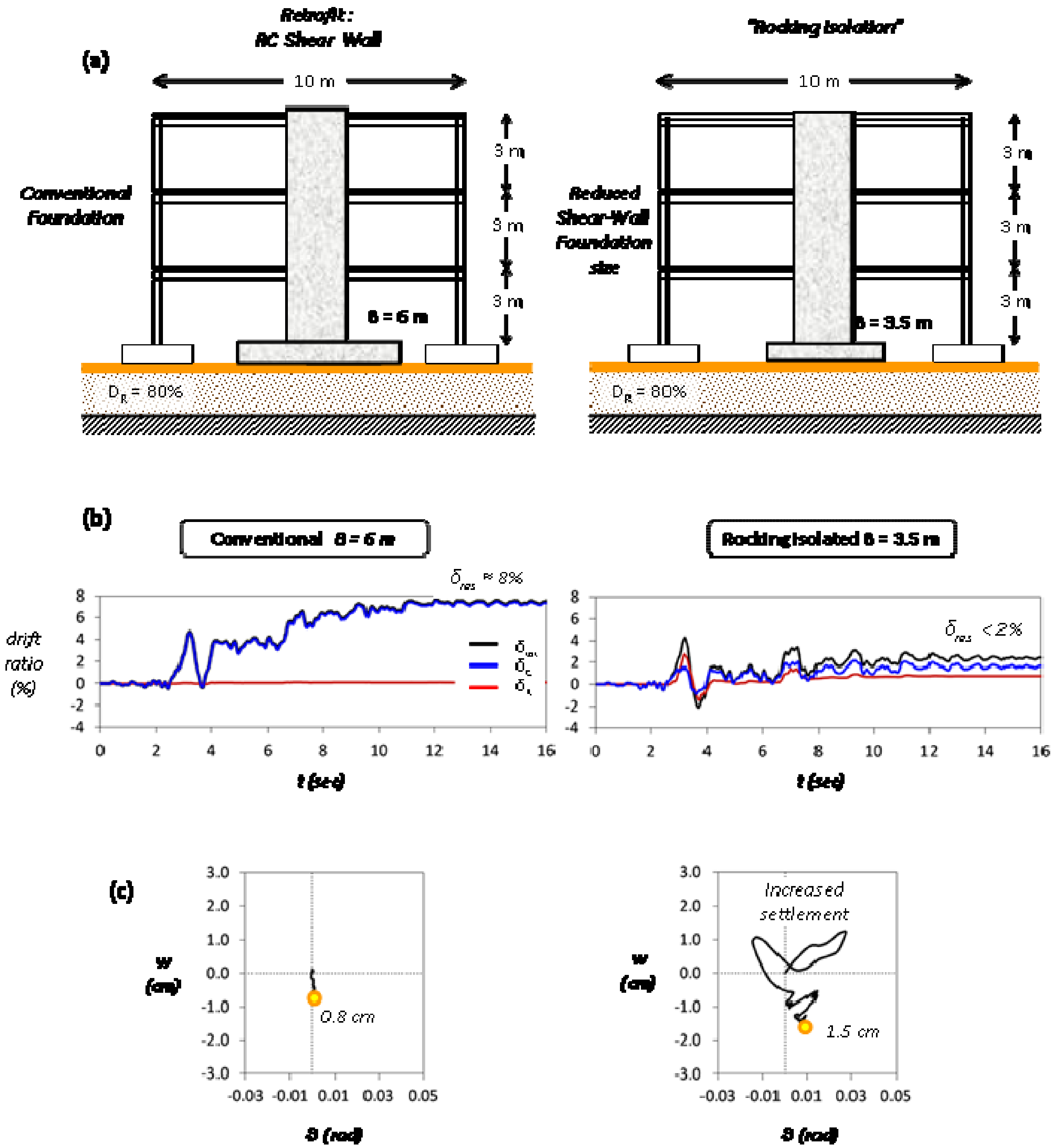

Figure 7. *(a)* Old frame retrofitted with stiff Shear Wall on two different foundations — conventional B = 6 m and unconventional B = 3.5 m; *(b)* time histories on top floor drift ratio; *(c)* settlement–rotation curves of the Shear Wall footings

task of the engineer to "accommodate" such settlements with proper design.

The results and conclusions of this paper are in harmony with the numerous experimental and theoretical findings of Professor Bruce Kutter and his coworkers at U.C. Davis, and of Professors Alain Pecker and Roberto Paolucci and their coworkers in Paris and Milano.

11 ACKNOWLEDGMENTS

The financial support for the work outlined in this paper has been provided through the research project "DARE", funded by the European Research Council (ERC), "IDEAS" Programme in Support of Frontier Research. Contract/number ERC–2–9–AdG228254–DARE.

12 REFERENCES – BIBLIOGRAPHY

Allotey N., El Naggar M.H. 2003. Analytical moment–rotation curves for rigid foundations based on a Winkler model. *Soil Dynamics and Earthquake Engineering,* 23, 367–381.

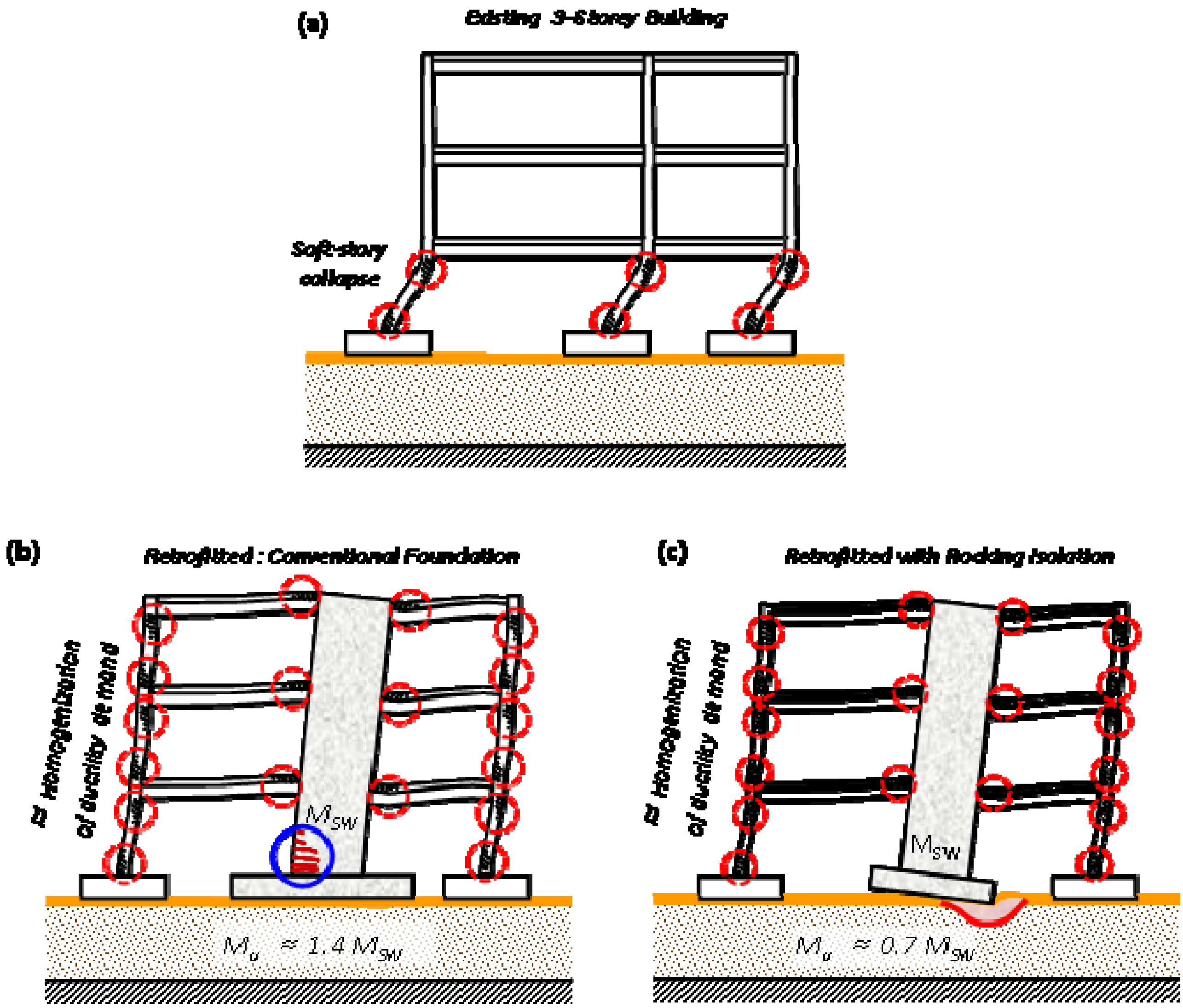

Figure 8. Sketches of damaged states of the three structures.

Allotey N., El Naggar M.H. 2007. An investigation into the Winkler modeling of the cyclic response of rigid footings, *Soil Dynamics and Earthquake Engineering,* 28, 44–57.

Anastasopoulos I., Gazetas G., Loli M., Apostolou M, Gerolymos N., 2010. Soil Failure can be used for Seismic Protection of Structures. *Bulletin of Earthquake Engineering*, 8, 309–326.

Anastasopoulos I., Gelagoti F., Kourkoulis R., Gazetas G. 2011. Simplified Constitutive model for Simulation of Cyclic Response of Shallow Foundations: Validation against Laboratory Tests. *Journal of Geotechnical and Geoenvironmental Engineering*, ASCE, 137(12), 1154-1168.

Anastasopoulos I. 2010. Beyond conventional capacity design : towards a new design philosophy. *Soil–Foundation–Structure Interaction*, Orense R.P., Chouw N., Pender M.J. (editors), CRC Press, Taylor & Francis Group : New York.

Anastasopoulos I., Georgarakos T., Drosos V., Giannakos S., and Gazetas G. 2009b. Towards a reversal of seismic capacity design: Part B, Shaking-table testing of bridge pier-foundation system. *Proceedings of the 3rd Greece-Japan Workshop on Seismic Design, Observation, and Retrofit of Foundations*, National Technical University of Greece, Santorini, 407–419.

Anastasopoulos I., Loli M., Georgarakos T., and Drosos V. 2013. Shaking Table Testing of Rocking−isolated Bridge Piers. *Journal of Earthquake Engineering,* 17(1), 1-32.

Aoi S., Kunugi T., Suzuki W., Morikawa N., Nakamura H., Pulido N., Shiomi K., and Fujiwara H. 2011. Strong motion characteristics of the 2011 Tohoku-oki earthquake from K-NET and KiK-NET. *SSA Annual Meeting*, 2011.

Apostolou, M., and Gazetas, G. 2005. Rocking of foundations under strong shaking: Mobilisation of bearing capacity and displacement demands. *1st Greece-Japan Workshop on Seismic Design, Observation, Retrofit of Foundations*, 11–12 October, 2005, Athens, Greece.

Apostolou M., Gazetas G., and Garini E. 2007. Seismic response of slender rigid structures with foundation uplifting, *Soil Dynamics and Earthquake Engineering* 27, 642–654.

Bartlett P. E., 1976. *Foundation Rocking on a Clay Soil*. ME thesis, Report No. 154, School of Engineering, University of Auckland, New Zealand.

Bienen B., Gaudin C., & Cassidy M.J. 2007. Centrifuge tests of shallow footing behavior on sand under combined vertical-torsional loading. *Int. J. Physical Modeling in Geotechnics*, 2, 1-21.

Borja R.I., Wu W.H., Amies A.P., Smith H.A. 1994. Nonlinear lateral, rocking, and torsional vibration of rigid foundations. *Journal of Geotechnical Engineering*, ASCE, 120(3), 491–513.

Borja R.I., Wu W.H., and Smith H.A. 1993. Nonlinear response of vertically oscillating rigid foundations. *Journal of Geotechnical Engineering* 119, 893–911.

Bransby M.F., Randolph M.F. 1998. Combined loading of skirted foundations. *Géotechnique*, 48(5), 637-655.

Butterfield R., Gottardi G. 1994. A complete three–dimensional failure envelope for shallow footings on sand. *Géotechnique*, 44(1), 181-184.

Chang B.J, Raychowdhury P., Hutchinson T., Thomas J., Gajan S. & Kutter B.L. 2006. Centrifuge testing of combined frame-wall-foundation structural systems. *Proc. 8th US National Conference on Earthquake Engineering*, April 18–22, San Francisco, CA, paper No. 998.

Chatzigogos C.T., Pecker A., and Salençon J. 2009. Macroelement modeling of shallow foundations. *Soil Dynamics and Earthquake Engineering* 29(5), 765–781.

Chen X.C., and Lai Y.M. 2003. Seismic response of bridge piers on elastic-plastic Winkler foundation allowed to uplift. *Journal of Sound Vibration* , 266, 957–965.

Chopra A.K., and Yim C.S. 1984. Earthquake response of structures with partial uplift on Winkler foundation, *Earthquake Engineering and Structural Dynamics,* 12, 263–281.

Crémer C., Pecker A., Davenne L. 2001. Cyclic macroelement for soil–structure interaction: material and geometrical nonlinearities. *International Journal for Numerical and Analytical methods in Geomechanics*, 25(12), pp. 1257–1284.

Cremer C., Pecker A., and Davenne L. 2002. Modeling of nonlinear dynamic behaviour of a shallow strip foundation with macro-element. *Journal of Earthquake Engineering* 6, 175–211.

Dobry R., and Gazetas G. 1986. Dynamic response of arbitrarily–shaped foundations, *Journal of Geotechnical Engineering* **113**, 109–135.

Drosos V., Georgarakos P., Loli M., Zarzouras O., Anastasopoulos I., Gazetas G. 2012. Soil–Foundation–Structure Interaction with Mobilization of Bearing Capacity : An Experimental Study of Sand. *Journal of Geotechnical and Geoenvironmental Engineering* (ASCE), 138(11), 1369-1386.

Faccioli E., Paolucci R., and Vanini M., 1998. *3D Site Effects and Soil-Foundation Interaction in Earthquake and Vibration Risk Evaluation*. Final report of the European research project TRISEE, European Commission, Brussels, Belgium.

Faccioli E., Paolucci R., and Vivero G., 2001. Investigation of seismic soil-footing interaction by large scale cyclic tests and analytical models. *Proceedings of the 4th International Conference on Recent Advances in Geotechnical Earthquake Engineering and Soil Dynamics* (S. Prakash, ed.), CD-ROM, S. Prakash Foundation publisher, San Diego, CA.

Fardis M. N. (ed.) 2010. *Advances in Performance-Based Earthquake Engineering*. Springer, University of Patras, Greece, pp. 485.

Federal Emergency Management Agency (FEMA), 2000. *Prestandard and Commentary for the Seismic Rehabilitation of Buildings, FEMA-356*, Washington, D.C.

Figini R.. 2010. *Nonlinear dynamic soil-structure interaction: Application to seismic analysis of structures on shallow foundations.* Ph.D. thesis, Politecnico di Milano, Italy.

Furumura T., Takemura S., Noguchi S., Takemoto T., Maeda T., Iwai K., Padhy S. 2011. Strong ground motions from the 2011 off-the Pacific-Coast-of-Tohoku, Japan (Mw=9.0) earthquake obtained from a dense nationwide seismic network. *Landslides* (available online, DOI: 10.1007/s10346-011-0279-3).

Gajan S., Kutter BL. 2008. Capacity, settlement and energy dissipation of shallow footings subjected to rocking, *Journal of Geotechnical and Geoenvironmetal Engineering*, ASCE 134(8), 1129-1141.

Gajan S., and Kutter B. L., 2009a. Contact interface model for shallow foundations subjected to combined loading. *Journal of Geotechnical and Geoenvironmental Engineering* 135, 407–419.

Gajan S., and Kutter B. L., 2009b. Effects of moment-to-shear ratio on combined cyclic load-displacement behavior of shallow foundations from centrifuge experiments. *Journal of Geotechnical and Geoenvironmental Engineering* 135, 1044–1055.

Garini E., Gazetas G., and Anastasopoulos I. 2011. Asymmetric 'Newmark' Sliding Caused by Motions Containing Severe 'Directivity' and 'Fling' Pulses. *Géotechnique,* 61(9), 753-756.

Gazetas G. 1991. Formulas and charts for impedances of surface and embedded foundations. *Journal of Geotechnical Engineering, ASCE*, 117(9), 1363–81.

Gazetas G., Anastasopoulos, I., and Apostolou, M., 2007. Shallow and deep foundations under fault rupture or strong seismic shaking. Chapter 9 in *Earthquake Geotechnical Engineering*, (K. Pitilakis, ed.), Springer Publishing, 185–215.

Gazetas G., Apostolou M., Anastasopoulos I. 2003. Seismic Uplifting of Foundations on Soft Soil, with examples from Adapazari (Izmit 1999, Earthquake). *BGA Int. Conf. on Found. Innov., Observations, Design & Practice*, Univ. of Dundee, Scotland, September 25, 37-50.

Gazetas G., Mylonakis G. 1998. Seismic soil–structure interaction: new evidence and emerging issues, emerging issues paper. *Geotechnique, Spec. Pub. ASCE*, 75, 1119–74.

Gazetas G. 1987. Simple physical methods for foundation impedances. Chapter 2 in *Dynamics of Foundations and Buried Structures* (P. K. Benerjee and R. Butterfield, eds), Elsevier Applied Science, Barking Essex, UK, 44–90.

Gazetas G. 1991. Formulas and charts for impedances of surface and embedded foundation. *Journal of Geotechnical Engineering* 117, 1363–1381.

Gazetas G., and Apostolou M. 2004. Nonlinear soil-structure interaction: Foundation uplifting and soil yielding. *3rd U.S.-Japan Workshop on Soil-Structure Interaction*, 29–30 March 2004, Menlo Park, CA.

Gazetas G., and Kavvadas M. 2009. *Soil–Structure Interaction.* NTUA Publications, Athens, Greece.

Gazetas G., Garini E., Anastasopoulos I. 2009. Effect of near–fault ground shaking on sliding systems. *Journal of Geotechnical and Geoenvironmental Engineering* 135, 1906–1921.

Gelagoti F., Kourkoulis R., Anastasopoulos I., Gazetas G. 2012. Rocking Isolation of Low- Rise Frame Structures founded on Isolated Footings", *Earthquake Engineering and Structural Dynamics,* 41, 1177-1197.

Georgiadis M., and Butterfield R. 1988. Displacements of footings on sands under eccentric and inclined loading. *Canadian Geotechnical Journal,* 25, 199–212.

Gerolymos N., Apostolou M., Gazetas G. 2005. Neural network analysis of overturning response under near-fault type excitation. *Earthquake Engineering and Engineering Vibration,* 4, 213–228.

Gottardi G., Houlsby G.T., Butterfield R. 1995. The displacement of a model rigid surface footing on dense sand under general planar loading. *Soils and Foundations,* 35, 71–82.

Gourvenec S. 2007. Shape effects on the capacity of rectangular footings under general loading. *Géotechnique*, 57(8), 637-646.

Gourvenec S., Randolph M.F. 2003. Effect of strength non–homogeneity on the shape and failure envelopes for combined loading of strip and circular foundations on clay. *Géotechnique*, 53(6), pp. 527-533.

Harden C., Hutchinson T. 2006. Investigation into the Effects of Foundation Uplift on Simplified Seismic Design Procedures. *Earthquake Spectra*, 22 (3), pp. 663–692.

Harden C.W., and Hutchinson T.C. 2009. Beam on nonlinear Winkler foundation modeling of shallow rocking–dominated footings. *Earthquake Spectra,* 25, 277–300.

Houlsby G.T., Amorosi A., & Rojas E. 2005. Elastic moduli of soils dependent on pressure: a hyperelastic formulation. *Géotechnique*, 55(5), 383–392.

Houlsby G.T., Cassidy M.J., Einav I. 2005. A generalized Winkler model for the behavior of shallow foundation. *Geotechnique* , 55, 449–460.

Housner G. W. 1963. The behavior of inverted pendulum structures during earthquakes, *Bulletin of the Seismological Society of America,* 53(2), 403–417.

Huckelbridge A.A., and Clough R. 1978. Seismic response of uplifting building frame. *Journal of Structural Engineering,* 104, 1211–1229.

Ishiyama Y. 1982. Motions of rigid bodies and criteria for overturning by earthquake excitations. *Earthquake Engineering Structural Dynamics* 10, 635–650.

Kausel E., & Roesset J.M. 1975. Dynamic stiffness of circular foundations. *J. Eng. Mech. Div., ASCE*, 101, pp. 771–85.

Kawashima K., Nagai T., and Sakellaraki D. 2007. Rocking seismic isolation of bridges supported by spread foundations. *Proceedings of 2nd Japan-Greece Workshop on Seismic Design, Observation, and Retrofit of Foundations*, Japanese Society of Civil Engineers, Tokyo, 254–265.

Kirkpatrick P. 1927. Seismic measurements by the overthrow of columns. *Bulletin of the Seismological Society of America* **17**, 95–109.

Knappett J.A., Haigh S.K., Madabhushi S.P.G. 2006. Mechanisms of failure for shallow foundations under earthquake loading. *Soil Dynamics and Earthquake Engineering,* 26, 91–102.

Koh A.S., Spanos P., and Roesset J.M. 1986. Harmonic rocking of rigid block on flexible foundation. *Journal of Engineering Mechanics* **112**, 1165–1180.

Kourkoulis R., Gelagoti F., Anastasopoulos I. 2012. Rocking Isolation of Frames on Isolated Footings : Design Insights and Limitations. *Journal of Earthquake Engineering,* 16(3), 374-400.

Kourkoulis R., Anastasopoulos I., Gelagoti F., Kokkali P. 2012. Dimensional Analysis of SDOF Systems Rocking on Inelastic Soil. *Journal of Earthquake Engineering*, 16(7), 995-1022.

Kutter B.L., Martin G., Hutchinson T.C., Harden C., Gajan S., Phalen J.D. 2003. *Status report on study of modeling of nonlinear cyclic load–deformation behavior of shallow foundations*. University of California, Davis, PEER Workshop, 2003.

Kutter B.L., Wilson D.L. 2006. Physical Modelling of Dynamic Behavior of Soil-foundation-superstructure Systems. *International Journal of Physical Modelling in Geotechnics*, 6(1), 1–12.

Kutter B.L., Martin G., Hutchinson T.C., Harden C., Gajan S., and Phalen J. D. 2006. *Workshop on modeling of nonlinear cyclic load-deformation behavior of shallow foundations.* PEER *Report* 2005/14, Pacific Earthquake Engineering Research Center, University of California, Berkeley, CA.

Le Pape Y., & Sieffert J.P. 2001.Application of thermodynamics to the global modelling of shallow foundations on frictional material. *International Journal for Numerical and Analytical Methods in Geomechanics*, 25, 1377-1408.

Luco J.E., and Westman R.A., 1971. Dynamic response of circular footings. *Journal of the Engineering Mechanics Division,* 97, 1381–1395.

Makris N., and Roussos, Y. 2000. Rocking response of rigid blocks under near source ground motions. *Géotechnique,* 50, 243–262.

Martin C.M., Houlsby G.T. 2001. Combined loading of spudcan foundations on clay : numerical modeling. *Géotechnique*, 51(8), 687-699.

Martin G.R., and Lam I.P., 2000. Earthquake resistant design of foundations: Retrofit of existing foundations. *Geoengineering 2000 Conference (GeoEng2000)*, 19–24 November 2000, Melbourne, Australia.

Maugeri M., Musumeci G., Novità D., & Taylor C.A. 2000. Shaking table test of failure of a shallow foundation subjected to an eccentric load. *Soil Dyn. and Earthq. Eng.*, 20 (5-8), 435-444.

Meek J. 1975. Effect of foundation tipping on dynamic response, *Journal of Structural Division,* 101, 1297–1311.

Mergos P.E., and Kawashima K. 2005. Rocking isolation of a typical bridge pier on spread foundation. *Journal of Earthquake Engineering*, 9(2), 395–414.

Meyerhof G.G. 1963. Some recent research on the bearing capacity of foundations. *Canadian Geotechnical Journal,* 1(1), 6–26.

Nakaki D.K., and Hart G.C. 1987. Uplifting response of structures subjected to earthquake motions. *U.S.-Japan Coordinated Program for Masonry Building Research, Report No 2.1-3* (Ewing, Kariotis, Englekirk, and Hart, eds.).

Negro P., Paolucci R., Pedrett S., and Faccioli E. 2000. Large-scale soil-structure interaction experiments on sand under cyclic loading. Paper No. 1191, *12th World Conference on Earthquake Engineering*, 30 January–4 February 2000, Auckland, New Zealand.

Nova R., & Montrasio L. 1991.Settlement of shallow foundations on sand. *Géotechnique*, 41(2), 243-256.

Panagiotidou A.I., Gazetas G., and Gerolymos N. 2012. Pushover and Seismic Response of Foundations on Overconsolidated Clay: Analysis with P-δ Effects, *Earthquake Spectra*, 28(4), 1589-1618.

Panagiotidou A.I. 2010. *2D and 3D inelastic seismic response analysis of foundation with uplifting and P-δ effects*. thesis, National Technical University, Athens, Greece.

Paolucci R. 1997. Simplified evaluation of earthquake induced permanent displacements of shallow foundations. *Journal of Earthquake Engineering* 1, 563-579.

Paolucci R. Shirato M., Yilmaz MT. 2008. Seismic behavior of shallow foundations : shaking table experiments vs. numerical modeling. *Earthquake Engineering & Structural Dynamics,* 37(4), 577-595.

Paolucci R., and Pecker A. 1997. Seismic bearing capacity of shallow strip foundations on dry soils. *Soils and Foundations* 37, 95–105

Paulay T., and Priestley M.J.N. 1992. *Seismic Design of Reinforced Concrete and Masonry Buildings*. John Wiley & Sons, New York, NY.

Pecker A. 2003. A seismic foundation design process, lessons learned from two major projects : the Vasco de Gama and the Rion Antirion bridges. *ACI International Conference on Seismic Bridge Design and Retrofit*, University of California at San Diego, La Jolla, USA.

Pecker A. 1998. Capacity design principles for shallow foundations in seismic areas. Keynote lecture, in *11th European Conference Earthquake Engineering* (P. Bisch, P. Labbe, and A. Pecker, eds.) A. A. Balkema, Rotterdam, The Netherlands, 303–315.

Pender M. 2007. Seismic design and performance of surface foundations. *4th International Conference on Earthquake Geotechnical Engineering*, Thessaloniki, Greece (CD-ROM).

Priestley M.J.N. 1993. Myths and fallacies in earthquake Engineering—Conflicts between design and Reality. *Bulletin, New Zealand Society for Earthquake Engineering* , 26, 329–341.

Priestley M.J.N. 2003. Myths and fallacies in earthquake engineering, revisited. *Ninth Mallet-Milne Lecture*, Rose School, IUSS Press, Instituto Universitario di Studi Superiori, Pavia, Italy.

Raychowdhury P. & Hutchinson T. 2009. Performance evaluation of a nonlinear Winkler-based shallow foundation model using centrifuge test results. *Earthquake Engineering and Structural Dynamics*, 38(5), 679-698.

Roesset J.M. 1980. Stiffness and damping coefficients of foundations, in *Dynamic Response of Foundations: Analytical Aspects* (M. W. O'Neil and R. Dobry, eds.). American Society of Civil Engineers, Reston, VA, 1–30.

Salençon J., and Pecker A., 1995. Ultimate bearing capacity of shallow foundations under inclined and eccentric loads. Part II: Purely cohesive soil without tensile strength. *European Journal of Mechanics, A:Solids,* 14, 377–396.

Shi B., Anooshehpoor A., Zeng Y., and Brune J. 1996. Rocking and overturning of precariously balanced rocks by earthquake. *Bulletin of the Seismological Society of America* 86, 1364–1371.

Shirato M., Kouno T., Nakatani S., and Paolucci R. 2007. Large-scale model tests of shallow foundations subjected to earthquake loads, in *Proceedings of the 2nd Japan-Greece Workshop on Seismic Design, Observation, and Retrofit of Foundations*, Japanese Society of Civil Engineers, Tokyo, Japan, 275–299.

Shirato M., Kuono T., Asai R., Fukui J., and Paolucci R. 2008. Large scale experiments on nonlinear behavior of shallow foundations subjected to strong earthquakes. *Soils and Foundations,* 48, 673–692.

Tassoulas J.L. 1984. An investigation of the effect of rigid sidewalls on the response of embedded circular foundations to obliquely-incident SV and P waves. *Dynamic Soil–Structure Interaction*, Rotterdam: A.A.Balkemal,. 55–63.

Ticof J. 1977. *Surface footings on sand under general planar loads*, Ph.D. Thesis, University of Southampton, U.K.

Ukritchon B., Whittle A.J., Sloan S.W. 1998. Undrained limit analysis for combined loading of strip footings on clay. *Journal of Geotechnical and Geoenvironmetal Engineering*, ASCE, 124(3), 265-276.

Veletsos A.S., & Nair V.V. 1975. Seismic interaction of structures on hysteretic foundations. *Journal of Structural Engineering, ASCE,* 101(1), 109–29.

Vesic A.S. 1973. Analysis of ultimate loads of shallow foundations. *Journal of Soil Mechanics Foundation Div.*, ASCE, 99, 45–73.

Vetetsos A.S., and Wei Y.T. 1971. Lateral and rocking vibration of footings. *Journal of the Soil Mechanics and Foundation Division* 97, 1227–1248.

Wolf J.P. 1988. *Soil–Structure Interaction Analysis in Time-Domain*.Prentice–Hall, Englewood Cliffs, NJ.

Zhang J., and Makris N. 2001. Rocking Response of Free-Standing Blocks Under Cycloidal Pulses. *Journal of Engineering Mechanics*, 127(5), 473–483.

The Ishihara Lecture, 18th International Conference on Soil Mechanics and Geotechnical Engineering, Paris 2013

Pressiorama – Application of Ménard Pressuremeter to Classify Several Geological Formations Encountered in Greece

A. Ritsos, A. Basdekis and M. Gambin

ABSTRACT : Pressuremeter tests carried out within several geological formations that can be found in Greece, are presented and commented basically by using the graphical display named Pressiorama© (Baud 2005, Baud and Gambin, 2013). With this graphical display the evaluation of the pressuremeter results and the pressuremeter parameters, in accordance with laboratory tests for the determination mainly of the physical properties in characteristic samples, is much more accurate and gives the possibility to determine more precisely the ground strength, several geotechnical engineering parameters and mathematical expressions needed for design purposes. Four typical case studies are presented using this graphical display, showing that this is an adequate process to provide useful information for the structure of several ground formations in relation to their strength.

RÉSUMÉ : Des série d'essais pressiométriques réalisés dans des formations géologiques diverses qui existent en Grèce, sont présentés et commentés notamment en utilisant le diagramme nommé Pressiorama© (Baud 2005, Baud et Gambin, 2013). Ce diagramme, permet que l'évaluation des résultats et des paramètres pressiométriques, en accord avec les essais de laboratoire pour la détermination surtout des propriétés physiques des échantillons caractéristiques, soit plus exacte, et donne la possibilité de déterminer plus précisément la résistance de sol, plusieurs paramètres géotechniques et expressions mathématiques nécessaires au niveau des études. Quatre études de cas caractéristiques, utilisant Pressiorama sont présentées, indiquant que c'est une procédure adéquate pour fournir des informations utile quant à la structure des formations diverses du sol par rapport à leur résistance.

KEYWORDS : Greece, pressiorama, parameters, soft soils, hard soils, weak rocks, tests, offshore tests, case studies.

MOTS CLES : Grèce, pressiorama, caractéristiques des sols, sols mous, sols raides, rocher altéré, essais en mer, études de cas.

1 INTRODUCTION

Ménard Pressuremeter Test (MPM) has been widely used during the last years in Greece, for the investigation of the ground conditions, and the determination of the ground strength parameters in several geotechnical projects (e.g. buildings, underground structures). The pressuremeter tests are usually performed in parallel with sampling boreholes, and other in situ and laboratory tests. The evaluation of the measured parameters is critical for the geotechnical design in any case.

'Pressiorama©' which has been introduced by J. P. Baud (Baud 2005, Baud and Gambin, 2013), is a spectral diagram where the graphical display of the main pressuremeter parameters, such as E_M, P^*_{LM}, and ratio E_M/P^*_{LM}, can be presented for several ground formations, for an overall classification, ranging from loose soils to hard soils and to weak rocks. This diagram is essential for the further evaluation of the test results, the principal qualitative characterization of the tested ground materials and the facilitation of the choice of a suitable value of the rheological factor 'α', used in the geotechnical design. The chosen values of 'α' takes the values of 1/4, 1/3, 1/2, 2/3, or 1, as initially proposed by Ménard and Rousseau (1962). The pressuremeter modulus E_M is related to the oedometer modulus Es, under the same pressure and strain conditions, by using the formula $E_s=E_M/\alpha$.

In the 'Pressiorama©' graphical display used hereby, $\log(P^*_{LM})$ given in the horizontal axis has an upper value of 10MPa, the ratio of $\log(E_M/P^*_{LM})$ in the vertical axis ranges between 4 and 100, and the third diagonal axis presenting $\log(E_M)$ takes values 0.30-3-30-300MPa. Ratio E_M/P^*_{LM} is characteristic of the ground structure, with higher values corresponding to well cemented or over consolidated material, and lower values indicating disturbed material during insufficient drilling or alluvial soils. E_M/P^*_{LM} values between 4 and 7 may correspond to saturated very loose material and sometimes are neglected during evaluation, when the drilling process is questionable.

The results of the pressuremeter tests, presented in this study, indicate that the pressuremeter curves are suitable. Also, the behavior of several geological formations tested varies significantly, classifying them from soft-even liquid ground material with water present or without, to hard soil and weak rock. The pressuremeter tests were performed on different soil materials, with varying weathering degree, from liquid to stiff and cemented. The permeability and porosity of these formations vary predominantly as well, depending on the depth, thickness, nature and sequence of stratigraphy.

The majority of the pressuremeter tests were performed during 2000 to 2012, at depth intervals of 2m and 3m, in several depths up to a maximum of about 50 m.

The maximum applied pressure to the ground was 10MPa. Several characteristic diagrams resulting from the tests are presented here, emphasizing on the 'Pressiorama©', where characteristic pressuremeter values for each classified formation are commented.

Four characteristic cases in several locations in Greece are concisely presented:

1. *Case 1: Athens* – Hard Soil and weak rock of Quarternary, Neogene, Alpine age, with emphasis to the Red Loam Clay that was used to make ceramic during ancient time.

2. *Case 2: Thessaloniki* – Quaternary to Neogene deposits underlying the archeological layer.

3. *Case 3: offshore tests* – Tests performed at relatively shallow sea depths using a stable temporary platform, in an almost liquid soft lean sandy to silty clay, where the CPT was not sufficient for measuring the ground strength.

4. *Case 4: Santorini, Thira* – Volcanic materials in Akrotiri area, where a 'Bronze age Pompeii' was found in the Ancient Aegean Sea, in the island described also in Jules Verne books.

The pressuremeter test results are discussed and in addition compared to data resulting from a series of sampling boreholes drilled in many cases next to the pressuremeter boreholes. The variation of ground geological structures as well as the strength and other geotechnical properties were also defined through laboratory testing, and other in situ tests (CPT, SPT) as well as using empirical correlations for similar formations based on literature. Based on the results of the current report, it may be concluded that the display of the pressuremeter test results on the 'Pressiorama©', is a useful graphical approach for the estimation of the expected range of critical geotechnical design parameters, for different ground formations.

2 CASE 1 : ATHENS

Athens is located in a basin surrounded by three mountains and the sea in the southern direction.

The geological formations tested refer generally to semi-cohesive to cohesive soils, hard soils and soft rocks. Most of the tests were carried out within Neogene and Quaternary clastic formations, of variable granulometry, as well as within the weathered mantle of the bedrock and the bed-rock known as 'Athenian Schists', which constitutes an important part of the stratigraphy of the basin. The lower parts of these formations are mainly coarse and poorly graded while the upper parts are fine and well graded. The geological formations from the youngest to the oldest are:

- *Quaternary formations.* Appear mainly in the south east part of the basin and are cemented or loose materials, with clay, sand, gravels, etc. These formations are more permeable, having periodically and locally a free aquifer. Their Pressiorama© is given in diagram 1, where the orientation of the non cemented and cemented material is distinct.

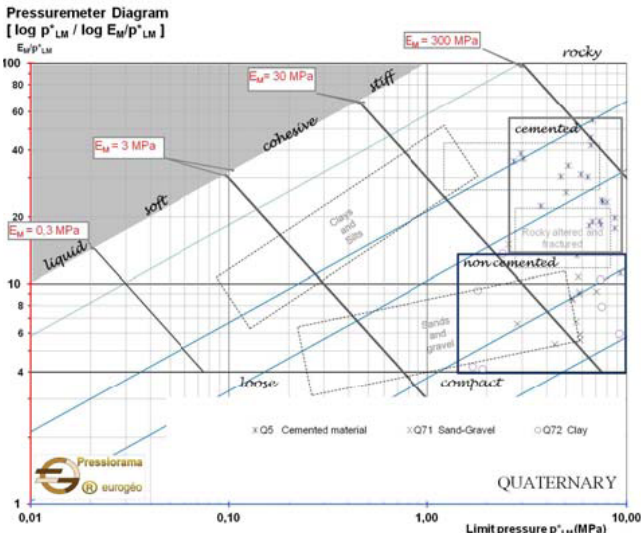

Figure 1. Pressiorama© - Quaternary, non cemented & cemented.

- *Neogene formations.* They have a semi-cohesive to cohesive nature, and include clastic sediments of variable grain size. The different materials are classified as Red Loams, Marls (clayey or calcitic), Mudstones, Siltstones, Sandstones, Marly Limestones. Their Pressiorama© is given in diagram 3, where the trend to the more compact and rocky behavior is distinct. The red loams are more homogenous materials.

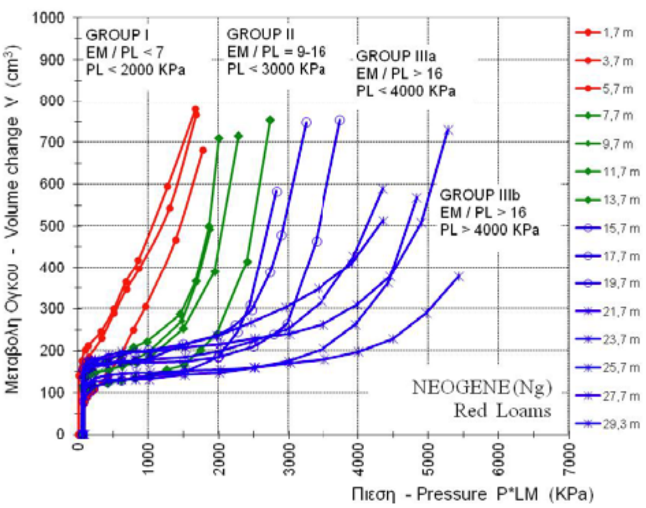

Figure 2. Red Loams (Ng) – Pressuremeter borehole 'Athmonon'.

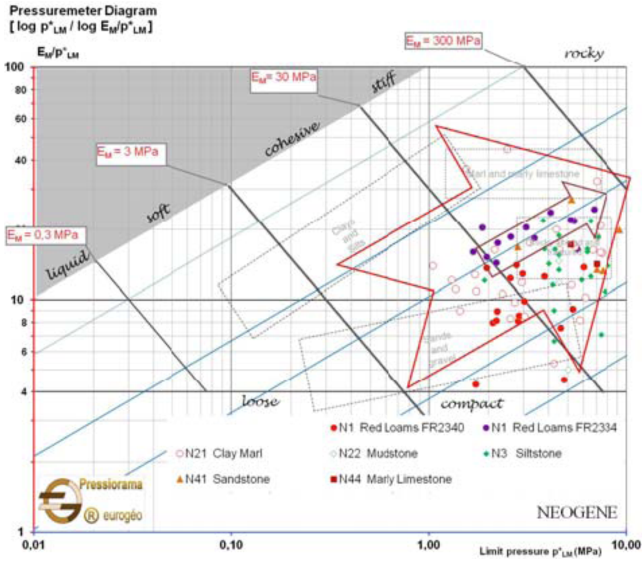

Figure 3. Pressiorama© - Neogene material (Ng)

- *Alpine formations.* The basin bedrock consists mainly of 'Athenian Schists'. This is a clastic formation of a specific flysch type character consisting of alternations of slightly dynamometamorphosed clayschists, black clayschists and sandstones, named meta-clayschist, meta-siltstones, meta-sandstones, with intercalations of marly to sandy crystalline limestones, conglomerates and locally ophiolitic olisthostromes or olistholites. Their Pressiorama© is given in diagram 4, where the trend to the well cemented and rocky behavior is clear.

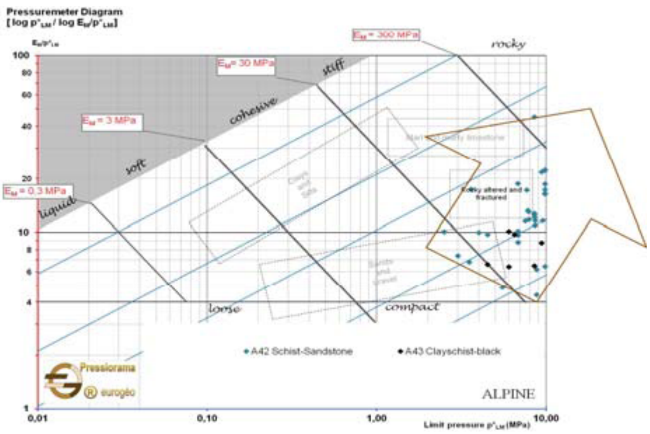

Figure 4. Pressiorama© - Alpine material.

Unfortunately, the performed tests for this time period couldn't exceed P*max=10MPa, due to the probe's capacity.

The *'Athenian schist'* presents variable mechanical properties which reflect directly to the mineral composition and the grade of weathering. The uppermost parts of the schist formations are locally totally weathered and refer to cohesive soil (elouvial mantle) of different thickness. The schists are generally not permeable, with certain permeability into the sandy-carbonate members. In certain cases, where hard rocky parts were encountered, the tests were not applicable (P_{max}=10MPa).

The *Red Loams (Ng) are* homogenous materials, investigated down to 33m depth. Historically, such material was used in ceramics and pottery, using the flowing water from the closest mountain. Borrow pits were found in the ancient location called 'Athmonon', an area close to the Olympic stadium of Athens. In diagrams 2 and 3 the measured values are presented, in which the homogenous behavior can be seen in a sorted relatively similar behavior with depth.

This material is classified as silty clay material, CL, ML (USCS), and as A-4, A-6, A-7-6 (AASHTO). UCS_{max}=135-600KPa. N_{SPT}=35 to refusal. P^*_{LM}=1.7-6.8MPa - E_M=7.4-166MPa - E_M/P^*_{LM}=5-25.

In the Athens basin urban area, (37) pressuremeter boreholes were evaluated, performed in 15 test locations, drilled during several stages usually next to sampling boreholes. A total number of about (518) pressuremeter tests were performed, in 2 to 3m intervals, up to maximum investigation depth of 40m. In (216) tests the pressuremeter parameters could be determined directly from the test diagrams.

The majority of the formations tested may be classified as cohesive, cemented, hard soils or soft rocks, with cohesive or granular composition with fines, with a varying percentage of clayey particles, in a progressive phase of weathering process.

From a total number of 518 performed tests, the 6% indicated that the ratio E_M/P^*_{LM}, that is indicative of the material structure, was E_M/P^*_{LM} < 7, the 42% had a value of 7-16, while for the rest 52% the ratio was higher than 16 with a maximum value of 75. A minimal value of E_M=1MPa was evaluated for the weathered clayey marl and a maximum value of E_M=2500MPa for the weathered Athenian schist.

In general, for all fine formations containing clayey particles, classified from soft, to cohesive, and up to stiff material, an accurate correlation between E_s (oedometer modulus) and P^*_{LM}, especially for values of P^*_{LM} between 1.0 to 6.5 MPa, is:

$$E_s = (16 \text{ to } 21)\ P^*_{LM} \qquad (1)$$

An a v e rage proposed equation (Ritsos et al, 2005) is:

$$E_s = 18.5\ P^*_{LM} \qquad (2)$$

3 CASE 2 : THESSALONIKI

Thessaloniki is located in an area with an amphitheatric relief, from hills and small mountains in the north, to sea in the south. Several rivers are crossing this plateau, and therefore the superficial ground material is mainly river deposits and lake or lagoon sediments. The bedrock of the area is mainly gneiss and schist formations of the Mesozoic period. The overburden ground material is upper Miocene to lower Pliocene Neogene deposits, consisting of stiff to hard red clays to silty clays with variable appearance of coarse material and Quaternary formations with sands, clays, gravels and locally conglomerates.

Historically, the city was founded in 315 BC, and that is why consecutive archeological layers of several historical periods can be found in the ground usually at an average depth of 7 to 10m. That archeological layer contains locally recent and manmade deposits consisting of coarse to fine material.

The Neogene and the Quaternary deposits consist of lacustrine, brackish and terrestrial phases which lithologically are dominated by clays of varying percentages of coarse fractions. These deposits cover the alpine background (geotectonic unity of Paeonia) and more specifically the metamorphic rocks of the Hortiati magmatic series. The geological formations in the area include the following formations from the youngest to the oldest:

- *Recent deposits & 'Archaeological layer'.* Silt to clay with local interlayer of gravels and sands, with presence of artificial materials such as bricks, bones, wood (etc) and weathering products. There may be loose deposits and voids which usually include materials mixed with ashes from historical fires that burnt the city.

- *Recent Quaternary deposits.* Alluvial and loose clastic deposits consisting mainly of silty clayey materials, including sands and gravels deposits from the ravines.

- *Old Quaternary deposits.* Clastic heterogeneous mixtures of clay and silts, locally including gravels to cobbles that present hard calcareous and manganese oxide phases.

- *Pliocene deposits, 'Sandstone and Marl series'.* Sea and lagoon phases of fine sand with local presence of hard calcareous phases which locally cause cementation.

- *Pontius deposits, such as 'red clays series'.* Lagoon to lake deposits with sequence of greenish, reddish to red brownish, stiff to very stiff and hard, silty clay to clayey silt with local presence of sands intercalations.

- *Alpine background.* Includes the metamorphic rocks of Hortiati magmatic series (Grs) with gneiss schists, green schists and sandstone schists.

The ground water level along the coast line is at the sea level. In the main land the ground water appears electively to the coarser sandy gravelly interlayer, at an average depth of 2 to 6m, which is unloaded when the continuation of this layer is interrupted by a finer clayey layer. Depending on the hydrologic conditions during the year, ground water appears periodically at the ravines and also free runoff water.

In the study area (22) pressuremeter boreholes were evaluated, drilled in several stages usually next to the sampling boreholes. A total number of about (300) pressuremeter tests were performed, of 2 to 3m intervals, up to an investigated maximum drilling depth varying from 22m to 50m. In all cases pressuremeter parameters could be determined directly from the test diagrams.

The pressuremeter values were correlated based on the nature of the ground material, classified according to the USCS as *fine grained soils* - such as clay (C) and silt (M) with at least 50% passing through No200 sieve – and *coarse grained soils* – such as gravel (G) and sand (S) with less than 50% passing through the No200 sieve. The ratio EM/P*LM ranges between 5 and 40. The 'rheological factor' α is estimated based on the nature of the tested ground material.

For the fine grained material, the proposed relation (1) between E_S and P^*_{LM}, that is E_S=(16 to 21)P^*_{LM}, is also valid, most effectively in the range of P^*_{LM} =1.0 to 6.5 MPa. In all the examined values the average ratio was equal to E_s/P^*_{LM} =19.40 which is within the proposed range of 16 to 21.

In diagrams 5 and 6, the 'Pressiorama©' of the fine grained, or coarse grained materials are presented. Silty and sandy to gravelly material have greater compact strength, progressively increasing towards the direction of the cemented material. Fine clayey material gives higher ratio of E_M/P^*_{LM} which is also evidence of good drilling technique.

In diagrams 7 and 8 ($\log P^*_{LM}$ vs $\log E_s$) the proposed linear relationship (2) is presented, which is valid mainly for the fine grained and the clayey material, along their average distribution. For the coarse grained material this relationship (2) can be used only as a lower limit, while their measured strength is 2 to 3 times higher than the fine grained material.

The classification of the material based on their nature and the sieve used is not always feasible and direct, while that is possible based only on their strength, progressively classifying them from compact and cohesive, to stiff and cemented.

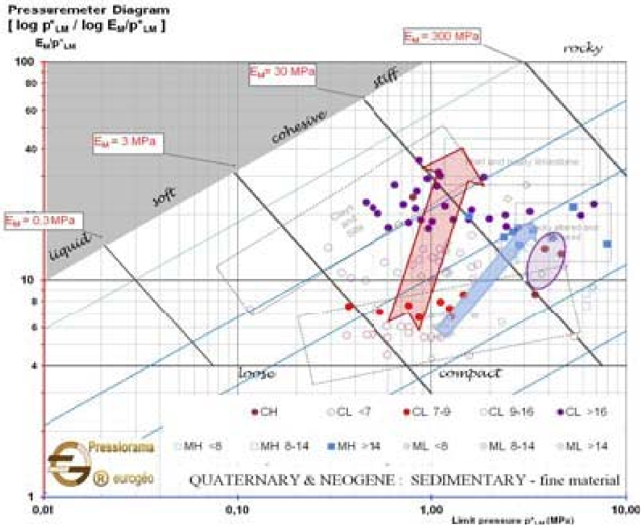

Figure 5. Pressiorama© - FINE material.

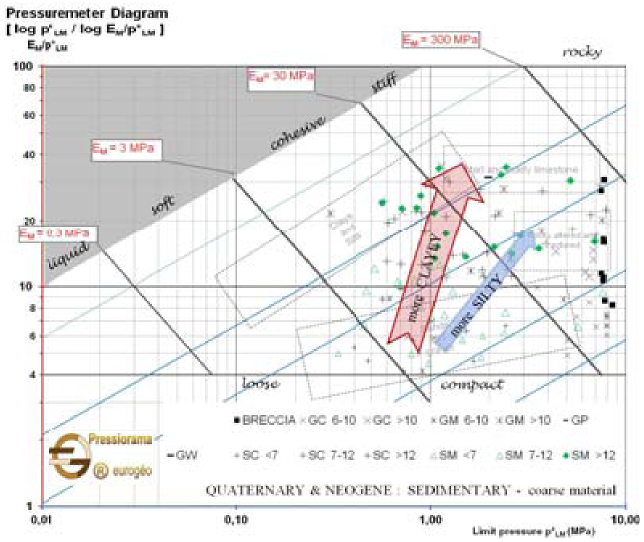

Figure 6. Pressiorama© - COARSE material.

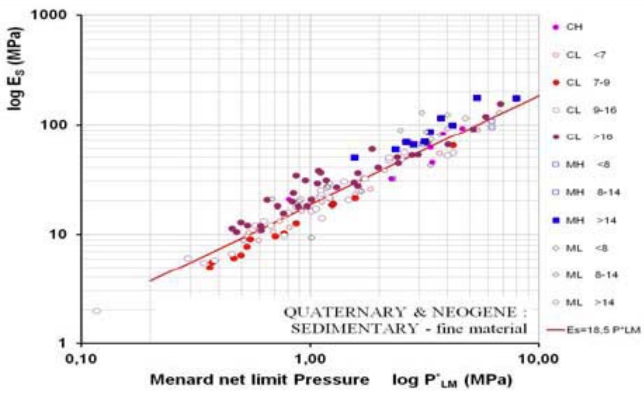

Figure 7. FINE material - logP*$_{LM}$ vs logE$_S$ [in MPa]

The measured parameters for each sieve classification are summarized in table 1.

4 CASE 3 : OFFSHORE TESTS

Offshore geotechnical investigations were performed, either from a floating platform, or from a temporary installed stable platform. The bottom of the sea was inclined with a maximum depth of 20m, measured from the sea level.

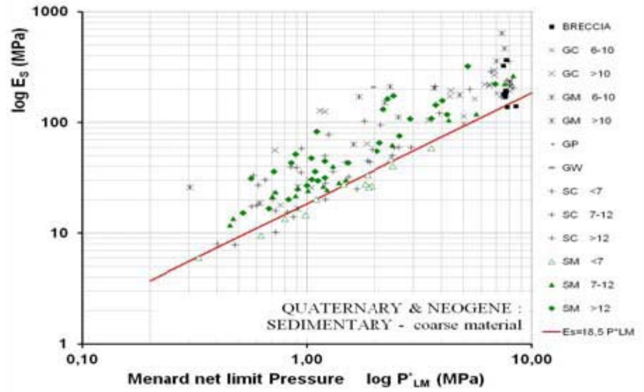

Figure 8. COARSE material - logP*$_{LM}$ vs logE$_S$ [in MPa]

Table 1. Thessaloniki – Range of pressuremeter parameters (USCS).

USCS	E_M/P^*_{LM}	E_M (MPa)	P^*_{LM} (MPa)	α	E_s (MPa)
CH	7 - 26	16 - 62.5	0.8 - 4.6	1/2 - 1	21 - 93
CL	5 - 6	3 - 30	0.5 - 5.4	1/3	9 - 91
	7 - 8	2.5 - 57	0.4 - 7.8	1/2	5 - 114
	9 - 15	1.3 - 37	0.1 - 4.2	2/3	2 - 56
	16 - 40	11 - 157	0.5 - 6.8	1	10 - 157
MH	<8	16	2.3	1/2	32
	8 - 14	33 - 55	2.7 - 6.2	1/2	66 - 110
	15 - 22	33 - 120	1.6 - 7.9	2/3	50 - 180
ML	<8	4 - 21	1.0 - 3.4	1/2	9 - 43
	8 - 14	4 - 65	0.5 - 6.7	1/2	9 - 130
	15 - 30	14 - 88	0.7 - 4.0	2/3	21 - 130
SC	<7	3 - 8	0.5 - 1.7	1/3	8 - 25
	7 - 11	3 - 75	0.4 - 8.0	1/3	8 - 219
	12 - 31	9 - 180	0.6 - 8.3	1/2	18 - 360
SM	<7	2 - 20	0.3 - 3.6	1/3	6 - 60
	7 - 11	4 - 88	0.5 - 8.3	1/3	12 - 266
	12 - 38	8 - 160	0.5 - 6.9	1/2	15 - 323
GC	5 - 9	4 - 60	0.8 - 8.0	1/4	18 - 240
	10 - 37	19 - 100	0.7 - 7.0	1/3	55 - 300
GM	5 - 9	4 - 45	0.9 - 4.8	1/4	16 - 180
	10 - 33	6 - 213	0.3 - 7.6	1/3	19 - 650
GP	11	8	0.7	1/3	24
GW	35	70	2.0	1/3	210
BRECCIA	8 - 32	70 - 246	7.5 - 8.5	1/2 - 2/3	138 - 367

The carried out ground investigations comprise a number of sampling boreholes, SPT tests, CPT tests, laboratory tests and pressuremeter boreholes. In those boreholes a total number of (23) pressuremeter tests performed, from the ground of the bottom of the sea, down to 40m depth (25m inside the ground).

The bearing layer in the ground was weathered and fractured schist. The above layered ground material comprises an alternation of fine to coarse, silty clayey to sandy, soft to lose material, with seaweeds and some gravels locally, down to a variable depth where the schist formation is encountered.

The SPT values in the soft ground range from 1 to 3 blows, indicating no strength in the ground for several meters. During the performance of the pressuremeter tests the following steps were adopted:

- Casing of the borehole up to one meter above the test depth.
- Slow drilling without casing up to the test depth. In several cases drilling wasn't necessary to reach the test depth. The probe was carefully self pressed into the ground.

The ground stratigraphy is the following:

- *Layer A-1 : Clay to Sand with some gravel*

Encountered in some of the boreholes, consisting of fines, sand (30%), gravels (38%) and shells, dark grey to grey in color, of low plasticity and maximum thickness 2.5m. Ground material classified as GM, GC, GP, SM (USCS).

- *Layer A-2 : Very soft lean sandy* Clay

Encountered in all boreholes, consisting of dark grey very soft lean clay with sand to soft lean clay (85%) of low to medium plasticity, with a few gravels (5%). Ground material classified as CL (USCS). Organic<2.5%. UCS=26KPa. N_{SPT}=1-8blows. Average: P^*_{LM}=0.30MPa - E_M=2.40MPa - E_M/P^*_{LM}=7-10.

- *Layer A-3 : Silty Sand to sandy Silt*

Appeared in all boreholes, consisting of very loose, non plastic silty sand (60%), sandy silt (20%) and interlayers of soft lean clay. Ground material classified as SM, SW, ML (USCS). N_{SPT}=1-12blows. P^*_{LM}=0.37MPa - E_M=4.60MPa - E_M/P^*_{LM}=13

- *Layer B : Fractured Schist with stiff sandy Clay*

Fractured ground material of very stiff sandy clay (60%) with gravel (15%). Material classified as GM, GC, CL (USCS). UCS_{max}=150-300KPa. N_{SPT}=17 to refusal. P^*_{LM}=0.4-1.10MPa - E_M=9.10MPa - E_M/P^*_{LM}=7-9

- *Layer C : Weathered Schist*

Locally weathered to slightly fractured, with veins of Quartz. P^*_{LM}=1.50MPa - E_M=18.0MPa - E_M/P^*_{LM}=10-12

- *Layer D : Schist.* Pressuremeter tests weren't performed.

The performance of the CPT tests was not regarded adequate for such lose and soft formation. In diagram 9, the classification of the ground material based on CPT test results (Robertson et al 1986, 2010) is given. The ground material that corresponds to Layer B is classified as silty clay, silt to silty clayey mixture. The ground material that corresponds to Layer C is classified as sand mixtures to silty sand. For Layer A (mainly for layers A-2 and A-3) the friction ratio was very low or zero, that corresponds to sensitive, soft to lose material.

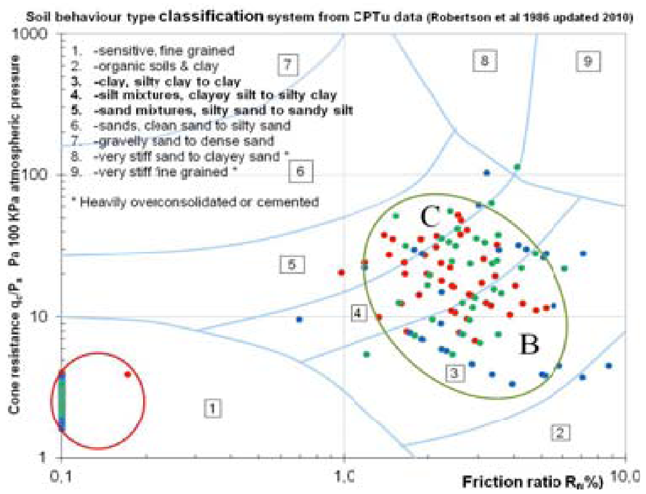

Figure 9. CPT - Offshore tests.

The pressuremeter tests were adequate for all ground Layers A, B, C, and the measured values were used for the design. In diagram 10 the 'Pressiorama©' of the sedimentary soft materials down to the schist formation, are presented. The progressive increase of the strength of the sediments with depth, by their self weight, is characteristic.

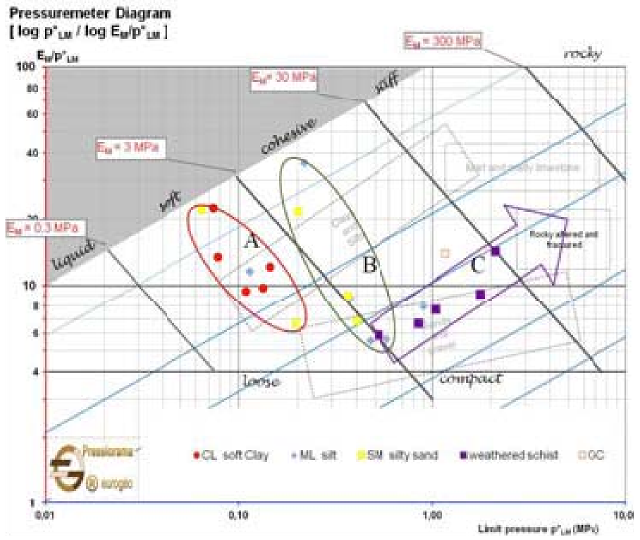

Figure 10. Pressiorama© - Offshore tests.

5 CASE 4 : SANTORINI ISLAND

The island of Santorini is located in the volcanic arc of Aegean Sea. The volcano located there is responsible for the current landscape of the island, with a volcanic activity known for at least 2 million years. The last catastrophic eruption was about 3600 years ago.

The investigations were performed at 'Akrotiri', where a prehistoric settlement was found under a layer of pumice of pozzolana in 1866. The French volcanologist Ferdinand Fouqué was one of the scientists who visited that time the island (1867). The settlement was destroyed during the volcanic eruption at about 1600 BC and was buried under the volcanic tuff and volcanic ash. Archeological excavations in the area were carried out the last years by Prof. S. Marinatos and by Prof. Ch. G. Doumas.

The biggest part of the island is covered by volcanic rocks with several volcanic series. In the broader area of Akrotiri the volcanic rocks include mainly the following units:

- *Upper Pumice Series.* The formation age is 3600 years old and comprises the Minoan IA time eruption. It is of white color and the magma is rhyodacite. At the base pumice is found and at the upper part chaotic volcanic ash deposits. The formation thickness is around 10 to 15 m.

- *Various volcanic Pyroclastic Series.* Formations average cemented, grey to yellow and reddish in color, products of various volcanic eruptions, including ash, lapilli, pumice and ignimbrites. According to literature the formation's thickness in the ground is about 200 m.

- *Lavas, tuffs and scorias.* Products of historical eruptions, aged about 1 million years old, found in the broader area of Akrotiri and mainly at the closest cape. The formation grey to reddish in color, is sufficiently cemented.

The old settlement was founded on the Pyroclastic Series, where the upper part consists of friable volcanic breccia and volcanic tuffs with lapilli and local intercalations or lenses of loose volcanic ash. The lower part consists of well cemented volcanic breccia with greater lapilli over imposed to lose volcanic tuffs and ash. Locally in the pyroclastic bedrock some discontinuities were found, with an average vertical length 150cm and locally 500cm, slightly open filled with sandy material (M. Ch. Alexiadou 2000).

Above the archeological findings and the Pyroclastic rock, based on the results of the geotechnical investigations, the main geotechnical formations are:

- *Layer I : Surface Deposits*

- *Layer II : Weathered Pumice Deposits*

- *Layer III : Volcanic ash*

- *Layer IV : Volcanic tuffs*

- *Layer V : Altereted Pyroclastic*

- *Layer VI : Archeological Layer*

The geotechnical design of special foundations with shaft piles, hand excavated in volcanic material of different ages was done by using the results of the geological supervision, the ground investigations and the pressuremeter tests. The need of almost dry sampling in the boreholes, and the performance of laboratory tests was a very difficult issue for such materials. For that reason the results of the pressuremeter tests were significant for the engineering purposes.

A total number of (17) pressuremeter tests were performed, in (2) pressuremeter boreholes next to the sampling boreholes, up to a maximum depth of about 25m. The tests were performed mainly inside layers III, IV, that are sandy to silty at layer V. Based on the tests, the Pyroclastic rock was sub-divided in two categories, the upper V_{α} formation, which is fractured and weathered, and the lower V_{β} formation, which is almost a weak rock. That classification was established from the pressuremeter strength measurements and was endorsed during the hand excavation of the shafts and the geological supervision of the pit.

The 'Pressiorama©' of the volcanic materials are displayed in diagram 11, where the progressive natural compaction, by the self weight of the volcanic material is visible. The proposed geotechnical parameters are summarized in table 2.

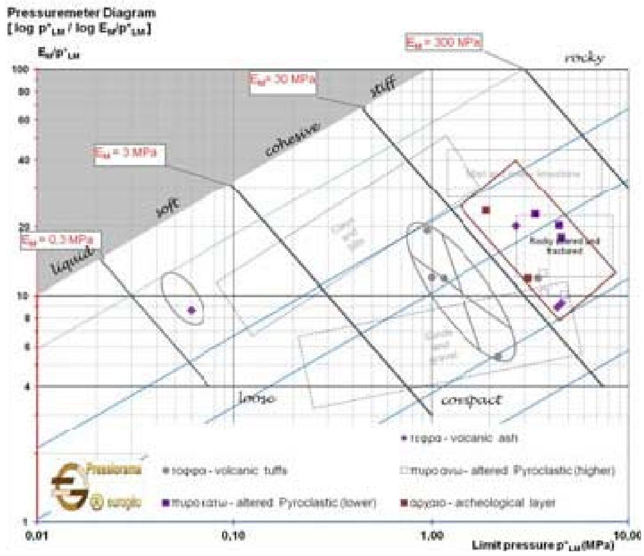

Figure 11. Pressiorama© - Volcanic material.

Table 2. Volcanic material geotechnical parameters

geotechnical	Volcanic – ash, tuffs, Pyroclastic rock			
parameters	III	IV	Va	Vb
P^*_{LM} (MPa)	3.90	1.76	4.06	4.15
E_M (MPa)	45.50	19.50	44.44	83.61
E_M/P^*_{LM}	10	10	10	17
φ (degrees)	36	31	39	39
c (KPa)	19	0	0	14.5

6 CONCLUSIONS

- Pressiorama© is a valuable tool in order to evaluate the pressuremeter results and hence the ground nature and response.

- Pressuremeter tests can be performed in all types of ground material from soft to hard soil and in weak rock.

- The increase of the probe loading capacity from 10MPa, to 25 and 50 MPa will increase the usefulness of the test.

- Useful data concerning the strength of the ground materials were withdrawn especially related to the transition from cohesive to coarser and cemented materials.

- The drilling technique is critical, in order to avoid disturbance and change in the cementation especially of coarse ground particles.

- The ground water conditions are critical, since the selective water circulation, pending water strata and the resulting variable weathering processes affect significantly the strength response.

- The use of the pressuremeter is sufficient for cases when other in situ and laboratory tests are not valid, such as in loose, in soft material and in coarse grained material.

- The numerical relations (1) and (2) between the oedometer modulus E_s and the P^*_{LM} are proposed, which are most valid for materials containing an important percentage of clay into their structure (classified as fine in USCS), from soft, to cohesive, and up to stiff material. These correlations are more accurate for values of P^*_{LM} between 1.0 to 6.5 MPa.

- The Geotechnical Engineering judgment is critical.

7 ACKNOWLEDGEMENTS

This paper gives us the opportunity to thank the senior author who, many years ago, taught us the use of the Ménard pressuremeter and the appraisal of the resulting design method.

Valuable was the exchange of information with J. P. Baud.

Special thanks to Prof. A. Anagnostopoulos, Prof. Ch. Fourniotis-Pavlatos, Prof. G. Migiros, and to Dr. A. Kollios, Dr. N. Naskos, E. Kolovaris, the geologists, the engineers and the drilling staff responsible for the performance of the tests, for the company EDAFOMICHANIKI S.A.

8 REFERENCES

Anagnostopoulos A. (2008). Καθιζήσεις Επιφανειακών Θεμελιώσεων. *5η Αθηναϊκή Διάλεξη Γεωτεχνικής Μηχανικής – HSSMGE, NTUA, Athens.*

Baguelin F., Jézéquel S.F., Shields D.H. (1978). The Pressuremeter and Foundation Engineering. *Trans Tech Publications, Germany*.

Baud J.P. (2005). Analyse des résultats pressiométriques Ménard dans un diagramme spectral et utilisation des regroupements statistiques dans la modélisation d'un site. *ISP5 - PRESSIO 2005*. Volume 1, 167-174.

Baud J.P. and Gambin M. (2005). Deriving a single Hyperbolic response to cylindrical expansion in a lithologically homogeneous soil by compilation of MPM curves. *ISP5 - PRESSIO 2005*. Volume 1, 175-186.

Baud J.P. (2005). Exercise for bearing capacity and settlement preliminary design in the case of a single pile. *ISP5 – PRESSIO 2005.* Volume 2, 549-560.

Baud J.P. and Gambin M. (2008). Homogenising MPM test curves by using a hyperbolic model. *ISC3 Taipei, Huang & Mayne (eds) London, 975-980.*

Baud J.P. and Gambin M. (2011). Soil and Rock classification based on High Pressure borehole expansion tests. *15th European Conference on SMGE, A. Anagnostopoulos et al., Athinai.* Part 1, 325-330.

Briaud J. L. (1992). The Pressuremeter. *A.A. Balkema / Rotterdam.* Clarke B.G. (1995). Pressuremeters in Geotechnical design. *Blackie Academic & Professional, London.*

Clarke B.G. and Gambin M. (1998). Pressuremeter testing in onshore ground investigation. *ISSMGE, Tech. Com. 16, ISC'98, Atlanta.*

EN-ISO 22476-4:2012(E). Geotechnical investigation and testing - Field testing - Part 4 : Ménard pressuremeter test.

Fourniotis-Pavlatos C., Alexiadou M.-Ch., Kollios A., Ritsos A. (2001). Pressuremeter tests in volcanic material*. 4th Hellenic Conference on G&GE, Athens.* Volume 1, 219-226.

Gambin M. and Rousseau J. (1988). The Ménard Pressuremeter - Interpretation and Application of Pressuremeter Test Results to Foundation Design. *General Memorandum, sols soils No 26*.

Ritsos A., Migiros G., Kollios A., Kolovaris E. (2005). Evaluation of Pressuremeter tests performed within the formations of the Athens basin. *ISP5 - PRESSIO 2005.* Volume 1, 645-652.

Ritsos A., Basdekis A., Naskos N. (2010). Performance of Pressuremeter tests in the Geotechnical Formations encountered at Thessaloniki. 6th *Hellenic Conference on G&GE, Volos.* Volume 1, 207-214.

Το άρθρο παρουσιάστηκε στο ISP6 - PRESSIO 2013 Parallel International Symposium on Pressuremeters, Paris, September 4, 2013 στα πλαίσια του 18th International Conference on Soil Mechanics and Geotechnical Engineering, Paris 2013 (Μέρος 4. Soil Classification / Classification des sols, άρθρο 4.7)

Compilation of a Local V_S Profile Database and Its Application for Inference of V_{S30} from Geologic- and Terrain-Based Proxies

Jonathan P. Stewart, Nikolaos Klimis, Alexandros Savvaidis, Nikos Theodoulidis, Elena Zargli, George Athanasopoulos, Panagiotis Pelekis, George Mylonakis, and Basil Margaris

Abstract: The time-averaged shear-wave velocity in the upper 30 m of a site (V_{S30}) is commonly used for ground-motion prediction. When measured velocities are unavailable, V_{S30} is estimated from proxy-based relationships developed for application on global or local scales. We describe the development of a local relationship for Greece, which begins with compilation of a profile database (PDB) from published sources and engineering reports. The PDB contains 314 sites; 238 have profile depths ≥ 30 m and 59 are within 100 m of accelerographs. We find existing relations for extrapolating a time-averaged velocity for depths less than 30 m to V_{S30} to overpredict V_{S30}. We present equations for these extrapolations. We then compile proxies for PDB sites, including terrain type, surface geology, and surface gradients at 30 and 3 arcsec resolution (from radar-derived digital elevation models [DEMs]). When checked against ground survey data, we find ground elevations from 3 arcsec DEMs to be more accurate relative to survey data than alternative 30, 9, and 1 arcsec DEMs. Drawing upon expert opinion, we develop geologic categories based on age, gradation, and depositional environment and assign such categories to PDB sites. We find an existing 30 arcsec gradient-based global model to be biased relative to local V_{S30} data for gradients >~0:05 m=m. Bias relative to a California model is also found for four of the eight well-populated geomorphic categories, and new (local) values are provided.We find statistically significant effects of the 3 arcsec gradient on V_{S30} for Quaternary and Tertiary materials but no gradient effect for those from the Mesozoic. Among Quaternary sediments, Holocene, mapped Quaternary (age unspecified), and mixed/fine-gradation materials exhibit consistent V_{S30}-gradient trends, whereas Pleistocene and coarse-gradation sediments have faster velocities. For the study region, we recommend use of the modified terrain- and geology-based methods in combination for proxy-based V^{S30} estimation.

Online Material: Profile database (spreadsheet) and figures of elevation residuals.

Introduction

Most ground-motion prediction equations (GMPEs) for major tectonic regimes worldwide use V_{S30} as the principal parameter representing site condition for the engineering characterization of site amplification. Arguments for and against V_{S30} have been presented elsewhere (Borcherdt, 1994; Castellaro et al., 2008; Seyhan et al., 2014), which wewill not repeat here. A premise for our work is simply that V_{S30} is a required parameter for the development and implementation of most major GMPEs, including those of the Next Generation Attenuation (NGA) projects (Bozorgnia et al., 2014).

The most straightforward way to evaluate V_{S30} for a given site is to measure seismic velocities to a depth of at least 30 m (deeper profiles are typically desirable to develop more complete insights of site response, but V_{S30} strictly requires a profile that is only 30 m deep). In this case, V_{S30} is simply computed as the ratio of 30 m to the shear-wave travel time through the upper 30 m of the site profile. When no geophysical data are available for a given site, V_{S30} is estimated from proxies, which may be based on geomorphology (using ground slope or terrain categories; Wald and Allen, 2007, and Yong et al., 2012, respectively), geology (e.g., Wills and Clahan, 2006), or geotechnical site categories (Chiou et al., 2008; Seyhan et al., 2014). The Wald and Allen (2007) proxy relationship is intended for global application in the sense that its proxy of ground slope at 30 arcsec resolution is globally available, and the correlation of slope to V_{S30} uses a global dataset.

Our objective in this paper is to develop local data resources and predictive tools that can be used within the study region (in this case, Greece) to estimate V_{S30}. The presumption is that such local relationships are more accurate and reliable within the applicable region than global methods. We begin by presenting a substantial profile database (PDB) developed from sources in the open literature, research reports, professional engineering reports, and personal communications. Each site in the PDB has geophysical measurements and is categorized according to proxies. We anticipate this database will be a useful product in its own right for engineering applications and future proxy-related research. We then utilize the PDB to test existing methods in the literature for extrapolating V_{SZ} (time-average velocity to depth zp) to V_{S30} when profile depths (zp) are less than 30 m. This extrapolation can be performed with relatively high confidence and substantially expands the size of the database.

The principal technical question that we address is the manner by which V_{S30} can be estimated from available proxies. We consider the proxies of surface geology, surface gradient, and geomorphic site categories. We describe a process by which geologic categories rresentative of local conditions were assigned to sites using the best-available, relatively large-scale geologic maps for Greece. We then test existing proxies for V_{S30} estimation using the PDB and, after finding shortcomings, develop recommended proxy-based relationships for V_{S30} prediction in the study region.

Using the results of this work, we develop protocols for assigning V_{S30} values and their related uncertainties to specific locations (e.g., strong-motion stations) in Greece that are of interest. These protocols are also expected to be directly useful for hazard or risk-mapping efforts within the study region when reliable geophysical data are unavailable. Moreover, the methodology developed here should be useful for other regions worldwide where there is a significant reliance on proxies for estimating site parameters.

Profile Database

Site Selection and Database Contents

The PDB is an inventory of sites in Greece where geophysical measurements have been undertaken to develop shear-wave velocity (V_S) profiles. To be included in the PDB, the profile depth must be at least 5–6 m and the data must be considered generally reliable, given local knowledge and generally accepted norms for geophysical testing. The PDB includes a relatively broad range of test types: crosshole, downhole (including seismic cone penetration tests), active and passive surface-wave methods, and seismic refraction. As with the Pacific Earthquake Engineering Research

Center Next Generation Attenuation of Ground Motions site database (Seyhan et al., 2014), we exclude refraction-microtremor-type measurements due to probable bias in V_S at depth. Inferred V_S profiles from penetration resistance data are not considered. Aside from the availability of a usable V_S profile of sufficient depth, the only other criteria for including a site in the PDB were that the measurement location be known (location is shown on the site plan or coordinates are provided) and that the data are available for use (either because it is already published or we obtained permission for its use).Ⓔ The PDB is given in Table S1 (available in the electronic supplement to this article). Figure 1 shows the locations of sites in the PDB overlayed on a geology map of Greece.

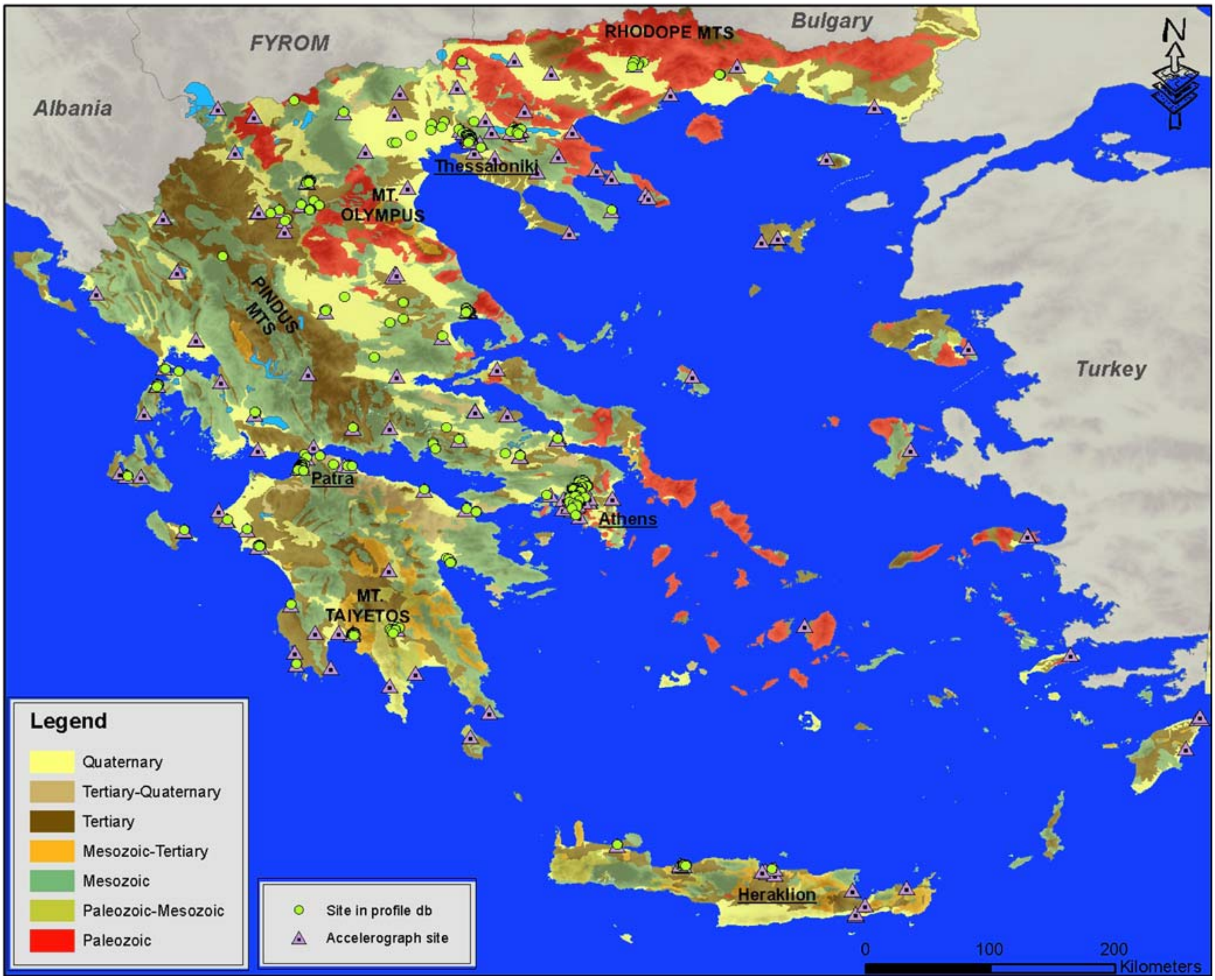

Figure 1. Geologic map of Greece showing locations of sites in profile database (PDB) and locations of strong-motion stations in site database. The geologic map used here is from digital sources (for ease of plotting) with a scale of 1:500,000. This map is for illustrative purposes only; higher-resolution maps were used to assign geologic conditions to particular sites. The color version of this figure is available only in the electronic edition.

A number of sites in the PDB have relevant information beyond the VS profile, such as a geotechnical borehole log and/or a description of local geology based on field observations by a geologist. Figure 2 shows a typical example of the available information for a site in the PDB (site number THETHE005b), including geophysical logs, borehole logs, and penetration resistance data.

The sites included in the PDB include the following:

- Strong-motion stations, many of which have been geophysically characterized for ground-motion studies. Where applicable, the distance of the profile to the nearest accelerometer is indicated in the PDB. Of the 314 sites in the PDB, 59 are located very near (within 100 m) accelerometers, and an additional 83 accelerometer sites are located within 1.0 km of a site in the PDB and have similar geology (according to Institute of Geological and Mineral Exploration [IGME] geologic maps at a scale of 1:50,000).

- Sites characterized as part of local microzonation projects or seismic-hazard/risk studies. In such cases, although V_{S30} is often mapped throughout a local area, we consider only the source measurements, not inferences of V_{S30} between measurements.

- Locations of civil infrastructure projects such as major buildings, industrial facilities, refineries, dams, pipelines, highways, tunnels, bridges, and harbors. In such cases, we utilize geotechnical design reports containing V_S profile data.

- Sites characterized as part of forensic investigations of heavily damaged regions following earthquakes (e.g., Thessaloniki, Argostoli, Aegio, Athens, Kalamata, the Kozani and Grevena area, Lefkada, and others).

Ⓔ The data source for each site in the PDB is indicated in Table S1 and includes journal and conference papers, research reports, private engineering consulting offices, and government offices.

The principal contents of the PDB are an identifier code, location (geodetic coordinates), metadata on the geophysical testing (data source, measurement type, profile depth), time-averaged shear-wave velocities over various depths (details below), surface geologic information (mapped description, assigned code, map source), ground slope gradi ents for 30 and 3 arcsec map resolutions, and geomorphic-terrain categories per Iwahashi and Pike (2007). Details on the shearwave velocity data, slope gradients, and terrain categories are given in the following subsections. Geologic categories are described in the next section.

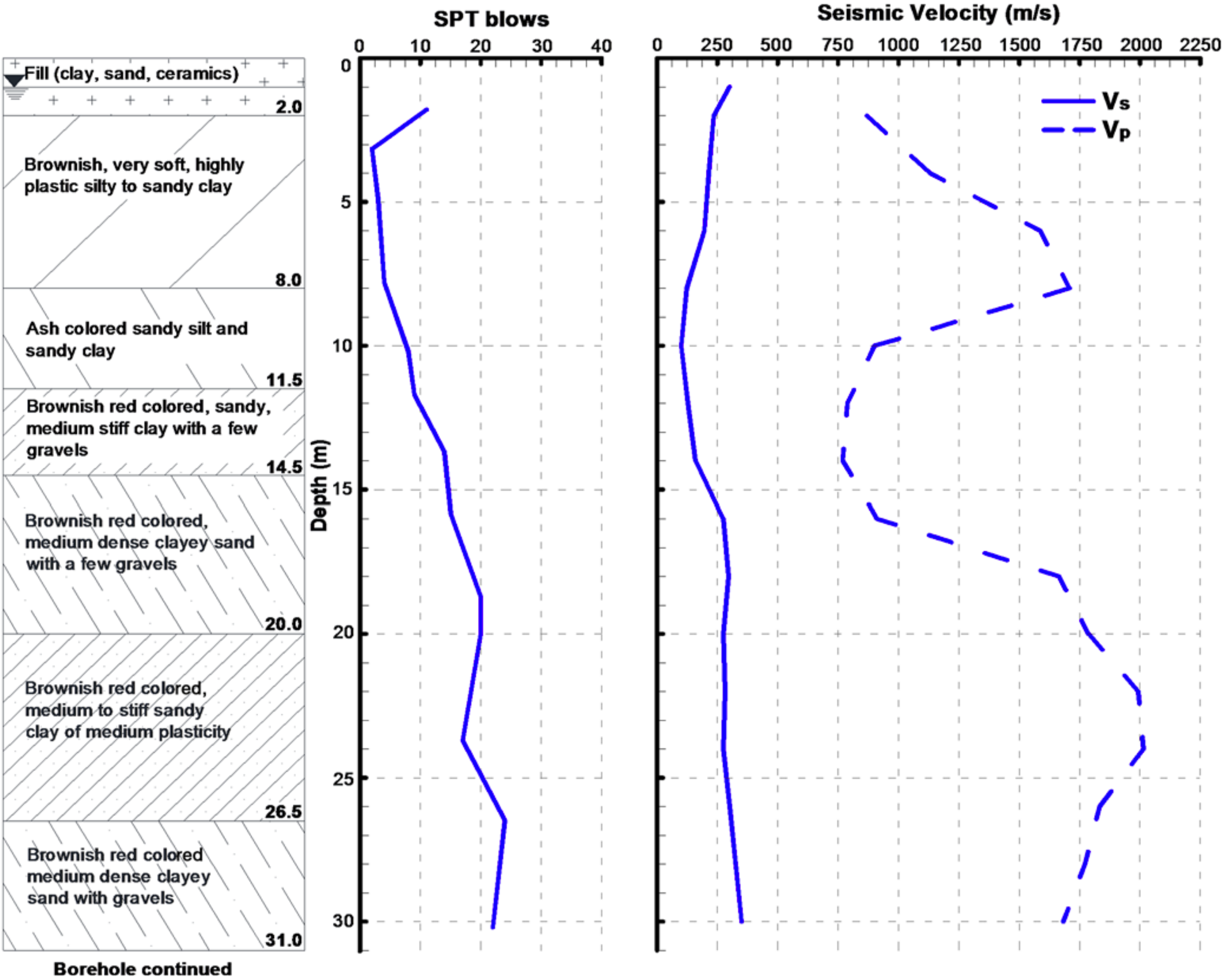

Figure 2. Example of compiled information for one site (THETHE005b) in the PDB, including seismic velocity profiles, geotechnical log, and penetration resistance. The velocity profiles in this case were derived from downhole logging. The color version of this figure is available only in the electronic edition.

VS Profile Data

Velocities shown in the PDB are V_{SZ} and V_{S30}. Velocity V_{SZ} is the time-averaged shear-wave velocity to profile depth zp and can be computed as

$$V_{SZ} = \frac{z_p}{\Delta t_z} \quad (1)$$

in which

$$\Delta t_z = \int_0^{z_p} \frac{dz}{V_S(z)} \quad (2)$$

Δt_z is the travel time for shear waves from depth z_p to the ground surface, and the integral is evaluated in practice through summation across velocities taken as constant within depth intervals. When the V_S profile extends to depths of 30 m or greater, V_{S30} can be computed directly from the profile data by replacing z_p with 30 m in equations (1) and (2).

When z_p < 30 m, V_{S30} cannot be calculated directly; this applies to 76 of the 314 sites in the PDB. Estimation of V_{S30} for these 76 sites requires V_{SZ}-to-V_{S30} extrapolation conditioned on profile depth z_p. Procedures for extrapolations of this type have been proposed by Boore (2004) and Boore et al. (2011) based on the analysis of VS profile data principally from California and Japan, respectively. Here, we test the applicability of these methods to the Hellenic data. We use 202 of the 238 sites in the PDB with $z_p \geq 30$ m (the additional 36 sites are excluded because the geophysics only provided V_{S30} and not shallower velocities), along with 23 additional sites that were excluded from the PDB solely because of unknown location (i.e., the profiles are good quality and have $z_p \geq 30$ m).

Figure 3 shows plots of V_{SZ} against V_{S30} for the 225 Hellenic sites for values of z_p = 5, 10, 14, and 20 m. The results generally indicate slower V_{S30} values for a given V_{SZ} from the Hellenic data as compared to the prior models, suggesting somewhat flatter velocity gradients on average from the Hellenic data. This discrepancy is greatest for the 5 m data, for which only the Boore et al. (2011) model has coefficients we can use for comparison. The large misfit in this case is expected because the prior model is considered applicable for relatively firm rock conditions in Japan (specifically K-NET sites with $z_p \approx 10$ m), in which the velocity gradients near the surface are often relatively steep. Because of the persistent differences, including at larger profile depths, we elected to not adopt the prior results, but instead fit the data with a linear relationship as shown in Figure 3 and given by

$$\log(V_{S30}) = c_0 + c_1 \log(V_{SZ}) \quad (3)$$

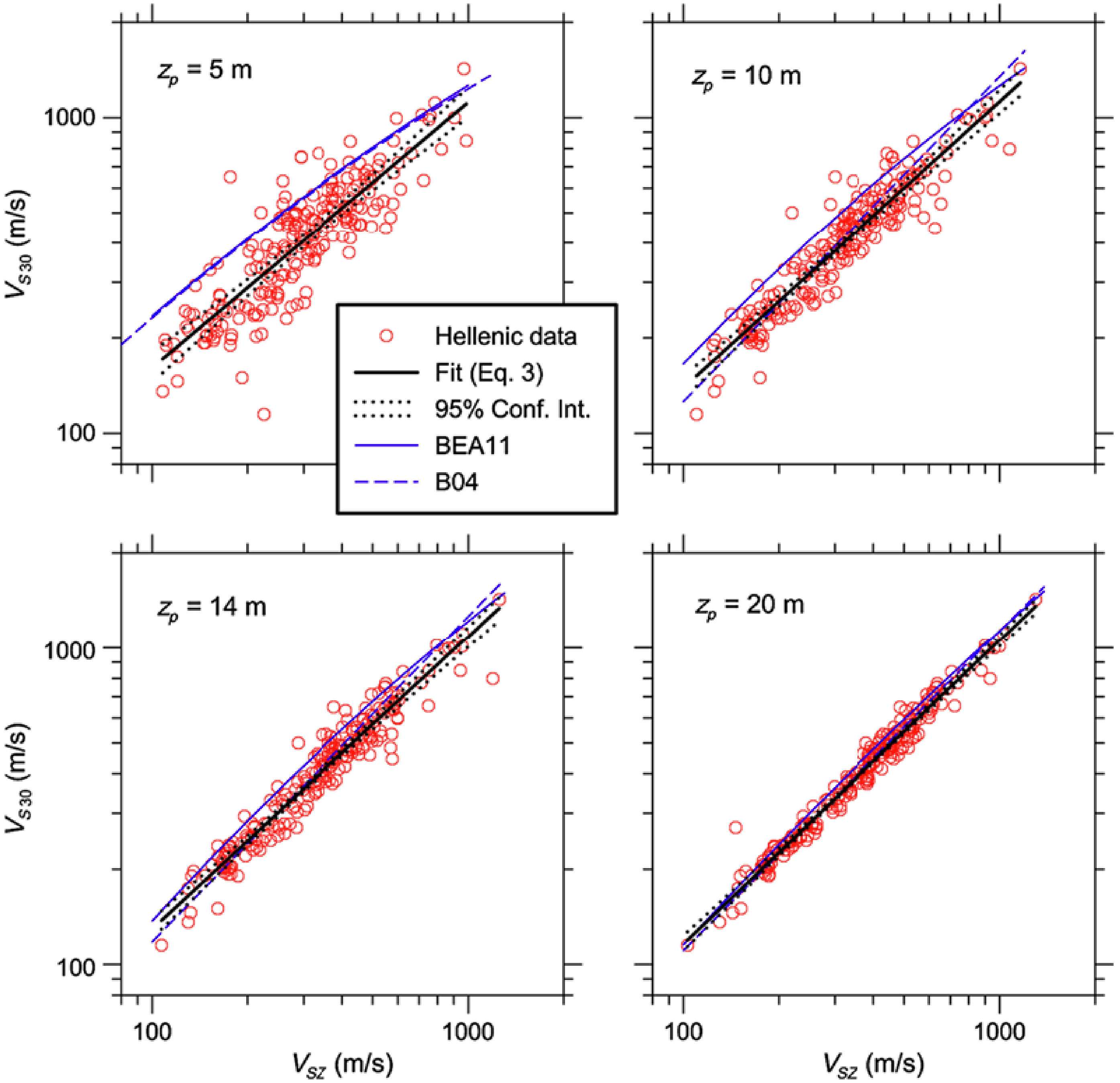

Figure 3. Comparison of VSZ–VS30 data from Greece with relationships developed by Boore (2004; shown as B04) and Boore et al. (2011; shown as BEA11). Linear fits through Hellenic data are shown with 95% confidence intervals. The color version of this figure is available only in the electronic edition.

A parabolic function was also considered but was not adopted because it produced results very similar to the linear function. In almost all cases, the prior models fall outside the confidence intervals of the present fits, suggesting statistically significant differences between the Hellenic data and the prior relations. Table 1 provides coefficients c_0 and c_1 for various profile depths between 5 and 28 m. Error term σe is the standard deviation of the fit residuals.

Because many of the sites in the PDB have profile depths z_p > 30 m, it is also possible to use the data to investigate the degree to which VS30 is correlated with deeper velocity structure. To illustrate this correlation, Figure 4 illustrates the relationship between V_{S30} and V_{S60}, which is possible for 24 sites. As shown in the figure, the two velocities are strongly correlated, with a coefficient of determination (R^2) of 0.94. This is very similar to results obtained previously for Japan by Boore et al. (2011), who investigated depths as great as 600 m. This correlation of V_{S30} with deeper velocity structure explains why V_{S30}, which is fundamentally a metric of the shallow site condition, has been found to cor-

Table 1
Model Coefficients for V_{SZ}-to-V_{S30} Extrapolation

z_p (m)	c_0	c_1	σ_e
5	0.522	0.842	0.233
10	0.331	0.907	0.156
12	0.287	0.919	0.138
14	0.261	0.925	0.121
16	0.240	0.930	0.107
18	0.165	0.955	0.086
20	0.144	0.960	0.076
22	0.088	0.978	0.054
24	0.064	0.984	0.045
26	0.038	0.991	0.033
28	0.014	0.997	0.015

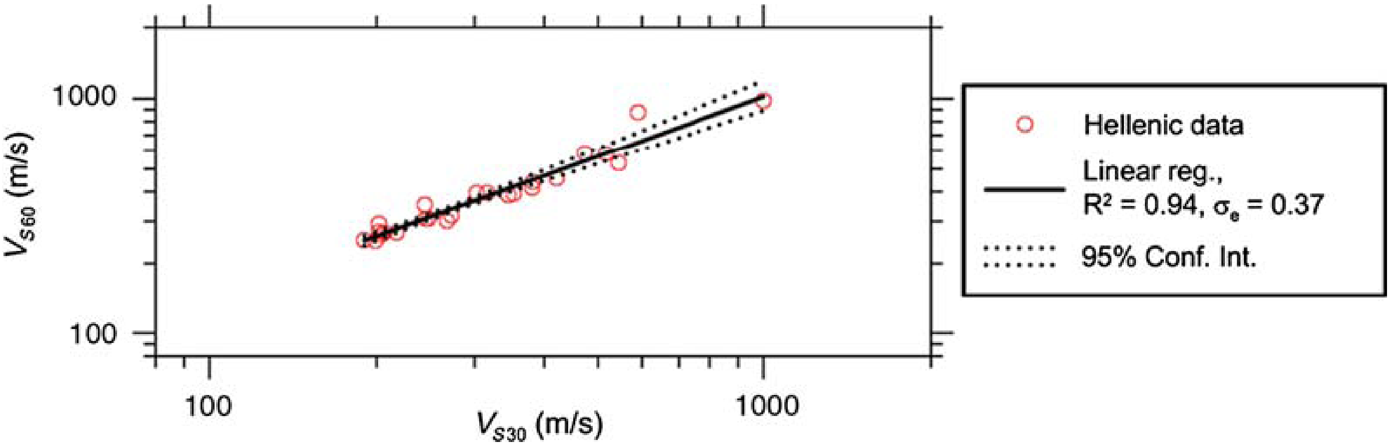

Figure 4. Relationship between VS60 and VS30 using Hellenic data. The color version of this figure is available only in the electronic edition.

relate well with site response at low frequencies involving wavelengths much longer than 30 m.

Ground Slope Gradients

The aforementioned slope gradients are based on digital elevation models (DEMs), which are available worldwide at various resolutions (30, 9, 3, and 1 arcsec) from the Shuttle Radar Topography Mission (SRTM; specific web resources used to access DEMs for the four resolution levels are indicated in the Data and Resources). For example, an SRTM map at 3 arcsec resolution will have a value for elevation on a grid of points separated horizontally by 3 arcsec in latitude and longitude. Gradients are computed by differencing elevations for adjacent points and dividing by horizontal separation distance. Given the gridded pattern of elevations, gradients can be measured in eight horizontal directions to adjacent points. To be consistent with past practice, we use the maximum of these eight gradients as computed from the grdgradient command in Generic Mapping Tool software (see Data and Resources). This process produces a map of gradients at the same level of resolution as the underlying DEM; the gradient for a given site is taken from the nearest grid point.

An important consideration when compiling gradients for proxy-based V_{S30} estimation is the level of horizontal resolution used in the gradient calculation. There are two critical factors affecting this choice: (1) possible bias in the gradient calculation and (2) the predictive power of the gradient for V_{S30}. We address the reliability of gradient calculations for the study region here; the effectiveness of gradients of different resolutions for V_{S30} estimation is examined subsequently.

Although the reliability of gradient calculations would appear to be enhanced at higher resolutions, canopy effects (e.g., from vegetation or buildings) can bias point estimates of elevations from high-resolution maps and, by extension, gradients measured from elevation changes. For example, Allen and Wald (2009) found gradients from 9 arcsec SRTM DEMs to be poorly resolved at low gradients, which was attributed to canopy effects. They considered gradients from 30 arcsec DEMs to be less affected by such effects “because the small-scale variations in elevation that are abundant in the high-resolution data are smoothed” (p. 940).

To evaluate the reliability of DEM-based elevations at different resolutions for our study region, we compiled elevations measured from ground-surveyed stations in the National Trigonometric Network (Hellenic Military Geographical Service; see Data and Resources) for comparison to the DEM elevations. Ⓔ Figures S1 and S2 show a representative example of elevation residuals (Δz is the surveyed elevation minus DEM elevations) versus surveyed elevation for resolutions of 1, 3, 9, and 30 arcsec for rural and urban areas in and surrounding Larissa (central Greece). The results show positive bias in elevations at all levels of resolution, but the smallest bias, and lowest standard deviation of residuals, occurs at 3 arcsec resolution. For the nonurban region (Ⓔ Fig. S1), bias and dispersion of Δz are highest at 30 arcsec resolution (24 and 50 m, respectively) and decrease with increasing resolution to minimums of 7.5 m (mean) and 6.8 m (standard deviation) at 3 arcsec resolution. The bias and dispersion then increase for the finest resolution considered of 1 arcsec (19 and 11 m, respectively), which we interpret as a canopy effect similar to that observed previously by Allen and Wald (2009) for other regions. The principal difference from that prior work is the level of map resolution at which the canopy effect becomes most evident (9 arcsec in the prior work, 1 arcsec here). The data for the urban region (Ⓔ Fig. S2) are relatively sparse due to its smaller size, but the same trends are evident.

On the basis of these findings, we consider gradients for elevations of 3 and 30 arcsec in the proxy development work to follow. We do not consider the 1 arcsec data due to the evidence of bias from canopy effects.

Terrain Categories

Application of the geomorphology-based scheme of Iwahashi and Pike (2007) requires information on gradient, convexity, and texture. Gradient is obtained from 30 arcsec SRTM maps, as described in the previous subsection. Local convexity, an expression of surface curvature, was derived by (1) applying a 3 × 3 Laplacian filter on DEM elevation to identify convex (positive curvature), concave (negative curvature), and planar (zero curvature) regions and (2) computing the percentage of convex cells within a 10-cell radius from any DEM grid node. Surface texture was computed by (1) identifying pits and peaks from the difference map between the original DEM and its smoothed version derived from 3 × 3 median filtering and (2) counting the number of pits and peaks within a 10-cell radius from any DEM grid node. The above three layers of geometric characteristics were then used in an automated classification framework to define 16 terrain classes using an iterative nested-means algorithm. The resulting 16 classes (Fig. 5a) range from steep (classes 1, 2, 3, 4) to gentle (classes 13, 15, 14, 16) according to the local DEM slope gradient, and from fine texture high convexity (classes 1, 5, 9, 13) to coarse texture low convexity (classes 4, 8, 12, 16), according to the other two terrain variables. Because the classification is automated, no region-specific geomorphological label can be assigned to terrain classes, although such labels could be developed based on local knowledge.

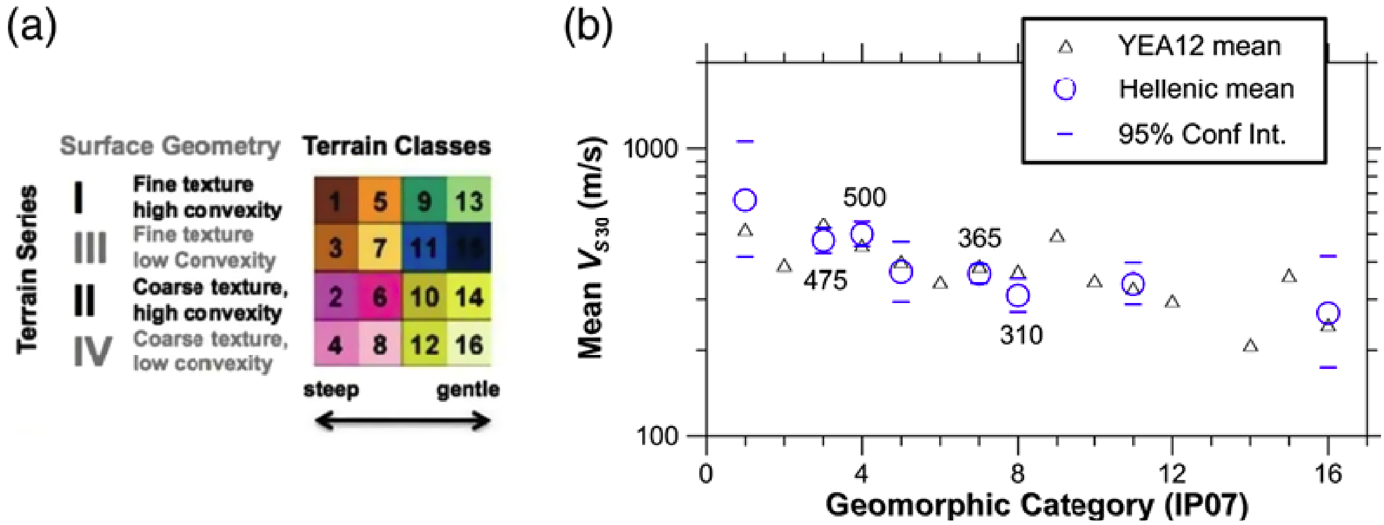

Figure 5. (a) Depiction of Iwahashi and Pike (2007) terrain categories; (b) category mean VS30 values as given by Yong et al. (2012; shown as YEA12) and from the Hellenic PDB (with confidence intervals). Numbers for categories 3, 4, 7, and 8 are category means judged sufficiently different from the YEA12 values that a change to these values is provided for applications in Greece. The color version of this figure is available only in the electronic edition.

Geologic Categories

This section concerns the use of surface geology as a proxy for VS30 estimation within Greece. Mountrakis (1985) and Higgins and Higgins (1996) provide an overview of Hellenic geology. The use of geology-related proxies to estimate V_{S30} has been surprisingly limited in scope worldwide. In California, Wills and Clahan (2006) developed 19 geologic categories for the state (many specific to certain regions) and computed V_{S30} statistics (mean and standard deviations) for profiles within those categories. That work was extended by Wills and Gutierrez (2008) to replace Quaternary categories with bins defined by 3 arcsec gradients, while retaining the use of categories for rock sites (Tertiary and Mesozoic). Scasserra et al. (2009) checked V_{S30} values for an Italian database against the category means of Wills and Clahan (2006), finding general compatibility for Quaternary categories but differences for older units. Similar to Wills and Clahan (2006), Matsuoka et al. (2006) defined categories they describe as geomorphic, but which we interpret to be more geologic in their description (e.g., mountain tertiary and alluvial fan), and compute VS30 statistics for applicable profiles within each category. Lee et al. (2001) related V_{S30}-based site categories to surface geologic conditions in Taiwan. Kottke et al. (2012) present preliminary relations between mean V_{S30} and 19 geologic categories in the central and eastern United States, although the data were only sufficient to provide stable means for nine of the categories. Within Greece, Zargli et al. (2013) investigate the relationship between geology, terrain, and slope gradient at 30 arcsec resolution but do not investigate relationships to V_{S30}. Outside of the aforementioned areas, we are not aware of other efforts in the archival literature to relate V_{S30} to geology.

Critical considerations associated with the use of geology as a V_{S30} proxy are map resolution and the consistency of mapping across the study region. Both of these issues presented challenges in the development of a geology-related proxy. The principal factor affecting resolution for paper-based maps is scale, which varies from 1:500,000 to 1:5000 in Greece. The largest scale available for the entire territory is 1:50,000 in 325 maps by the IGME (see Data and Resources). The consistency of these maps is relatively poor in the sense that the geologic terms used to describe units (lithostratigraphic and structural names) are not standardized, which results from the geologic mapping upon which the maps are based having occurred over a period of six decades by various geologists. A particular problem is that the currently used model for the geotectonic zones of Greece was developed after 1970 (Nikolakopoulos and Tsombos, 2010). There are many examples of adjacent geologic maps depicting different conditions at their boundaries, especially if one map predates the 1970 geotectonic model and its neighbor is more recent.

Despite these challenges with consistency, we utilize the IGME maps due to their relatively good resolution and general availability. Following extensive internal discussions and consultation with an experienced panel of geologists (listed in Acknowledgments), we developed the set of categories descriptive of depositional environment and material gradation shown in Table 2. These conditions can be related to the much more diverse set of geologic terms used on the maps to describe units (the total number of mapped units on the source maps is 69). The conversion of the 69 mapped units to those given in Table 2 was by expert opinion of the authors and our team of geologists. Accordingly, the PDB shows the geology as-mapped for each site, including age and lithostratigraphic description, and our interpretation of the geology based on the depositional environment and gradation as given in Table 2.

The site categorization with respect to gradation is motivated by a general understanding that fine-grained sediments tend to have lower seismic velocities than coarse grained sediments, with mixed gradation being an intermediate case. The use of gradation-based categories, especially for Quaternary sediments, is well established in prior work (e.g., Fumal, 1978; Fumal and Tinsley, 1985; Stewart et al., 2003). The categorization by depositional environment is motivated by practicality (this information is often directly indicated on geologic maps) and a general understanding that high-energy depositional environments (e.g., fast-flowing streams) produce coarser and stiffer sediments than do low-energy environments (e.g., lakes, bays, or seas). The categorization of geologic conditions according to depositional environment for ground-motion or seismic velocity studies has strong precedent in the literature (e.g., Borcherdt, 1970; Park and Elrick, 1998; Stewart et al., 2003; Wills and Clahan, 2006).

Figure 1 shows the 314 sites in the PDB relative to a map indicating geologic age. The map used in the figure is relatively small scale (1:500,000) for illustrative purposes, but the actual age assigned to a site in the PDB is based on the 1:50,000 IGME maps. The major age groups and the number of PDB sites in each are given in Table 3. A significant majority of the sites are Quaternary (Holocene, Pleistocene, or mapped Quaternary). The depositional environment

Table 2
Categories of Grain Gradation and Deposition Environment

Grain Gradation	Deposition Environment
1. Coarse grained	A. Nonmarine
2. Fine grained	Terrestrial: (1) desert, (2) loess
3. Mixed grained	Subaqueous: (3) fluvial, (4) lacustrine, (5) paludal, (6) spelean
	Glacial: (7) subglacial, (8) glacier-terminus, (9) estuarine
	B. Transitional
	(10) Deltaic
	(11) Lagoonal
	(12) Estuarine
	C. Marine
	Coastal: (13) beach, (14) tidal-flat, (15) muddy shoreline, (16) reefy shoreline, (17) prodelta
	Shelf: (18) siliciclastic, (19) carbonate
	Abyssal: (20) continental slope, (21) submarine canyon/fan/abyssal plain, (22) open deep ocean

classes of fluvial (class 3) and lacustrine (class 4) dominate the PDB sites, with 210 and 55 occurrences, respectively. Material gradations are more uniformly distributed, with 85 coarse, 46 fine, and 172 mixed occurrences.

Table 3
Breakdown of Sites in PDB According to Geologic Age

Geologic Age	Number of Sites
Holocene	94
Pleistocene	61
Mapped Quaternary (more specific age unknown)	67
Tertiary: Neogene	63
Mesozoic and Paleozoic	29

Proxy-Based VS30 Estimation

In this section, we test existing methods for V_{S30} estimation using terrain- and gradient-related proxies. Some revisions to the terrain mean VS30 values are provided as a result of misfits. We then develop a VS30 estimation procedure based on geology and gradient.

Terrain and Gradient

Wald and Allen (2007) use the proxy of ground slope gradient at 30 arcsec resolution to estimate V_{S30} using global data segregated into active crustal regions and stable continental regions (the data for active regions were from California, Italy, Taiwan, and Utah). The data indicate increasing V_{S30} with increasing gradient. The Yong et al. (2012) procedure for estimating V_{S30} considers gradient and geomorphologic factors related to convexity and texture. Those factors are jointly analyzed using an automated topography classification scheme by Iwahashi and Pike (2007) to segregate terrain types into 16 categories, which were then linked by Yong et al. (2012) to log-average V_{S30} values within the categories using data from California.

Figure 6 shows the ranges of V_{S30} provided byWald and Allen (2007) as a function of the 30 arcsec gradient, along with the data from the Hellenic PDB. Also shown are V_{S30} means and their 95% confidence intervals within approximately equally spaced gradient bins (on a log scale). We find the slope gradient proxy-based estimates to be unbiased with respect to the Hellenic data for relatively flat slopes (gradient <~0:05 m=m). For sites with steeper gradients, there is a slight overprediction bias. The bias of the model for steeper gradients is significantly less than that found for California data by Seyhan et al. (2014) but is reasonably consistent with what has been found for European data as a whole by Lemoine et al. (2012). This prior European study included few of our sites, so the present analysis comprises a largely independent check of the method. On the basis of these results, application of the 30 arcsec gradient proxy can be supported. However, as discussed further below, for the study region we are recommending a combination of gradient and geology in lieu of gradient alone. With regard to geomorphic site categories, we have computed mean V_{S30} values (specifically, the exponent of the mean of the logs) of the Hellenic data within each category and show the results in Figure 5b, along with their 95% confidence intervals. Also shown in the figure are the values provided by Yong et al. (2012) based on California data. For categories for which the California means fall very near or outside the confidence intervals for the mean of the Hellenic data, we update the category means based on the Hellenic database with the new values marked in the figure.

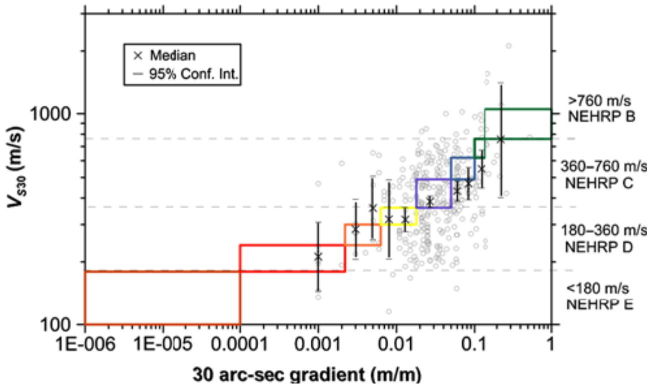

Figure 6. Trends of V_{S30} against a 30 arcsec gradient using data from Greece as compared to ranges for active crustal regions provided by Wald and Allen (2007). Binned means of data are shown with their 95% confidence interval. The color version of this figure is available only in the electronic edition.

Geology-Based Proxy

Age- and Gradient-Based Analysis. In this section, we describe the relationship between geology and V_{S30} using data from the PDB with the intention of developing recommendations specific to the study region for proxy-based estimation of V_{S30}. To begin, Figure 7 shows histograms of V_{S30} for different geologic age categories. For the Quarter-nary, we separately consider those sites mapped as Qua-ternary (i.e., no information on whether age is Holocene or Pleistocene), sites mapped into the Holocene or Pleistocene age groups, and all Quaternary (Holocene, Pleistocene, and mapped Quaternary). Through visual inspection, the histogram shape is considered to be better represented as log

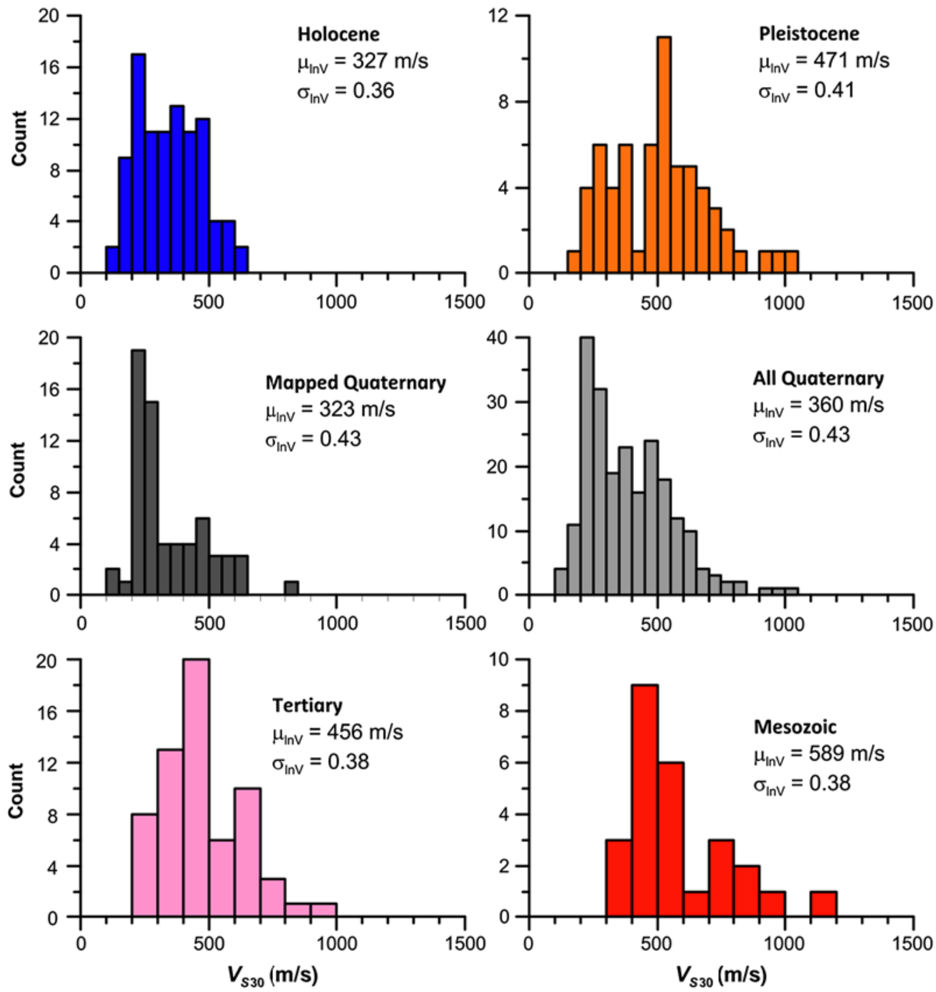

Figure 7. V_{S30} values from the PDB, sorted by geologic age. μ_{lnV} is the exponent of the mean of the logs of V_{S30}, whereas σ_{lnV} is the standard deviation of the logs. The color version of this figure is available only in the electronic edition.

normal than normal, so we compute the mean and standard deviation of logs, which are written as μ_{lnV} and σ_{lnV}, respectively.

When compared with California (Wills and Clahan, 2006), the mean VS30 values from Greece are generally higher than the California values for Quaternary (and its subsets) and Mesozoic formations (which are mostly Cretaceous for California). The California and Hellenic mean V_{S30} values are similar for Tertiary formations.

We parsed the data in various ways to investigate factors beyond age affecting V_{S30}, including gradient (at 30 and 3 arcsec resolution), depositional environment, and gradation (per Table 2). Figure 8 shows V_{S30} against 3 arcsec gradient for Quaternary sediments. For flat gradients (<~0:015), the data are dominated by the Holocene and mapped Quarternary units. For gradients of approximately 0.015–0.15, all categories are present, with Holocene data having slower velocities. In the same figure, we also show binned means (μ_{lnV}; four bins per log cycle of gradient) for Holocene, Pleistocene, and all Quaternary data. The Holocene and Quaternary trends are very similar before diverging (Q being higher) beyond a gradient of about 0.1. Pleistocene velocities are consistently higher and have a similar dependence on gradient.We fit the following power law relationship through three data sets (all Quaternary, Holocene, and Pleistocene):

$$\overline{\ln(V_{S30})} = a_0 + a_1 \ln(s) \qquad (4)$$

in which V_{S30} is in meters per second, slope gradient s is in meters/meter, coefficients a_0 and a_1 are given in Figure 8, and $\overline{\ln(V_{S30})}$ is the model prediction for a given set of coefficients and gradient. Although the Pleistocene and Holocene fits lie above and below the Quaternary fit, respectively, only the Pleistocene fit lies outside of the 95% confidence intervals for the Quaternary. Additional analyses have been undertaken for 30 arcsec gradient with similar results but slightly flatter slopes (a_1). We adopt the 3 arcsec gradient due to its slightly stronger correlation with V_{S30} in Quaternary sediments (i.e., higher a_1 terms) and slightly lower standard deviations for the Holocene and Pleistocene age groups (σ_{lnV} = 0:36 and 0.41 for 30 arcsec, as compared to 0.35 and 0.39 for 3 arcsec for the Holocene and Pleistocene, respectively).

A similar set of plots and fits are shown for the Tertiary and Mesozoic age groups in Figure 9. Because the Tertiary results are very similar to those for the Pleistocene, these two age groups were combined for regression, with the resulting fit and confidence intervals shown in the figure. The Mesozoic velocities do not have a significant trend with gradient, hence the use of the category mean from Figure 7 is recommended over the power law relationship. A similar lack of trend in velocity with gradient for Mesozoic sites was found by Wald et al. (2011).

Effects of Material Gradation and Depositional Environment. To investigate possible effects of material gradation, we plot the Quaternary data in Figure 10 (as in Fig. 8) with the data points segregated according to coarse, fine, and mixed

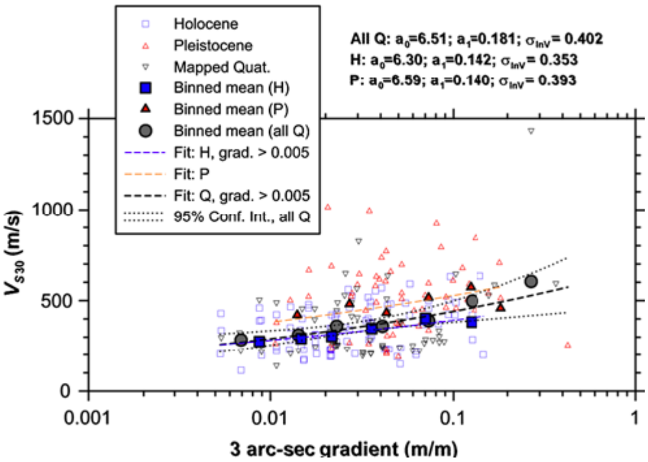

Figure 8. V_{S30} compared with gradient for Quaternary data, with binned means and fit curves per power law relationship (equation 4). 95% confidence intervals for Quaternary fit encompass the Holocene fit, suggesting the difference is not statistically significant, whereas the Pleistocene fit is at faster velocities that are generally above the confidence intervals. The color version of this figure is available only in the electronic edition.

gradations. The data reflect the expected pattern of coarse sites at steeper gradients and fine/mixed sites at flatter gradients. Also shown are power law fits (equation 4) for the coarse and mixed gradation groups. The fine gradation group is poorly populated but is generally similar to the mixed group. The coarse fit falls well above the confidence intervals for the mixed fit, indicating that the differences between these groups are statistically significant. The coarse group also has higher dispersion than most geologic categories considered previously. Although not shown in Figure 10 directly, the mixed fit is quite close (yet slightly lower) than the Quaternary fit in Figure 8. The corresponding regression coefficients for the two well-populated classes are given in Figure 10. Until more information becomes available, the fine group can be approximated using coefficients for the mixed group. Overall, these data indicate that material gradation is a viable indicator for V_{S30} estimation in Quaternary sediments. For Tertiary sites, the

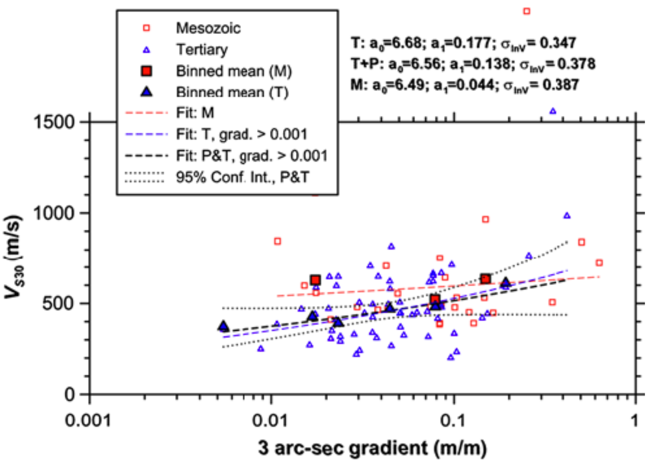

Figure 9. V_{S30} compared with gradient for Tertiary (T) and Mesozoic (M) data, with binned means and fit curves per power law relationship (equation 4). Because the Tertiary results are similar to those from the Pleistocene (P), these categories are combined with the resulting fit shown (P&T). Note that the Tertiary fit is well within the 95% confidence intervals for the combined P&T results. The Mesozoic fit is at faster velocities generally above the P&T confidence intervals and has no significant trend with gradient. The color version of this figure is available only in the electronic edition.

material gradations are almost entirely mixed and fine (with similar means); the coarse group contains only seven sites in this case. Accordingly, we have not developed gradation-based fits for Tertiary sites.

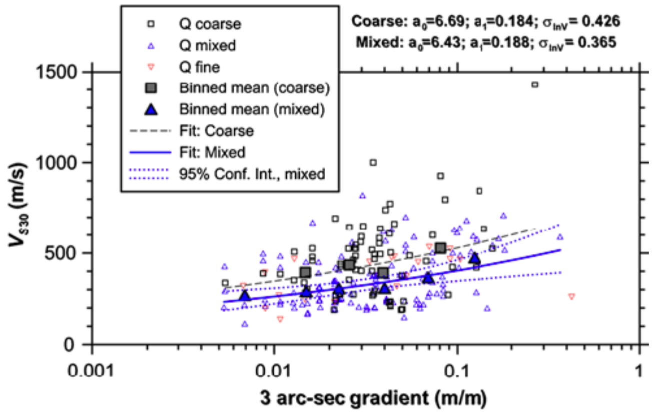

Figure 10. V_{S30} compared with gradient for Quaternary sediments, sorted by material gradation. Binned means and fit curves per power law relationship (equation 4) are shown for the wellpopulated coarse and mixed groups. The coarse fit is above the 95% confidence intervals for the mixed group, so the two categories are judged to be distinct. The color version of this figure is available only in the electronic edition.

The gradation-based Quaternary coefficients given in Figure 10 do not account for the previously observed trend of Pleistocene sites having relatively fast velocities as compared to other Quaternary sites (Fig. 8). To investigate Pleistocene misfit, we compute velocity residuals (RV) as

$$R_V = \ln(V_{S30}) - \overline{\ln(V_{S30})} \qquad (5)$$

Figure 11 indicates these residuals for Pleistocene sites, which have a flat trend with respect to gradient and a bias (i.e., mean of residuals, $\bar{R}_V$) of 0.145, indicating model underprediction. As also indicated in the figure, residuals for all other age groups are practically zero. The bias for the Pleistocene can be removed by adding 0.145 to a0 for these sites when using the material gradation equations.

We were unable to consider depositional environment as a means by which to parse the Quaternary data because the vast majority of sites (87%) are fluvial, with the remainder mixed among various categories (mostly lacustrine). Because meaningful statistics could not be compiled for these other categories, we have no basis for judging distinction from fluvial. For Tertiary sites, the situation is marginally better, although in this case it is the fluvial category that is sparsely populated with nine sites. We present histograms for fluvial and (the relatively well-populated) lacustrine groups in Figure 12. As expected, lacustrine sites are softer on average than fluvial, but more data will be needed before proxies that consider depositional environment can be provided.

Recommended Geology-Based Approach for V_{S30} Estimation. When V_{S30} is to be estimated using a geology-based proxy within the study region (Greece), we recommend the following:

1. Quaternary sediments: Use equation (4) with the applicable gradation group and its associated coefficients in Figure 10.

    - Exception: If the Quaternary age is Pleistocene, add0.145 to the a0 values in Figure 10.

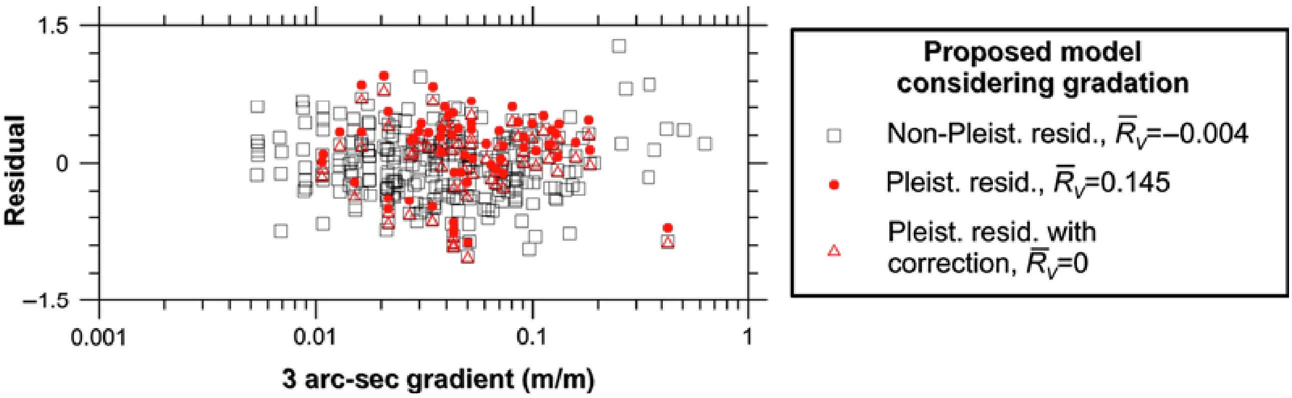

Figure 11. Residuals compared with the gradient for non-Pleistocene and Pleistocene sites. Data residuals are computed relative to proposed power law relationship (equation 4). Gradation-based coefficients are applied for the Quaternary. For the Tertiary and Mesozoic, we apply T coefficients from Figure 9 and the binned mean from Figure 7, respectively. The color version of this figure is available only in the electronic edition.

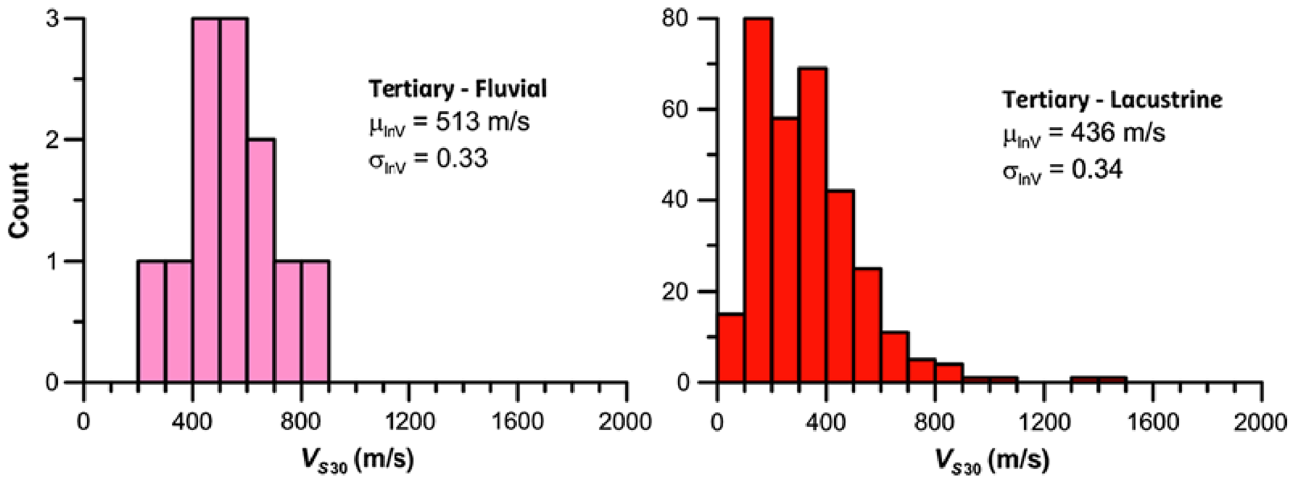

Figure 12. VS30 values from Tertiary sites, sorted by depositional environment. We consider the data to be too sparse to consider depositional environment for VS30 estimation. The color version of this figure is available only in the electronic edition.

- If material gradation is unknown and the geologic age is Holocene or Quaternary (subgroup not specified), use equation (4) with the "all Q" coefficients in Figure 8.

- If material gradation is unknown and geologic age isPleistocene, use equation (4) with the "P&T" coefficients in Figure 9.

2. Tertiary rock sites: Use equation (4) with the "P&T" coefficients in Figure 9.

3. Mesozoic sites: Use the category mean of 589 m/s (equivalent to a_0 = 6:378 and a_1 = 0).

Implementation

Proxies and Weighting

Best practices in site characterization are to develop full V_S profiles (extending to rock) derived from geophysical data. When it is necessary to estimate VS30 for sites lacking such data, given currently available proxy relationships (including those in this paper), there are three options for sites in Greece: (1) the gradient-based approach of Wald and Allen (2007), (2) the terrain-based approach of Yong et al. (2012) with the updated category means shown in Figure 5, and (3) the geology and gradient proxy presented in the previous section.

We recommend use of the latter two approaches, not the gradient-only approach of Wald and Allen (2007). That approach is marginally less desirable due to misfit in some gradient groups (Fig. 6) and modest correlation between the 30 arcsec slope gradients and the 3 arcsec gradients considered in the proposed geology-based proxy (the approximate range of correlation coefficients is 0.3–0.6 depending on geologic category). It should be emphasized that because the Wald and Allen (2007) approach is based on a globally available proxy, it will be the only practical approach for many regions around the world. Our recommendation of alternates in this case is predicated on the availability of a suitable local proxy relationship.

Because we are recommending two proxy methods, there will be two estimates of VS30 for any given site lacking measurements. Protocols developed in the NGA-West 2 project (Seyhan et al., 2014) are to compute a weighted average of available proxy-based V_{S30} values, with the weights inversely related to the residual sum of squares (i.e., $\bar{R}_V^2 + \sigma^2_{\ln V}$). In our case, the mean biases ($\bar{R}_V$) are practically zero, because the proxies are applied in the region that produced the data used in their development. Thus, the weights are dependent only on the variance of residuals ($\sigma^2_{\ln V}$). The overall standard deviations for the two approaches are 0.396 and 0.394, respectively. Given that these are practically identical, the two proxies can be equally weighted.

Standard Deviation of VS30 for Sites with Measurements

When multiple VS profiles are developed for a given site, between-profile variations of VS will be encountered and different VS30 values will be computed for each profile. The

V_{S30} dispersion among profiles is denoted $\sigma_{\ln V}$, as with the proxies.

In the NGA-West 2 project, $\sigma \ln V$ was computed for sites in active crustal regions worldwide having multiple measurements. Separation distances were on the order of 10 to about 100 m, and only measurement methods considered reliable were used. As described by Seyhan et al. (2014), these calculations showed that variations among measurement types were small and the principal factor causing high variability is when the surface geology is variable across the site. Excluding such conditions, the range of $\sigma_{\ln V}$ was approximately 0.02–0.12, with an average of about 0.06. A value of 0.1 was applied to sites with measurements in the NGA-West 2 site database.

There are eight clusters of sites in Greece where this analysis can be applied, with the results in Table 4. The values of $\sigma_{\ln V}$ range from 0.02 to 0.16, with an average of 0.09. These results support the value of 0.1 applied in NGA-West 2.

Table 4
Clusters of VS Profiles for which Group Statistics can be computed

Site Cluster (3 or more)	V_{S30} Values (m/s)	$\mu_{\ln V}$	$\sigma_{\ln V}$
AIGAMY: 002a, 004c, 003d, 003a	463, 545, 466, 524	498	0.083
ATHPIR047: a, b, c	514, 547, 701	582	0.164
ATHPIR: 054b, 055a, 056b, 057b	299, 267, 280, 329	293	0.090
KALKAL: 006a, 007a, 008a	402, 518, 525	478	0.150
KORKOR: 001a, 001b, 001c	356, 333, 374	354	0.058
LEFLEF: 001a, 002a, 003e	218, 273, 276	254	0.133
PATPAT: 010a, 011a, 012a, 012e	376, 381, 369, 385	378	0.018
VLVZAG: 007e, 008a, 008c, 008e	234, 217, 234, 210	224	0.044

The spacing between profiles is generally 100 m or less.

Protocols for Assigning VS30 and Its Uncertainty

The results of this research will be applied subsequently for establishing a site database for recording stations in Greece. On the basis of the findings presented here, a value of V_{S30} and its uncertainty can be assigned to any site with a known location, as given in Table 5.

Discussion and Conclusions

The time-averaged shear-wave velocity in the upper 30 m of a site (V_{S30}) is commonly used as the principal site parameter for ground-motion prediction. Parameter V_{S30} and other metrics of site condition used in GMPEs (principally depth to a VS horizon) are best developed from site-specific measurements. However, it is common that such data are unavailable, which necessitates V_{S30} estimation from proxies. Because of regional variations in geologic conditions, proxy-based estimation of VS30 is best undertaken at a local level, as seemingly similar conditions in different regions can have different velocity structures. This has been shown in past work to be particularly true for rock-site conditions (Scasserra et al., 2009).

In this paper, we describe the results of a large project having the goal of enabling reliable, proxy-based estimates that are customized for a local region (in this case, Greece). The process begins with the exacting task of assembling a database of VS profiles, the PDB. Our PDB was compiled from published sources and a variety of research and engineering reports. It contains 314 sites, 238 of which have profile depths of 30 m or more and 59 of which are near (within 100 m) strong-motion stations. In addition to basic site information (name, location), the PDB includes information on geophysical test type, profile depth, time-averaged shear-wave velocity to the profile depth (V_{SZ}), and V_{S30}. We utilize the data for sites with profile depths $z_p \geq 30$ m to test V_{SZ}-to-V_{S30} extrapolation methods from the literature that have been developed principally from data from California and Japan. We find these models overpredict V_{S30} for Hellenic sites, suggesting flatter gradients in Greece. We present depth-dependent linear models for performing this extrapolation. We also use the subset of the data having profile depths significantly more than 30 m to illustrate a phenomenon widely observed elsewhere—the strong correlation of VS30 to time-averaged velocities for greater depths. We demonstrate this feature using a profile depth of 60 m.

A major aspect of our project was to compile proxies for all PDB sites, including ground slope gradient at 30 and 3 arcsec resolution, terrain type as given by Iwahashi and Pike (2007), and surface geology. Surface geology was a particular challenge, due principally to lack of consistent naming conventions for geologic units. We overcame this problem by consulting with a network of local expert geologists to develop uniform criteria for characterization of local geology for use in V_S-related applications. The results, given in Table 2, provide five age categories, three material gradation categories, and 22 depositional environment categories. The most well-populated conditions are Quaternary sediments of coarse or mixed gradation, derived from fluvial or lacustrine depositional environments. There are also a significant number of rock sites, mostly in the Tertiary age group (Neocene).

Table 5
Recommended Protocols for Assigning V_{S30} and Its Uncertainty to Recording Stations

Code	Data Source Type
0	Assign from measured velocity profile with $z_p \geq 30$ m in proximity of site (within approximately 100 m). $\sigma_{\ln V} = 0.1$.
1	Estimate from measured velocity profiles with depths $10 \leq z_p < 30$ m and located within approximately 100 m using $V_{SZ} - V_{S30}$ relationships described above. $\sigma_{\ln V} = \sqrt{0.1^2 + \sigma_e^2(z_p)}$, in which the depth-dependent σ_e is from Table 1.
2	Estimate from velocity profile at a different site but in the vicinity of instrument (generally within 1 km) on the same surface geology. $\sigma_{\ln V} = 0.2$ if $z_p \geq 30$ m. $\sigma_{\ln V} = \sqrt{0.2^2 + \sigma_e^2(z_p)}$ if $z_p < 30$ m.
3	Inferred from average of terrain- and geology-related proxies as given above ($\sigma_{\ln V} = 0.4$).

The lowest code number that can be applied given the available site data should be used.

We plot the data against the Wald and Allen (2007) gradient-based model, and find the model to overpredict the V_{S30} data for 30 arcsec gradients >~0:05 m=m. Bias is also found for four of the eight well-populated geomorphic categories, and new values are provided when previous values from Yong et al. (2012) are rejected by the data. These differences confirm the presence of variable geophysical conditions, even for apparently similar geology, in the local application region of Greece as compared to California and Japan (where most of the prior data was derived).

We develop a geology-based V_{S30} estimation procedure by plotting the data within geologic classes against gradient. We find that gradients measured at 3 arcsec resolution produce stronger trends (i.e., steeper slopes in V_{S30}-gradient space), and reduced dispersion, than results for 30 arcsec. We find an effect of gradient for Quaternary and Tertiary materials, but no gradient effect for those from the Mesozoic. Among Quaternary sediments, Holocene, mapped Quaternary (age unspecified), and mixed/fine gradation materials exhibit reasonably consistent V_{S30}-gradient trends, whereas Pleistocene and coarse-gradient sediments exhibit faster velocities. We develop a simple procedure for VS30 estimation that considers these factors. For application, we recommend giving equal weight to estimates from the modified terrain-based method and the proposed geology-based method.

One of the principal applications of a PDB and proxies for V_{S30} estimation is to establish site parameters for use in the development of GMPEs. Such applications require site parameters at each recording station. We provide protocols that emphasize the use of data when they are available and proxies otherwise. We also provide recommendations on the uncertainty of V_{S30}, which is established from residuals analysis for the proxies, and from analysis of clustered V_S profiles for V_{S30} established from data. The results are used for ongoing ground-motion research conducted for Greece.

Limitations of our study are that certain geologic conditions are poorly represented (especially hard rock), and site parameters considered in some GMPEs are not addressed directly (site period and the depth to shear-wave horizon).

Data and Resources

The velocity profile data utilized in this study are derived from a variety of sources, including the open literature, research reports, and reports from private consulting engineers and government offices.Ⓔ Sources for individual profiles are given in the electronic supplement materials. The information directly used in the analyses presented in this paper is presented in its entirety in the electronic supplement.

The following digital elevation models (DEMs) were used to obtain gradients considered in this study: a nearglobal, 30-arcsec-resolution, DEM comprising a combination of data from the Shuttle Radar Topography Mission (SRTM), flown in February 2000, and the U.S. Geological Survey (USGS) GTOPO30 data set (https://lta.cr.usgs.gov; last accessed May 2014); 9 arcsec resolution model obtained from ACE2 (http://tethys.eaprs.cse.dmu.ac.uk/ACE2/; last accessed May 2014), which is also SRTM based; a 3 arcsec DEM from USGS SRTM Digital Terrain Elevation Data (DTED) Level 1 (https://lta.cr.usgs.gov; last accessed May 2014); and a 1 arcsec DEM, from the National Aeronautics and Space Administration website, The Advanced Spaceborne Thermal Emission and Reflection Radiometer (ASTER) Global Digital Elevation Model (GDEM) (http://asterweb.jpl.nasa.gov/; last accessed May 2014). SRTM data at 1 arcsec resolution are not available for Greece from the USGS. Gradients were computed from elevation data using the grdgradient command in Generic Mapping Tools software (http://gmt.soest.hawaii.edu/, last accessed May 2014).

Elevation data used for the validation of DEM-based gradients were obtained from the Hellenic Military Geographical Service, National Trigonometric Network website (http://web.gys.gr/portal/page?_pageid=33,36834&_dad=portal&_schema=PORTAL; last accessed May 2014).

The geology discussed in our work was based on various maps from the Institute of Geological and Mineral Exploration (IGME), available as Geologic Sheets of Greece in 1:50.000 scale, www.igme.gr (last accessed May 2014).

Acknowledgments

This research was partially co-funded by the following research projects: (1) European Union (European Social Fund [ESF]) and Hellenic national funds through the Operational Program "Education and Lifelong Learning" of the National Strategic Reference Framework (NSRF)—Research Funding Program "THALES"; (2) European Neighborhood and Partnership Instrument (ENPI) and Hellenic national funds in the framework of the cross-border cooperation program, Black Sea Basin Joint Operational Project 2007–2013 (MIS-ETC 2614); and (3) "ARCHIMIDIS III: Research Teams Reinforcement in ASPETE" (MIS: 383576) of the Operational Program "Education and Lifelong Learning," co-funded by the European Union and national funds.

We extend sincere thanks to the panel of geologists who assisted with the assignment of geologic categories for profile database (PDB) sites, including V. Marinos, P. Marinos, K. Papatheodorou, D. Rozos, N. Nikolaou, and K. Dimaras. We also thank R. E. Kayen, who assisted with V_S profiling for some sites in the PDB, and Dimitri Atmatzidis who assisted in the procurement of essential equipment for V_S profiling. Students T. Bika, F. Kapeti, and A. Kokkinou of the Institute of Engineering Seismology & Earthquake Engineering (Greece), as well as E. Psaroudakis, K. Iordanis, El. Petala, Th. Lazaridis, Ch. Charharidi, and K. Mimidis of the Democritus University of Thrace, who assisted in the compilation of the PDB. Finally we thank David Wald of the U.S. Geological Survey and one anonymous reviewer for their insightful comments.

References

Allen, T. I., and D. J.Wald (2009). On the use of high-resolution topographic data as a proxy for seismic site conditions (VS30), Bull. Seismol. Soc. Am. 99, 935–943.

Boore, D. M. (2004). Estimating VS30 (or NEHRP site classes) from shallow velocity models (depths < 30 m), Bull. Seismol. Soc. Am. 94, 591–597.

Boore, D. M., E. M. Thompson, and H. Cadet (2011). Regional correlations of V_{S30} and velocities averaged over depths less than and greater than 30 m, Bull. Seismol. Soc. Am. 101, 3046–3059.

Borcherdt, R. D. (1970). Effects of local geology on ground motion near San Francisco Bay, Bull. Seismol. Soc. Am. 60, 29–61.

Borcherdt, R. D. (1994). Estimates of site-dependent response spectra for design (methodology and justification), Earthq. Spectra 10, 617–653.

Bozorgnia, Y., N. A. Abrahamson, L. Al Atik, T. D. Ancheta, G. M. Atkinson, J. W. Baker, A. Baltay, D. M. Boore, K. W. Campbell, B. S.-J. Chiou, et al. (2014). NGA-West2 research project, Earthq. Spectra 30, 973–987.

Castellaro, S., F. Mulargia, and P. L. Rossi (2008). V_{S30}: Proxy for site amplification? Seismol. Res. Lett. 79, 540–543.

Chiou, B. S.-J., R. Darragh, D. Dreger, and W. J. Silva (2008). NGA project strong-motion database, Earthq. Spectra 24, 23–44.

Fumal, T. E. (1978). Correlations between seismic wave velocities and physical properties of near-surface geologic materials in the southern San Francisco Bay region, California, U.S. Geol. Surv. Open-File Rept. 78-1067, 114 pp.

Fumal, T. E., and J. C. Tinsley (1985). Mapping shear wave velocities of near surface geologic materials, in Evaluating Earthquake Hazards in the Los Angeles Region—An Earth-

Science Perspective, J. E. Ziony (Editor), U.S. Geol. Surv. Profess. Pap. 1360, 101–126.

Higgins, M. D., and R. Higgins (1996). A Geological Companion to Greece and the Aegean, Duckworth Publishers, Ithaca, New York.

Iwahashi, J., and R. J. Pike (2007). Automated classifications of topography from DEMs by an unsupervised nested-means algorithm and a threepart geometric signature, Geomorphology 86, nos. 3/4, 409–440.

Kottke, A. R., Y. M. A. Hashash, J. P. Stewart, C. J. Moss, S. Nikolaou, E. M. Rathje, W. J. Silva, and K. W. Campbell (2012). Development of geologic site classes for seismic site amplification for central and eastern North America, Proc. 15th World Conf. on Earthquake Eng., Lisbon, Portugal, 24–28 September 2012, Paper Number 4557.

Lee, C.-T., C.-T. Cheng, C.-W. Liao, and Y.-B. Tsai (2001). Site classification of Taiwan free-field strong-motion stations, Bull. Seismol. Soc. Am. 91, 1283–1297.

Lemoine, A., J. Douglas, and F. Cotton (2012). Testing the applicability of correlation between topographic slope and VS30 for Europe, Bull. Seismol. Soc. Am. 102, 2585–2599.

Matsuoka, M., K.Wakamatsu, F. Fujimoto, and S. Midorikawa (2006). Average shear-wave velocity mapping using Japan engineering geomorphologic classification map, J. Struct. Mech. Earthq. Eng. 23, 57s–68s.

Mountrakis, D. M. (1985). The Geology of Greece, University Studio Press, Thessaloniki, Greece.

Nikolakopoulos, K., and P. Tsombos (2010). Updating the 1:50.000 geological maps of IGME with remote sensing data, GPS measurements and GIS techniques: The case of Antiparos Island, in Remote Sensing for Science, Education, and Natural and Cultural Heritage (EARSel), R. Reuter (Editor), European Association of Remote Sensing Laboratories, Paris, France, 281–287.

Park, S., and S. Elrick (1998). Prediction of shear wave velocities in southern California using surface geology, Bull. Seismol. Soc. Am. 88, 677–685.

Scasserra, G., J. P. Stewart, R. E. Kayen, and G. Lanzo (2009). Database for earthquake strong motion studies in Italy, J. Earthq. Eng. 13, 852–881.

Seyhan, E., J. P. Stewart, T. D. Ancheta, R. B. Darragh, and R. W. Graves (2014). NGA-West2 site database, Earthq. Spectra 30, 1007–1024.

Stewart, J. P., A. H. Liu, and Y. Choi (2003). Amplification factors for spectral acceleration in tectonically active regions, Bull. Seismol. Soc. Am. 93, 332–352.

Wald, D. J., and T. I. Allen (2007). Topographic slope as a proxy for seismic site conditions and amplification, Bull. Seismol. Soc. Am. 97, 1379–1395.

Wald, D. J., L. McWhirter, E. Thompson, and A. Hering (2011). A new strategy for developing VS30 maps, Proc. 4th Int. Effects of Surface Geology on Seismic Motion Symp., Santa Barbara, California, 23–26 August 2011, 12 pp.

Wills, C. J., and K. B. Clahan (2006). Developing a map of geologically defined site-condition categories for California, Bull. Seismol. Soc. Am. 96, 1483–1501.

Wills, C. J., and C. Gutierrez (2008). Investigation of geographic rules for improving site-conditions mapping, Calif. Geo. Sur. Final Tech. Rept. 20 pp. (Award Number 07HQGR0061).

Yong, A., S. E. Hough, J. Iwahashi, and A. Braverman (2012). Terrain-based site conditions map of California with implications for the contiguous United States, Bull. Seismol. Soc. Am. 102, 114–128.

Zargli, E., S. Liodakis, P. Kyriakidis, and A. Savvaidis (2013). Classification of topography using DEM data and its correlation with the geology of Greece, 1st Int. Conf. on Remote Sensing and Geoinformation of the Environment (RSCy2013), D. G. Hadjimitsis, K. Themistocleous, S. Michaelides, and G. Papadavid (Editors), Proc. of SPIE, Vol. 8795, 87950S.

Bulletin of the Seismological Society of America, Vol. 104, No. 6, pp. –, December 2014, doi: 10.1785/0120130331

ΝΕΑ ΑΠΟ ΤΙΣ ΕΛΛΗΝΙΚΕΣ ΚΑΙ ΔΙΕΘΝΕΙΣ ΓΕΩΤΕΧΝΙΚΕΣ ΕΝΩΣΕΙΣ

ISSMGE Technical Committee
TC203 Earthquake Geotechnical Engineering and Associated Problems
www.earthquake-issmge.org

In Memoriam: Professor Michele Maugeri

On 1 November 2014, after a strong battle against illness, Professor Michele Maugeri passed away. Prof. Maugeri was a long-time Italian member of the ISSMGE Technical Committee on 'Earthquake Geotechnical Engineering and Associated Problems' (TC203).

Born in Acireale (Sicily) in 1944, he got the degree in Civil Engineering from the Politecnico di Torino, winning the award for the best thesis ("Technical aspects of a bridge across the Messina Strait") and the second prize in an international competition for the fixed link road and railway between Sicily and the mainland, banned by the Ministry of Public Works.

The brilliant academic career developed at the University of Catania, where he was teaching since 1972, becoming Associate Professor in 1979 and then Full Professor of Geotechnical Engineering in 1990. His career was full of countless tasks of primary importance: he was a member of the Board of Public Works, member of the National Commission UNI "Construction Structural Engineering", member of the Task Group no. 6 on "Geotechnical Earthquake Engineering and Microzonation" of the European Association for Earthquake Engineering, chairman of the "ERTC 12 - Evaluation of Geotechnical Aspects of EC8", member of scientific and organizing committees of numerous national and international conferences.

He also actively contributed to the life of his native Sicily, as a director of Banca Popolare Santa Venera at Acireale, and of Credit Valtellina today.

He was Guest Editor of several special issues of national and international journals (including the recent issue n.3 of the Bulletin of Earthquake Engineering in 2014) and authored more than 300 scientific publications.

Since 1990, Prof. Maugeri delivered keynote and special lectures in international conferences and workshops of different disciplines, helping extend the TC203 mission beyond the core industry. Recently, Prof. Maugeri was the Chairman of the very successful 2nd International Conference on "Performance-Based Design in Earthquake Geotechnical Engineering" of TC203, held in Taormina, 2012.

He was a scientific "ambassador" of geotechnical earthquake engineering at events organized by other learned societies. He often focused on engineering issues relevant to Italy in the fields of seismic geotechnics, mitigation of natural hazards and geosynthetics. Through his contributions, the Italian geotechnical community has maintained a strong and beneficial dialogue with the world.

He died at his home in Sicily, just one day after he retired from University of Catania. Burial services were held on November 3 at the cathedral in his home town of Acireale. We extend our thoughts and sympathies to his family and friends. He will be remembered warmly and missed by many of us.

Ciao, Michele.

ΔΙΑΚΡΙΣΕΙΣ ΕΛΛΗΝΩΝ ΓΕΩΜΗΧΑΝΙΚΩΝ

Ο καθηγητής της Σχολής Πολιτικών Μηχανικών ΕΜΠ **Γιώργος Γκαζέτας** προσκλήθηκε από τους διοργανωτές του 12th Australia New Zealand Conference on Geomechanics (ANZ 2015) να παρουσιάση την πρώτη Keynote Presentation του συνεδρίου, την Κυριακή 22 Φεβρουαρίου 2015, με τίτλο «Avoiding Over-Conservatism and Conventional Dogmas in Seismic Geotechnical Design».

ΠΡΟΣΕΧΕΙΣ ΓΕΩΤΕΧΝΙΚΕΣ ΕΚΔΗΛΩΣΕΙΣ

Για τις παλαιότερες καταχωρήσεις περισσότερες πληροφορίες μπορούν να αναζητηθούν στα προηγούμενα τεύχη του «περιοδικού» και στις παρατιθέμενες ιστοσελίδες.

7th International Conference on Scour and Erosion (ICSE-7), 2nd – 4th December 2014, Perth, Western Australia, http://www.2014icse.com

Underground Infrastructure & Deep Foundations UAE, 7-10 December 2014, Dubai, United Arab Emirates, enquiry@iqpc.ae, ujwal.nayak@iqpc.com, www.iqpc.com

2nd Arabian Tunnelling Conference and Exhibition Abu Dhabi, United Arab Emirates, 9-10 December 2014, www.atc2014.ae

Third Australasian Ground Control in Mining Conference 2014, Sydney, Australia, www.mining.unsw.edu.au/node/608

Proceedings of the Institution of Civil Engineers, Geotechnical Engineering, THEMED ISSUE 2015, Construction processes and installation effects, Editors: Benoît Jones, University of Warwick, UK and Stuart Haigh, University of Cambridge, UK, sarah.walker@ice.org.uk

IGS Chennai 2015 6th International Geotechnical Symposium on Disaster Mitigation in Special Geoenvironmental Conditions, January 21-23, 2015, IIT Mandras, Chennai, India, http://igschennai.in/6igschennai2015

Spritzbeton - Tagung 2015 / Shotcrete Conference and Exhibition, January 29-30, 2015, Congress Centre Alpbach, Austria, http://www.spritzbeton-tagung.com

Geosynthetics 2015, February 15 – 18, 2015, Portland, Oregon, USA, http://geosyntheticsconference.com

Environmental Connection Conference, February 15–18, 2015, Portland, Oregon, USA, www.ieca.org/conference/annual/ec.asp

12th Australia New Zealand Conference on Geomechanics (ANZ 2015), 22-25 February 2015, Wellington, New Zealand, http://www.anz2015.com

GeoProc2015: International Conference on Coupled THMC Processes in Geosystems, 25-27 February 2015, Salt Lake City, USA, https://secureweb.inl.gov/geoproc2015

International Conference & Exhibition on Tunnelling & Underground Space 2015 (ICETUS 2015) Sustainable Transportation in Underground Space Development, 3 – 5 March 2015, Kuala Lumpur, Malaysia, http://icetus2015.iemtc.com

AFRICA 2015 - Water Storage and Hydropower Development for Africa, 10 to 12 March 2015, Marrakesh, Morocco http://www.hydropower-dams.com/AFRICA-2015.php?c_id=89

Third United Nations World Conference on Disaster Risk Reduction, 14 -18 March 2015, Sendai City Miyagi Prefecture Japan, http://www.wcdrr.org

16th African Regional Conference on Soil Mechanics and Geotechnical Engineering, April 27 to 30, 2015 in Hammamet, Tunisia, http://www.cramsg2015.org

cs so

2nd Annual Underground Space Engineering
Driving Innovation: Redefining Tunnels & Underground of the Future
28 - 29 April 2015, Singapore

The tunnelling and underground industry is booming around the world. As the world's cities continue to grow, so too does the demand for new infrastructure. With numerous opportunities emerging from tunnels and underground projects, now is the time to build new relationships that are essential to winning works. Following the success of the 2014 event, TRUEVENTUS 2ND ANNUAL UNDERGROUND SPACE ENGINEERING continues its journey to the Asian underground city-Singapore! Mega tunnel and underground projects comes with all sorts of engineering challenges. This year's conference will bring together decision-makers from across the industry to provide a unique insight into the complexity and challenges of tunneling in city areas, mitigating construction risk, tunneling through di-cult ground conditions, managing groundwater in ows and mircotunelling as well as issues relevant to the design and construction of underground works.

For further details, contact
John Karras
T: +603 2775 0001 | F: +603 2775 0005
E: admin@registerforaconference.com, johnk@trueventus.com

cs so

ISP7-PRESSIO2015 1 to 2 May 2015, Hammamet, Tunisia, http://www.cramsg2015.org/isp7-pressio2015

13th ISRM International Congress on Rock Mechanics Innovations in Applied and Theoretical Rock Mechanics 10–13 May 2015, Montreal, Canada, www.isrm2015.com

Shale and Rock Mechanics as Applied to Slopes, Tunnels, Mines and Hydrocarbon Extraction, Special One day Symposium, May 12, 2015, Montreal, Quebec, Canada, www.isrm2015.com/Page/PageContent/ShaleSymposium

World Tunnel Congress 2015 and 41st ITA General Assembly: Promoting Tunnelling in South East European (SEE) Region, 22 - 28 May 2015, Dubrovnik, Croatia, http://wtc15.com

ꕥ

www.2015.compdyn.org

In the last few decades significant developments have been made to provide more accurate and reliable design methods for structures, infrastructures and foundations, particularly, when subjected to dynamic (mainly seismic) actions. Numerical methods have played a major role in these advances. Nevertheless, their remarkable potential should be broadened and improved, since geotechnical earthquake engineering hazards are still difficult to mitigate.

The Mini-Symposium "*Progress and challenges in geotechnical earthquake engineering*" will offer an opportunity for the presentation and discussion on several geotechnical issues related to earthquake engineering problems. All those involved with computational, related to earthquake geotechnical engineering are welcome to present their recent experience and research findings. Contributions related to hybrid, analytical as well as experimental methods in the field of soil dynamics are also welcome.

This Mini-Symposium aims to attract academic staff, researchers, post-graduate students and professional engineers dealing with advanced topics, which include but are not limited to: *Performance-based design*; *Liquefaction and other types of major soil failures*; *Dynamic soilstructure interaction*; *Codes, standards and safety evaluation*; *Foundations and Ground Improvement*; *Retaining structures; Slopes, dams and embankments*; *Tunnels and lifelines; Wind turbines; Man-made vibrations.*

MS Organizers

Castorina Silva Vieira, University of Porto, Portugal, cvieira@fe.up.pt

Yiannis Tsompanakis, Technical University of Crete, Greece, jt@science.tuc.gr

ꕥ

5th International Congress on Construction History
June 3rd-7th, 2015, Chicago, USA
www.5icch.org

The Construction History Society of America is proud to announce that it will be hosting the 5th International Congress on Construction History from June 3rd to 7th, 2015 at the Palmer House Hilton Hotel in Chicago. This will be the first time the Congress will be held outside Europe, following the four previous events hosted by Madrid (2003), Cambridge (2006), Cottbus (2009) and Paris (2012). The 5th International Congress on Construction History will include over two hundred papers on topics ranging from construction guilds and unions, to the evolution of building materials, as well as the construction of specific buildings and types. Papers will be delivered by delegates from six continents. Five keynote speakers will also present papers during the conference, and seven tours will be offered. In addition, there will be ample time for networking at several evening receptions. We look forward to welcoming you to Chicago in June!

Conference Topics

- History and construction of specific projects
- History of the building trades or specific builders
- Organization of construction work
- Wages and the economics of construction
- The development of building codes and regulations
- Trade unions and guilds
- Structural analysis and the development of structural forms
- Development of construction tools, cranes, scaffolding, etc
- Building techniques in response to their environments
- Building materials, their history, production and use
- History of services (heating, lighting etc.) in buildings
- The changing role of the professions in construction
- Building archaeology
- Computer simulation, experimentation and reconstruction
- Use of construction history for dating of historic fabric
- Recording, preservation and conservation
- Construction in architectural writing
- The role of construction history in education
- The bibliography of construction history
- The theory and practice of construction history

Construction History Society of America
P. O. Box 93461, Atlanta, GA
30377–0461 USA
chs@coa.gatech.edu

ꕥ

2nd International Course on Geotechnical and Structural Monitoring, 4-5-6 June 2015, Poppi, Tuscany, Italy, www.geotechnicalmonitoring.com/en/home-2

83rd ICOLD Annual Meeting & Congress Hydropower' 15, June 2015, Stavanger, Norway, www.icoldnorway2015.org

ISFOG 2015 3rd International Symposium on Frontiers in Offshore Geotechnics, Oslo, Norway, 10-12 June 2015, www.isfog2015.no

DMT 15 The 3rd International Conference on the Flat Dilatometer, Rome 15-17 June 2015, www.dmt15.com

ICGE 2015 International Conference in Geotechnical Engineering – Colombo-2015, 10 - 11 August 2015, Colombo, Colombo, Sri Lanka, http://www.slgs.lk/?p=564

China Shale Gas 2015 - an ISRM Specialized Conference, 6-8 September 2015, Wuhan, China, http://english.whrsm.cas.cn/ic/ic/201405/t20140509_120692.html

16th European Conference on Soil Mechanics and Geotechnical Engineering "Geotechnical Engineering for Infrastructure and Development", 13 - 17 September 2015, Edinburgh, UK, www.xvi-ecsmge-2015.org.uk

Workshop on Volcanic Rocks & Soils, 24 - 25 September 2015, Isle of Ischia, Italy, www.associazionegeotecnica.it

EUROCK 15 ISRM European Regional Symposium & 64th Geomechanics Colloquy, 7 – 9 October 2015, Salzburg, Austria, www.eurock2015.com

International Conference on Engineering Geology in New Millennium, 26-31 October 2015, New Delhi, India, http://isegindia.org/pdfs/1st%20circular-international-IAEG.pdf

6th International Conference on Earthquake Geotechnical Engineering, 2-4 November 2015, Christchurch, New Zealand, www.6icege.com

SEOUL 2015 - 25th World Road Congress Roads and Mobility – Creating New Value from Transport, 2–6 November, 2015, Seoul, Republic of Korea, http://www.aipcrseoul2015.org

4ο ΠΑΝΕΛΛΗΝΙΟ ΣΥΝΕΔΡΙΟ ΑΝΑΣΤΗΛΩΣΕΩΝ

Η ΕΤΑΙΡΕΙΑ ΕΡΕΥΝΑΣ ΚΑΙ ΠΡΟΩΘΗΣΗΣ ΤΗΣ ΕΠΙΣΤΗΜΟΝΙΚΗΣ ΑΝΑΣΤΗΛΩΣΗΣ ΤΩΝ ΜΝΗΜΕΙΩΝ (ΕΤΕΠΑΜ) οργανώνει στην Θεσσαλονίκη τον Νοέμβριο 2015, το 4ο Πανελλήνιο Συνέδριο Αναστηλώσεων. Οι ακριβείς ημερομηνίες και ο τόπος διενέργειας θα ανακοινωθούν αργότερα.

Αντικείμενο – Θεματολογία

Στο αντικείμενο του Συνεδρίου εμπίπτουν τα σχετικά με την Αναστήλωση των ιστορικών κτισμάτων (και των λειψάνων τους) ζητήματα, που αφορούν

α) στην φιλοσοφία και μεθοδολογία των επεμβάσεων,

β) στη σεισμική επικινδυνότητα των μνημείων

γ) στην τεχνολογική έρευνα (τεκμηρίωση, τεχνικές, υλικά κλπ) και εφαρμογή

δ) στην ανάδειξη μνημείων και αρχαιολογικών χώρων.

Το Συνέδριο απευθύνεται σε επιστήμονες που προέρχονται από τους χώρους των φυσικών επιστημών και της τεχνολογίας και συνεισφέρουν στο αναστηλωτικό έργο.

Η διάρκεια του συνεδρίου θα είναι τριήμερη και δύο από τις συνεδρίες θα αφιερωθούν στα ειδικά θέματα με τίτλους:

«Αναστηλώσεις νεώτερων μνημείων με φέροντα στοιχεία από χάλυβα και οπλισμένο σκυρόδεμα» και

«Οι επιπτώσεις του σεισμού της Κεφαλλονιάς στα μνημεία».

Πληροφορίες

ΕΤΑΙΡΕΙΑ ΕΡΕΥΝΑΣ ΚΑΙ ΠΡΟΩΘΗΣΗΣ ΤΗΣ ΕΠΙΣΤΗΜΟΝΙΚΗΣ ΑΝΑΣΤΗΛΩΣΗΣ ΤΩΝ ΜΝΗΜΕΙΩΝ, Θερμοπυλών 42, Θεσσαλονίκη , ΤΚ 54248 e-mail : etepam.etepam@gmail.com, ιστοσελίδα : www.etepam.gr.

The 15th Asian Regional Conference on Soil Mechanics and Geotechnical Engineering, 9-13 November 2015, Fukuoka, Japan, http://www.15arc.org

15th Pan-American Conference on Soil Mechanics and Geotechnical Engineering, 15 - 18 November 2015, Buenos Aires, Argentina, http://conferencesba2015.com.ar

VIII South American Congress on Rocks Mechanics, 15 - 18 November 2015, Buenos Aires, Argentina, http://conferencesba2015.com.ar

Sixth International Conference on Deformation Characteristics of Geomaterials IS Buenos Aires 2015, November 15th to 18th 2015, www.saig.org.ar/ISDCG2015

Geo-Environment and Construction, 26-28 November 2015, Tirana, Albania, Prof. Dr. Luljeta Bozo, lulibozo@gmail.com; luljeta_bozo@universitetipolis.edu.al

2015 6th International Conference Recent Advances in Geotechnical Engineering and Soil Dynamics, December 7-11, 2015, New Delhi (NCR), India, wason2009@gmail.com; wasonfeq@iitr.ernet.in, sharmamukat@gmail.com; mukutfeq@iitr.ernet.in, gvramanaiitdelhi@gmail.com, ajaycbri@gmail.com

Southern African Rock Engineering Symposium an ISRM Regional Symposium, 5 January 2016, Cape Town, South Africa, http://10times.com/southern-african-rock

GeoAmericas 2016 3rd Panamerican Conference on Geosynthetics, 11 – 14 April 2016, Miami Beach, USA, www.geoamericas2016.org

World Tunnel Congress 2016 "Uniting the Industry", April 22-28, 2016, San Francisco, USA, http://www.wtc2016.us

ISRM

Southern African Rock Engineering Symposium - an ISRM Regional Symposium
May 2016, Cape Town, South Africa

Contact Person: William Joughin
Telephone: +27-11-441-1214
E-mail: wjoughin@srk.co.za

84th ICOLD Annual Meeting, 16-20 May 2016, Johannesburg, South Africa, www.sancold.org.za/index.php/activities/icold-annual-meeting-2016

7th In-Situ Rock Stress Symposium 2016 - An ISRM Specialised Conference, 10-12 May 2016, Tampere, Finland, www.rs2016.org

GEOSAFE: 1st International Symposium on Reducing Risks in Site Investigation, Modelling and Construction for Rock Engineering - an ISRM Specialized Conference
25 – 27 May 2016, Xi'an, China

Contact

Telephone: 0086 27 87198913
Fax: 0086 27 87198413
E-mail: xtfeng@whrsm.ac.cn

NGM 2016 - The Nordic Geotechnical Meeting, 25 - 28 May 2016, Reykjavik, Iceland, www.ngm2016.com

EUROC 2016 - ISRM European Regional Symposium Rock Mechanics & Rock Engineering: From Past to the Future, 29-31 August 2016, Ürgüp-Nevşehir, Cappadocia, Turkey http://eurock2016.org

3rd ICTG
International Conference on Transportation Geotechnics

4 - 7 September 2016, Guimaraes, Portugal
www.spgeotecnia.pt/cpgt

The Transportation Geotechnics International Conference series began under the auspices of ISSMGE-TC 3 and was initiated in 2008 at the University of Nottingham, UK, as an International event designed to address the growing requirements of infrastructure for societies. The 2nd International Conference on Transportation Geotechnics took place in 2012, at Sapporo, Japan, under the ISSMGE-TC202 that follows the TC-3 activities for the period 2009-2013. To continue the successful of these conferences and the output of ISSMGE-TC-202, the 3rd was scheduled for 2016, at Guimarães, Portugal. Following the previous one, the challenges addressed by this conference will include a better understanding of the interactions of geotechnics on roads, rails, airports, harbours and other ground transportation infrastructure with the goal of providing safe, economic, environmental, reliable and sustainable infrastructures. The 3rd ICTG will be composed of workshops and several types of sessions, as well as a technical exhibition, to better disseminations of findings and best practices. A special attention will be paid to the publication of all the peer review papers, some of them in specialised international journals. On behalf of the organizing committee I am honoured to invite you to the 3rd ICTG in the City of Guimarães, UNESCO World Heritage (September 4-7, 2016).

Contact person: Prof. A. Gomes Correia (Chair)
Address: University of Minho, School of Engineering
Campus de Azurém
4800-058, Guimarães, Portugal
Phone: +351253510200, +351253510218
Fax: +351253510217
E-mail: 3ictrgeo2016@civil.uminho.pt, agc@civil.uminho.pt

EuroGeo 6 – European Regional Conference on Geosynthetics
25 – 29 Sep 2016, Istanbul, Turkey
www.eurogeo6.org

eguler@boun.edu.tr

ARMS 9
9th Asian Rock Mechanics Symposium
ISRM Regional Symposium
October 2016, Bali, Indonesia
rkw@mining.itb.ac.id

Contact Person: Dr Ridho Wattimena
Indonesian Rock Mechanics Society (IRMS)
Telephone: +22 250 2239

ᏈᏋ ᏈᏋ

GeoAsia 6

6th Asian Regional Conference on Geosynthetics, 8-11 November 2016, New Delhi, India, uday@cbip.org

ᏈᏋ ᏈᏋ

GeoAfrica 2017

The 3rd African Regional Conference on Geosynthetics, 9 – 13 October 2017, Morocco

ᏈᏋ ᏈᏋ

11th International Conference on Geosynthetics (11ICG)

16 - 20 Sep 2018, Seoul South Korea
csyoo@skku.edu

ΕΝΔΙΑΦΕΡΟΝΤΑ ΓΕΩΤΕΧΝΙΚΑ ΝΕΑ

Βραχοπτώσεις από το Ronchi di Termeno

Βράχος όγκου 160 m^3 "έγλυψε" την αγροικία.

Εντυπωσιακές εικόνες από τις ελεγχόνες ανατινάξεις για την άρση της επικινδυνότητας του φαινομένου στους παρακάτω συνδέσμους:

https://www.youtube.com/watch?v=EV0l5N28Nl8

https://www.youtube.com/watch?v=uu3WOB-xC7s

https://www.youtube.com/watch?v=3YgVPWI_BD8

https://www.youtube.com/watch?v=CfGC15nWtKM

Frana Provocata Valle d'Aosta

Landslide caused to remove a giant boulder that hung on the SS26 Aosta Valley between the towns of Bard and Arnad on March 29, 2010 at 15.00.

https://www.youtube.com/watch?v=Nl5kPhlAVug

ΕΝΔΙΑΦΕΡΟΝΤΑ - ΣΕΙΣΜΟΙ

Software utilises satellite radar to monitor fracking and land stability

New technology could help fracking companies avoid areas where gas drilling may be most likely to cause earth tremors.

Researchers from Nottingham University have developed software that uses satellite radar data to identify millimetre-scale vertical movements in the landscape in a way that was previously impossible in rural areas.

This could allow landowners, local authorities and fracking firms to identify areas of high seismic activity that may be more likely to produce tremors if hydraulic fracturing (fracking) is used to drill for gas beneath them.

'What this system gives us is regional coverage so we can see how large areas are moving over time,' said Dr Colm Jordan from the British Geological Society, who has been working with the Nottingham researchers to validate the software. 'This gives a more complete picture of what's happening in rural areas.'

The technique could also be used to monitor whether fracking is causing seismic activity in an area during and after drilling operations – but only if fracking is found to cause surface movement.

'This system would only look at surface motion, and fracking occurs at great depth,' said Jordan. 'If fracking is occurring and it does produce a surface motion this might be one system that could help us monitor that.'

Existing seismic detection systems can use satellite radar data to monitor how the land in urban areas rises or falls due to seismic activity. The time taken for the radar signal to bounce off a fixed object such as a building enables scientists to work out its distance from the satellite, and so over time see if it has moved.

But in rural areas the continual growth of vegetation and the lack of buildings to act as clear reference points over a wide area mean traditional systems were unable to build an accurate picture of the height of the land when viewed from above.

The new software, developed by Dr Andrew Sowter in the Nottingham's Department of Civil Engineering, uses a technique called Intermittent Small Baseline Subset (ISBAS) to combine over 30 radar images and identify areas of the signal reliable enough to calculate the height of the land.

'We think that if you look at a forest from the air you can see that the canopy has holes in it that give good measurements from where you can see the ground or dry tree trunks that reflect ground motion,' he said.

While research from Durham University Energy Institute has found that seismic activity caused by fracking is nearly undetectable by humans, Sowter said there was concern over what might happen from the knock-on effects of injecting fracking fluids into sections of rock that were already under high stress.

A report from the Royal Academy of Engineering has recommended improved monitoring of shale gas exploration sites in order to ensure their safety.

The new software, dubbed "PUNNET GEO", recently won the overall prize in the European Copernicus Masters Earth Monitoring Competition that recognises innovative uses of satellite observation data.

(Stephen Harris / theengineer, 5 November 2014, http://www.theengineer.co.uk/1019452.article?cmpid=tenews_655654)

Stanford engineers build, test earthquake-resistant house

Twenty-five years after the Loma Prieta earthquake, a Stanford team develops inexpensive design modifications that could be incorporated into new homes to reduce damage in an earthquake.

A Stanford team has developed inexpensive design modifications that might replace the need for residential earthquake insurance. Seismic isolators let a house skate along the trembling ground instead of collapsing.

Stanford engineers have built and tested an earthquake-resistant house that stayed staunchly upright even as it shook at three times the intensity of the destructive 1989 Loma Prieta temblor 25 years ago.

The engineers outfitted their scaled-down, boxy two-story house with sliding "isolators" so it skated along the trembling ground instead of collapsing. They also including extra-strength walls, to create a home that might replace the need for residential earthquake insurance, said project leader Gregory Deierlein, Stanford's John A. Blume Professor in the School of Engineering.

The modifications are inexpensive and could be incorporated into new homes as soon as designers and contractors decide to try them, according to the researchers.

"We want a house that is damage free after the big earthquake," said Eduardo Miranda, an associate professor of civil and environmental engineering. He co-led the project with Deierlein and Benjamin Fell, an associate professor in the Department of Civil Engineering at California State University, Sacramento.

Residential homes already do a good job of keeping the people inside safe when a temblor hits. But earthquakes typically do a lot of minor structural damage. For example, after the 1994 Northridge quake, the majority of the $25.6 billion in repair costs paid for fixes to 500,000 residential structures.

Most of those homes were not destroyed, but nonetheless thousands of families had to find a new place to live while their houses were repaired. Even if the walls stay up in a quake, wall finishes like drywall and stucco, along with architectural fixtures like cabinetry, are damaged because of the large sideways movements caused by earthquakes, Deierlein said.

The house that Stanford built had two major modifications to stave off earthquake damage. For one, it was not affixed into a foundation, but rested on a dozen steel-and-plastic sliders, each about 4.5 inches in diameter. Under those sliders were either plates or bowl-shaped dishes made of galvanized steel. These units are called seismic isolators.

"The idea of seismic isolation is to isolate the house from the vibration of the ground," Miranda said. "When the ground is moving, the house will just slide." Seismic isolators already protect large structures like San Francisco City Hall and structures at San Francisco International Airport, Deierlein said, but they are quite expensive. He and his team adapted the technology for residential use by incorporating inexpensive materials into their scaled-down isolators.

Second, the engineers developed what they call a "unibody" design, a term borrowed from the automobile industry, in which every element of the structure contributes to its strength. Instead of simply screwing drywall to the wood framing, as in typical construction, they used glue to affix extra-thick, 5/8-inch drywall more securely. On the outside, they used strong mesh and additional screws to attach the white stucco tightly. These elements made the house stiffer and stronger, leading to a significantly better seismic performance.

How do you test an earthquake-resistant house? It takes a big earthquake simulator called a shake table. Deierlein and colleagues constructed their 36-by-22-foot three-bedroom home atop the biggest such platform in the country, the Large High Performance Outdoor Shake Table at the University of California, San Diego. The facility uses computer-controlled hydraulic pistons to move the platform back and forth in a pattern selected by the engineers, so it can replicate specific earthquakes like Loma Prieta.

The table is part of the George E. Brown, Jr. Network for Earthquake Engineering Simulation (NEES), with sites across the United States funded by the National Science Foundation. The engineers tested partial versions of their design earlier at Stanford, California State University, Sacramento, and a NEES site at the University of California, Berkeley.

After a seven-week build, in September it was time to rumble the house. First, the engineers tested the isolators, the flat versions and the dish shape. The dishes are designed so that after the temblor ceases, the isolators' pegs will settle back into the lowest point of the dish. That way, the house always winds up where it started. Although flat pads are easier to build, they also leave the house more vulnerable to migrating from its original location.

While it is difficult to put the simulations on the Richter scale, the engineers shook the table at three times the intensity of the ground shaking during Loma Prieta, which measured 6.9 magnitude. The house slid from left to right, but held together. "Under the isolators, the house basically saw no damage," Deierlein said. Even in a strong quake like Northridge, a 6.7 on the Richter scale, isolators should protect a home, he said.

Next, the researchers bolted the house to the shake table, to test how well the unibody system held up without isolators. They had developed computer models to predict when the house would fall, but it outperformed their expectations.

"We are really seeing very little damage," said Ezra Jampole, a doctoral candidate at Stanford whose T-shirt read, "I'm an earthquake engineer… If I run you run." Under the triple-Loma Prieta conditions, a few cracks appeared in the stucco and drywall, and a swinging light in the garage shattered. The test window and steel door stayed put, as did the table and chair that furnished the test house.

Encouraged, the engineers cranked up the table to shake 50 percent faster, the maximum quake the table can simulate. That did it. The engineers whooped and clapped as the house sashayed from side to side. The window and door fell out and stucco sheared off. The house wound up listing to the side like the Tower of Pisa.

"It came really close to collapse," Deierlein said. He said the engineers still have some work to do to figure out precisely how much shaking a unibody house can withstand before crumbling.

Want your own earthquake-resistant home? Though it should be possible to retrofit houses with these modifications, it would be simpler to incorporate them into a new construction, Deierlein said. He and his colleagues intentionally designed protective features that were not only effective, but also affordable. The unibody system, requiring some glue, mesh and screws, should add less than a few thousand dollars to the cost of building a building the size of the test house, and very little time to the construction process, Miranda said.

Deierlein estimated that building a house on this type of seismic isolators would add about $10,000 to $15,000 to the total cost of a 1,500- to 2,000-square-foot house; and it would take contractors about four extra days to install them before building the home on top. However, he said, that one-time cost is minimal compared to annual earthquake insurance with high deductibles. Californians paid an average premium of $676 in 2013, according to the California Department of Insurance, but the majority of homeowners don't carry a policy at all.

Contractors could start incorporating these changes into new homes anytime, Deierlein said, though it will likely take a few pioneering engineers to add them to designs and work with building departments to incorporate them into existing building codes.

"We are always cautious never to talk about earthquake-proof," he said, "but our resistance is getting better and better."

(Amber Dance / Stanford Report, October 16, 2014, http://news.stanford.edu/news/2014/october/shakehouse-quake-engineering-101614.html)

Engineers at Stanford Develop Cost-Effective Earthquake-Resistant House

In 1989, California's central coast was rocked by a 6.9 magnitude earthquake, destroying infrastructure and buildings in San Francisco, Oakland, and a host of coastal cities. The Loma Prieta Earthquake caused an estimated $6 trillion in damage, prompting researchers to develop techniques for management of severe seismic activity in urban centres. Twenty five years later, a team of engineers at Stanford University have invented a cost-effective foundation for residential buildings capable of withstanding three times the magnitude of the catastrophic 1989 earthquake.

Of the estimated 10,000 earthquakes California receives annually, approximately 15-20 are capable of producing serious damage to millions of structures across the state. Earthquake insurance is levied on homeowners to offset costs associated with major reconstruction of infrastructure and housing, costing homeowners an average of $673 annually. The team of engineers at Stanford set about to develop a foundation that could withstand California's harshest seismic activity, potentially bringing a significant reduction in the costs of insurance. The resulting home utilizes automotive unibody technology to create a reinforced structure able to endure some of the strongest earthquakes likely in California.

The premise behind the technology is simple: "When the ground is moving, the house will just slide," says Edouardo Miranda, an associate professor of engineering at Stanford. During an earthquake, the house would skate along a series of "isolators," 4.5 inch steel and plastic sliders resting atop bowl-shaped dishes of galvanized steel, minimizing the destructive effects of intense structural vibration. When combined with the unibody structural frame, the isolators minimize vibration from the ground, eliminating the destructive effects created by earthquakes. The technology is similar to the seismic isolators already used on many public buildings in California, except at a dramatically lower price: researchers estimate the cost of implementing the system at only $10,000 to $15,000, adding four days to construction time. One-time installation costs pale in comparison to earthquake insurance costs, say researchers.

https://www.youtube.com/watch?v=Z30rcg3buuw

Tests on the structure were carried out at the University of California San Diego, home to the largest earthquake simulator in the United States. The 'shake table' measures 36' by 22' and was able accommodate the two-storey, three bedroom home constructed by the project team. Simulations were programmed based on historic earthquakes with significant residential damage, including the 1994 quake in Los Angeles damaging 500,000 homes and incurring $25.6 Billion in repair costs. The house underwent trials with and without isolators, designed to test the resiliency of the house's reinforced structure. According to Stanford, the house "outperformed" expectations during testing, and only showed structural damage upon being tested at maximum capacity by the simulator.

Stanford's earthquake-resistant technology is now ready to be implemented in zones of seismic activity worldwide, having completed and passed rigorous safety tests. Its next hurdle will be zoning approval and inclusion in residential design. Read more about the project at Stanford News, .

(Finn MacLeod / Architecture News, California, Earthquake Engineering, Stanford University, 15 November 2014, http://www.archdaily.com/567766/engineers-at-stanford-develop-cost-effective-earthquake-resistant-house)

Πολύκροτη υπόθεση
Ανατράπηκε η καταδίκη σεισμολόγων για «μη προειδοποίηση» του σεισμού στην Άκουιλα

Η ανατροπή της καταδίκης προκάλεσε ανακούφιση στους κατηγορουμένους αλλά οργή στους κατοίκους, που φώναζαν στο δικαστήριο

Απάλλαξε τελικά το Εφετείο τους έξι σεισμολόγους της ιταλικής «Επιτροπής Μεγάλων Κινδύνων» που είχαν αρχικά καταδικαστεί σε εξαετή κάθειρξη επειδή δεν είχαν προειδοποιήσει επαρκώς για τον κίνδυνο σεισμών στην Άκουιλα, τις παραμονές της καταστροφής του 2009.

Μόνο η καταδίκη του αξιωματούχου που ήταν επικεφαλής της επιτροπής επικυρώθηκε, αν και μειώθηκε σε δύο χρόνια

Η απόφαση έγινε δεκτή με ανακούφιση από τους κατηγορουμένους, αλλά προκάλεσε την οργή των κατοίκων που φώναζαν στο δικαστήριο «ντροπή» μετά την ετυμηγορία.

Οι επτά (έξι σεισμολόγοι και ο αναπληρωτής επικεφαλής της επιτροπής Μπερνάντο ντε Μπερναντίνις) είχαν καταδικαστεί πρωτόδικα το 2012 σε έξι χρόνια φυλάκισης για ανθρωποκτονία από αμέλεια.

Στο επίκεντρο της υπόθεσης είχαν βρεθεί ανακοινώσεις της επιτροπής λίγες ημέρες πριν τον σεισμό, και κυρίως το εάν είχαν σχηματίσει -υπό πολιτική πίεση- καθησυχαστική εικόνα που διαψεύστηκε με τον τραγικότερο τρόπο όταν χτύπησε ο Εγκέλαδος με 6,3 βαθμούς.

Την Άκουιλα, που έχει περάσει αρκετούς σεισμούς στην ιστορία της, είχαν ανησυχήσει σειρά μικρότερων δονήσεων πριν τον ισχυρό σεισμό της 6ης Απριλίου.

Η αρχική καταδίκη είχε προκαλέσει έντονες αντιδράσεις στη διεθνή επιστημονική κοινότητα, η οποία έβλεπε κίνδυνο να μην τολμούν πλέον επιστήμονες στα πεδία φυσικών καταστροφών να προβούν σε εκτιμήσεις εξαιτίας του κινδύνου καταδίκης τους.

(Newsroom ΔΟΛ, 11 Νοε. 2014, http://news.in.gr/world/article/?aid=1231362762)

ΕΝΔΙΑΦΕΡΟΝΤΑ - ΛΟΙΠΑ

theENGINEER

The Engineer has seen a lot of change in its long history which dates back to 1856. From the opening of the Brooklyn Bridge to the tragic sinking of the Titanic, The Engineer has been at the forefront of every engineering news story for the past 157 years including:

1859 - Death of Isambard Kingdom Brunel
1912 - The Titanic Inquiry
1923 - The Construction of Wembley Stadium (see image reference above)
1936 - First Flight of the Hindenberg
1956 - The World's First Nuclear Power Station
1969 - Apollo 11 Mission

View The Engineer archive online >>

Times have changed, and although theengineer.co.uk is now the UK's leading online resource for the engineering industry The Engineer maintains its print format. In a world where the sheer volume of information and news can often be overwhelming, the magazine is a must-read monthly digest of news, features, and analysis on the most important, inspiring and innovative stories from across industry.

We look forward to sending you the most established engineering magazine in the UK.

The Engineer

The Engineer is available free of charge to individuals who meet our qualifying criteria. We try to only invite people who we think might qualify for complimentary copies. If you do not meet the terms of control we will inform you of this and contact you with details of how to subscribe. Offer available in the UK only.

The Engineer is a division of Centaur Media PLC, Wells Point, 79 Wells Street, London W1T 3QN.

Registered in England No. 4948078

Transportation official: Grid must handle natural disasters

The nation's transportation grid must be built to withstand a new normal of more serious natural disasters and it won't be cheap or easy, a top official of the U.S. Transportation Department warned Wednesday.

Creating a resilient transportation system is "the most significant challenge we have in the century going forward," Peter Rogoff, the department's undersecretary for policy told a forum sponsored by the Eno Center for Transportation.

Rogoff said such things as building highways and rail lines higher and better protected to withstand storms and sea level rise makes financial sense.

But it will also be more expensive in the short-run he told dozens attending the forum. The think-tank sponsoring the event works to make transportation systems more efficient and safer.

Rogoff said the damage from Superstorm Sandy two years ago in the New York City area proved the worst transportation disaster in the nation's history.

The storm flooded subway tunnels, cut power to electric train lines, snarled traffic because of road and other damage and caused lines at gas stations when new supplies could not be brought in.

"**We need to break away from a cost-benefit process that justifies projects solely on what happened in the past**," Rogoff said. "**Taxpayers shouldn't be footing the bill for in-frastructure and transportation assets that are not designed for the new normal.**"

He noted some of the tunnels in New York that flooded during Sandy flooded just a year earlier in Hurricane Irene.

Changing the way America builds its transportation system will require convincing "a skeptical public, a skeptical bureaucracy and a skeptical Congress," Rogoff added.

America is more interconnected with communications than ever before, said Lillian Borrone, who chairs the board of the Eno Center. "But what good does it do if we're connected?" she asked, if people can't get to hospitals, to grocery stores or are cold and can't get heating fuel.

The economy depends on moving goods in a transportation system that is both public and private said Leslie Blakey the president of a nonprofit that works for increased federal investment in the nation's freight infrastructure.

"The response to a destructive event is going to always be very challenging because so many players are involved and yet the stakes could not possibly be higher," she said.

She said that the cost to the economy of a disaster is generally much higher than dealing with the immediate damage.

(Associated Press, November 12, 2014, http://www.foxbusiness.com/markets/2014/11/12/transportation-official-grid-must-handle-natural-disasters)

Γνωρίστε τον «μπριντγκμανίτη»
Το πιο άφθονο ορυκτό της Γης επιτέλους αποκτά όνομα

Ίχνη του «μπριντγκμανίτη» κρύβονταν σε έναν μετεωρίτη που έπεσε τον 19ο αιώνα στην Αυστραλία (Πηγή: Chi Ma)

Το ορυκτό που λέγεται ότι καταλαμβάνει περισσότερο από το ένα τρίτο του πλανήτη απέκτησε επιτέλους όνομα. Η ειρωνεία όμως είναι ότι τα μόνα γνωστά δείγματα του «μπριντγκμανίτη» δεν προέρχονται από τη Γη, αλλά από το Διάστημα.

Το παράξενο ορυκτό, το οποίο περιέχει μαγγάνιο, πυρίτιο και οξυγόνο και έχει τον τύπο $MgSiO_3$, είναι σταθερό μόνο σε συνθήκες ακραίας πίεσης, σε βάθη 670 έως 2.900 χιλιομέτρων μέσα στο γήινο μανδύα.

Για να γίνει επίσημα αποδεκτό ένα νέο ορυκτό, σύμφωνα με τους κανόνες της Διεθνούς Ένωσης Ορυκτολογίας, οι επιστήμονες πρέπει να περιγράψουν όχι μόνο τη χημική του σύσταση αλλά και την κρυσταλλική δομή του. Η σύσταση του μπριντγκμανίτη ήταν γνωστή, ωστόσο η διάταξη των ατόμων στον κρύσταλλο παρέμενε απροσδιόριστη.

Η ανάσυρση δειγμάτων από το μανδύα είναι πρακτικά αδύνατη, ωστόσο μια πέτρα που έπεσε από τον ουρανό στην Αυστραλία το 1879 έδωσε τελικά τη λύση. Προηγούμενες μελέτες είχαν δείξει ότι ο λεγόμενος μετεωρίτης του Τέναμ είχε υποστεί αλλεπάλληλες συγκρούσεις με άλλους αστεροειδείς και έφερε φλέβες ορυκτών που είχαν λιώσει από την πίεση και τη θερμοκρασία.

Η νέα μελέτη, η οποία δημοσιεύεται στο κορυφαίο περιοδικό Science, δείχνει ότι οι συγκρούσεις εξέθεσαν απότομα τον εξωγήινο βράχο σε θερμοκρασία 2.200 βαθμών Κελσίου και σε πίεση 240.000 ατμοσφαιρών. Το ψύχος του Διαστήματος και η αυξημένη πίεση στο εσωτερικό του αστεροειδή διατήρησαν σταθερή την κρυσταλλική δομή του μπριντγκμανίτη, ο οποίος βρέθηκε υπό τη μορφή μικροσκοπικών σφαιριδίων, με διάμετρο μερικών μικρομέτρων.

Το νέο όνομα του ορυκτού, το οποίο έγινε επίσημα δεκτό τον περασμένο Ιούνιο, τιμά τον αμερικανό φυσικό Πέρσι Μπρίντγκμαν, ο οποίος βραβεύτηκε με Νόμπελ Φυσικής το 1946 για τις μελέτες του στο σχηματισμό ορυκτών σε συνθήκες ακραίας πίεσης.

Σύμφωνα με προηγούμενες μελέτες, οι οποίες μεταξύ άλλων εξέταζαν τη διάδοση σεισμικών κυμάτων μέσα στον μανδύα της Γης, έχουν δείξει ότι το 70% του κατώτερου μανδύα, σε βάθος 660 έως 2.900 χιλιόμετρα, αποτελείται κατά 70% από «μπριντγκμανίτη».

Αυτό σημαίνει ότι το ακριβοθώρητο ορυκτό αντιστοιχεί στο 38% του συνολικού όγκου της Γης.

(Βαγγέλης Πρατικάκης / Newsroom ΔΟΛ, 28 Νοε. 2014, http://news.in.gr/science-technology/article/?aid=1231367027)

ΝΕΕΣ ΕΚΔΟΣΕΙΣ ΣΤΙΣ ΓΕΩΤΕΧΝΙΚΕΣ ΕΠΙΣΤΗΜΕΣ

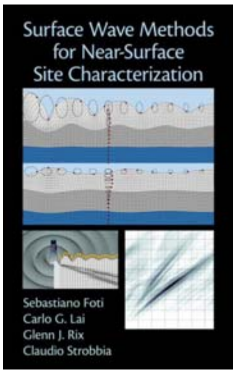

Surface Wave Methods for Near-Surface Site Characterization

Sebastiano Foti, Carlo G. Lai, Glenn J. Rix, Claudio Strobbia

Using examples and case studies directly drawn from the authors' experience, this book addresses both the experimental and theoretical aspects of surface wave propagation in both forward and inverse modeling. This book accents the key facets associated with surface wave testing for near-surface site characterization. It clearly outlines the basic principles, the theoretical framework and the practical implementation of surface wave analysis. In addition, it also describes in detail the equipment and measuring devices, acquisition techniques, signal processing, forward and inverse modeling theories, and testing protocols that form the basis of modern surface wave techniques.

Review Examples of Typical Applications for This Geophysical Technique

Divided into eight chapters, the book explains surface wave testing principles from data measurement to interpretation. It effectively integrates several examples and case studies illustrating how different ground conditions and geological settings may influence the interpretation of data measurements. The authors accurately describe each phase of testing in addition to the guidelines for correctly performing and interpreting results. They present variants of the test within a consistent framework to facilitate comparisons, and include an in-depth discussion of the uncertainties arising at each stage of surface wave testing.

- Provides a comprehensive and in-depth treatment of all the steps involved in surface wave testing
- Discusses surface wave methods and their applications in various geotechnical conditions and geological settings
- Explains how surface wave measurements can be used to estimate both stiffness and dissipative properties of the ground
- Addresses the issue of uncertainty, which is often an overlooked problem in surface wave testing
- Includes examples with comparative analysis using different processing techniques and inversion algorithms
- Outlines advanced applications of surface wave testing such as joint inversion, underwater investigation, and Love wave analysis

Written for geotechnical engineers, engineering seismologists, geophysicists, and researchers, this book offers practical guidance, and presents a thorough understanding of the basic concepts.

(CRC Press, August 2014)

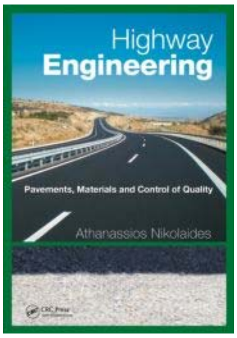

Highway Engineering: Pavements, Materials and Control of Quality

Athanassios Nikolaides

Highway Engineering: Pavements, Materials and Control of Quality covers the basic principles of pavement management, highlights recent advancements, and details the latest industry standards and techniques in the global market. Utilizing the author's more than 30 years of teaching, researching, and consulting experience, this text focuses on the design, construction, maintenance, and management of pavements for roads and highways, and covers the main topics in highway engineering. The author integrates pavement materials, material testing for acceptability and quality assurance, asphalt mix design, flexible and rigid pavement design, construction, maintenance and strengthening procedures, quality control of production and acceptance of asphalts, pavement evaluation, asphalt plants, and pavement recycling. He also includes both European and American (ASTM and AASHTO) standards and practice, and is extensively illustrated with references, tables, graphs, charts, and photographs.

The book contains 18 chapters that cover:

- Soils for roadworks
- Aggregates for unbound, hydraulically bound materials, and bituminous mixtures
- Bitumen and bituminous binders
- Laboratory tests and properties of paving bitumen and bitumen emulsion
- Hot and cold bituminous mixtures
- Fundamental mechanical properties of bituminous mixtures and testing
- Production, transportation, laying, and compaction of bituminous mixtures
- Quality control and acceptance of bituminous mixtures
- Methods for determining stresses and strains in pavements
- Pavement design and construction
- Thickness design methodologies for flexible and rigid pavements
- Pavement maintenance
- Rehabilitation and strengthening
- Pavement evaluation
- Equipment for measuring surface and structural characteristics
- Pavement management
- Pavement recycling

Written for civil engineering students and engineers engaged in highway projects or laboratory testing, **Highway Engineering: Pavements, Materials and Control of Quality** covers pavement engineering comprehensively as a textbook for undergraduates and graduates, and a valuable reference for practicing professionals.

(CRC Press, November 24, 2014)

ΗΛΕΚΤΡΟΝΙΚΑ ΠΕΡΙΟΔΙΚΑ

www.geoengineer.org

Κυκλοφόρησε το Τεύχος #117 του **Newsletter του Geoengineer.org** (Νοεμβρίου 2014) με πολλές χρήσιμες πληροφορίες για όλα τα θέματα της γεωμηχανικής. Υπενθυμίζεται ότι το Newsletter εκδίδεται από τον συνάδελφο και μέλος της ΕΕΕΕΓΜ Δημήτρη Ζέκκο (secretariat@geoengineer.org).

ΕΚΤΕΛΕΣΤΙΚΗ ΕΠΙΤΡΟΠΗ ΕΕΕΕΓΜ (2012 – 2015)

ΕΕΕΕΓΜ
Τομέας Γεωτεχνικής
ΣΧΟΛΗ ΠΟΛΙΤΙΚΩΝ ΜΗΧΑΝΙΚΩΝ
ΕΘΝΙΚΟΥ ΜΕΤΣΟΒΙΟΥ ΠΟΛΥΤΕΧΝΕΙΟΥ
Πολυτεχνειούπολη Ζωγράφου
15780 ΖΩΓΡΑΦΟΥ

Τηλ. 210.7723434
Τοτ. 210.7723428
Ηλ-Δι. secretariat@hssmge.gr ,
geotech@central.ntua.gr
Ιστοσελίδα www.hssmge.org (υπό κατασκευή)

«ΤΑ ΝΕΑ ΤΗΣ ΕΕΕΕΓΜ» Εκδότης: Χρήστος Τσατσανίφος, τηλ. 210.6929484, τοτ. 210.6928137, ηλ-δι. pangaea@otenet.gr, ctsatsanifos@pangaea.gr, editor@hssmge.gr

«ΤΑ ΝΕΑ ΤΗΣ ΕΕΕΕΓΜ» «αναρτώνται» και στην ιστοσελίδα www.hssmge.gr